Modeling the Environmental Fate of Polybrominated Diphenyl Ethers in Lake Thun

Diploma Thesis

Markus Bläuenstein
Department of Environmental Science
Swiss Federal Institute of Technology Zürich, ETH Zürich (Switzerland)

Tutor
PD Dr. Martin Scheringer
Supervisor
Prof. Dr. Konrad Hungerbühler

Safety & Environmental Technology Group
Institute for Chemical and Bioengineering, ETH Zürich (Switzerland)

September 2007

ETH
Eidgenössische Technische Hochschule Zürich
Swiss Federal Institute of Technology Zurich

Safety and
Environmental
Technology Group

-

Executive Summary

Polybrominated diphenyl ethers (PBDEs) are applied as flame retardants in many consumer products. Their production and use have increased rapidly during the last decades and have caused increasing emissions into the environment. Evidence of long-range transport and exponentially increasing levels have been observed in the environment. This is of concern since PBDEs are persistent, bioaccumulative, toxic and can act as endocrine disruptors. Many studies have therefore addressed PBDEs in the environment by taking and analyzing environmental samples or modeling the fate of these chemicals in the environment.

While measurements of contaminant levels in the environment characterize the partitioning between various media, they do not give direct conclusive information about the processes and factors that determine the measured concentrations. Multimedia box models, in contrast, provide concentrations in, and mass fluxes between different environmental media. These are derived from input values for chemical properties and emission mass fluxes on one side and parameters describing transfer processes in the environment on the other side. Furthermore, a multimedia model provides the possibility to calculate scenarios that do not represent the current state of the environment. A model can thus assess the outcome for different emission scenarios and investigate in depth the effect of a change in certain parameters on contaminant levels in the environment.

Methodology

A multimedia mass balance model for a lake was set up with MATLAB giving the option to change input parameters in order to calculate various scenarios. The model consists of three bulk compartments: atmosphere, lake water and sediment. The atmosphere includes the free gas phase and two different aerosol size fractions, the lake water consists of the water (dissolved) phase, suspended particles and fish and the sediment consists of solid sediment and pore water.

Mass balance equations for each compartment were set up, which include advective and diffusive mass transfer processes between the three model compartments as well as across the system boundaries.

The model was applied to PBDEs in Lake Thun. PBDE homologues were modeled, whereas a homologue represents all PBDE congeners with the same number of bromine substitutions. Thus, 9 compounds from Di-BDE (2 bromines) to Deca-BDE (10 bromines) were considered. Formation of lower brominated homologues from higher brominated ones by debromination was included into the mass balance equations.

The model was calibrated to the measured PBDE concentration in the atmosphere by defining a flow into the atmospheric compartment containing the measured PBDE concentrations. The concentrations were seasonally adapted, since some temperature dependence of the bulk atmospheric concentration (gas + particle bound concentrations) has been observed in the samples. An additional input via

rivers was included, where measurements from the tributaries Aare and Kander were used. A sensitivity analysis was performed to determine the influence of individual parameters on specific model outputs and model uncertainty was analyzed with both an analytical uncertainty propagation method and with Monte Carlo simulation.

Results

Modeled steady-state concentrations: Steady-state calculations were evaluated and compared with measured concentrations.

Measured concentrations are close to the model point estimates and lie within the model uncertainty with only a few exceptions. Modeled Hexa-BDE and Deca-BDE concentrations in the dissolved water phase are too low compared to measurements and modeled Hexa-BDE and Hepta-BDE concentrations on suspended particles are too low compared to measurements. This has probably been caused by the sampling and analytics methods. Many values were below the detection limit and the dissolved phase still contains some particles, since a 0.7 µm filter was used in sampling. Concentrations in fish are in agreement except for Hexa-BDE. This homologue seems to be underestimated in the tributaries and/or in the atmospheric input leading to too low modeled concentrations in all media. Since the model assumes equilibrium between water and fish, it can be concluded that no biomagnification occurs in the fish. This is in contrast to PCBs, which were used to further evaluate the model, where measured concentrations are systematically higher than modeled and biomagnification is thus observed.

Measured concentrations in sediment lie within the range of uncertainty of the modeled concentrations. However, the modeled point estimates of lower brominated congeners tend to be higher than measured concentrations. A likely reason is that some degradation takes place in the sediment, which lowers measured concentrations. Modeled concentrations represent the sediment at the top, which is in interaction with the open water, while the measured concentration represent material deposited about one year before sampling.

Other scenarios: A model run without input by tributaries resulted in concentrations that were further away from measurements. However, due to the high uncertainties in the model it can not be concluded that rivers significantly change the concentrations in the lake by their additional input. In another scenario debromination was ceased. The result was close to the basic scenario where debromination is included and therefore no additional information about the extent of debromination occurring in the environment could be gained from the model.

Mass balance and inventories: The input of substances into the lake is mainly from the atmosphere, except for Hepta-BDE and Deca-BDE where the input from tributaries is higher. Particle deposition is the main pathway for homologues with six or more bromines, while input via diffusion and dissolution in rainwater is the main pathway for homologues with five or less bromines. The substances leave the lake water compartment mainly by sedimentation. Only for the lower brominated homologues degradation and output with rivers reach some importance. Consequently most of the total mass in the modeled system is present in the solid sediment. Compared to the total mass in the system, the water compartment only

holds 17% for Di-BDE, 11% for Tri-BDE, 1.7% for Tetra-BDE and less than 1% for the other homologues.

Dynamic solution: Seasonal variations have been observed to lie within 0.5 and 1 order of magnitude and are mainly caused by the seasonal change in the atmospheric input concentration. Generally concentrations in summer are higher than in winter in all media, caused by higher atmospheric concentrations and thus higher inputs into the lake.

An overall half-time for depletion from Lake Thun (water compartment + sediment compartment) in case of ceasing input into the lake is between 3.4 and 9.5 years, whereas higher brominated homologues tend to have longer half-lives. This is rather high compared to a 1.3 years 'half-life' of water in the lake and reflects the fact that most of the PBDEs are in the sediment.

Conclusions

A model has been developed that can be used to assess the environmental fate of chemicals in a lake. The general and straightforward nature of the model enables to use the model for other lakes and other chemicals. The environmental fate of PBDEs in Lake Thun case study led to satisfactory outcomes. Only a few significant deviations from measurements were observed for which reasonable explanations are presented.

Some problems in the analytical solution for the dynamic model (level IV model) occurred and therefore the use of the numerical solution is suggested unless the problems can be solved. For the model uncertainty calculation, Monte Carlo simulation should be favored, since the model includes non-linear relationships between inputs and outputs, which limit the applicability of the analytical uncertainty propagation method.

Acknowledgments

I want to thank PD Dr. Martin Scheringer from the Safety and Environmental Technology Group at the ETH Zurich Institute for Chemical and Bioengineering for supervising this diploma thesis, helping me with various modeling issues and providing me a good introduction into environmental fate modeling. Furthermore, I want to thank all the members of the Safety and Environmental Technology group for their help in various modeling issues. A special thank deserves Fabian Soltermann, who did his diploma thesis at the same time about global modeling of PBDEs. Mainly his effort in finding and assessing property data, in particular PBDE degradation data, was of high value for me, and he was a good partner to discuss various aspects of the environmental fate of PBDEs. I also want to thank Dr. Martin Scheringer and Dr. Matthew MacLeod for the introductory lectures given in environmental fate modeling.

I thank Prof. Konrad Hungerbühler for giving me the opportunity to perform my diploma thesis in his research group.

A special thank also goes to Christian Bogdal, Dr. Martin Kohler and their research group from the Swiss Federal Laboratories for Materials Testing and Research (Empa) in Dübendorf, who measured endocrine disrupting chemicals in and around Lake Thun. The collaboration with this group was extremely valuable for this diploma thesis. I thank Christian Bogdal for showing me the sampling techniques in the field and explain me to the analytical steps in the laboratory. I further want to thank Michael Naef, diploma student at the Empa, for providing further data on chemical concentrations in whitefish and discussing issues regarding whitefish in Lake Thun with me and I thank Andreas Gerecke for giving me information about degradation of PBDEs. At this point I also thank Dr. Martin Kohler for inviting me to the final conference of the national research project (NRP 50) on endocrine disrupting chemicals in Magglingen, and I thank the Steering Committee of the NRP 50 for this successful event and for giving me the opportunity to take part in it.

Further thanks go to Thomas Bosshard, diploma student at the Institute for Atmospheric and Climate science (ETH), for collecting and providing meteorological data, Christoph Küng from the inspectorate of fisheries of the Canton of Bern for additional information on whitefish in Lake Thun, Andreas Buser and Leo Morf from Geo Partner AG for the discussion about modeling PBDEs, and Markus Zeh from the laboratory of water and soil protection of the Canton of Bern for giving me chemical and physical data for Lake Thun.

Last but not least I would like to thank all my friends who accompanied me not only during this diploma thesis but also through my whole studies and my parents for supporting me in any aspect.

Contents

Abbreviations

Only abbreviations used in the text are included in this list. A list of used variables is included in the Appendix.

BAFU	Bundesamt für Umwelt (Swiss Federal Office of the Environment)
BFR	Brominated flame retardants
DeBDE	Decabromodiphenylether, commercial product
OcBDE	Octabromodiphenylether, commercial product
OC	Organic carbon
OM	Organic matter
PCB	Poly-chlorinated biphenyl
PeBDE	Pentabromodiphenylether, commercial product
(P)BDE	(Poly-)brominated diphenyl ether
PM(10)	Particulate matter (aerosols) with diameter smaller than 10 µm
PM(2.5)	Particulate matter (aerosols) with diameter smaller than 2.5 µm
(Q)SAR	(Quantitative) structure activity relationship
SMSL	Surface mixed sediment layer

1. Introduction

Multimedia box models are used in environmental chemistry to investigate the environmental fate of chemicals. Contaminant levels and mass fluxes can be calculated on the basis of chemical properties, environmental parameters and emission mass fluxes. Models are a complement to field measurements. While measurements in the environment can provide a footprint of the contamination by some chemicals, models provide the possibility to investigate the factors and processes influencing environmental concentration levels and they further give the option to calculate outcomes under varying environmental conditions. Hence, models have the possibility to analyze the effect of changing emission patterns as a result of for example, new regulatory measures or changing consumer behavior.

Polybrominated diphenyl ethers (PBDEs) are a class of brominated flame retardants (BFRs) and used in various consumer products such as textiles, electronic devices and plastics. They are persistent, bioaccumulative, toxic and act as endocrine disruptors. (deWit, 2002; and Darnerud, 2003)

Concerns about PBDEs and other brominated flame retardants have been rising in the recent past since measured concentrations have increased exponentially during the last 30 years (Hites, 2004). Ikonomou et al. (2002) observed exponentially increasing PBDE levels in ringed seal in the Canadian arctic showing that long-range transport of these compounds is an issue and that remote areas far away from their emission sources can become affected. Levels of PBDE in Lake Thun sediment show a continuous increase over the last two decades and are still rising, which is in contrast to polychlorinated biphenyls (PCBs) and polychlorinated naphtalenes (PCNs) that reached a maximum in the 1960s (Bogdal, 2007).

PBDEs consist of two phenyl rings linked with one oxygen atom (ether). Diphenyl ether molecules contain 5 hydrogen atoms on each ring, which can be replaced by bromine. Consequently, polybrominated diphenyl ethers can hold between 1 and 10 bromine atoms. Due to their similarity to PCBs, the same nomenclature has been used for the 209 possible congeners. The structure of a PBDE molecule is shown in Figure 1-1. The substitution scheme of the PBDEs used in this study is listed in *Appendix I – Substances.*

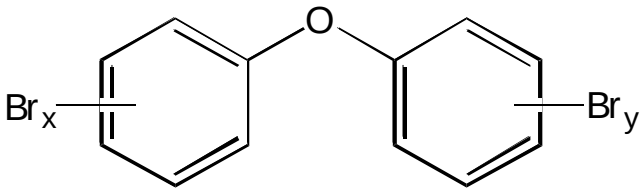

Figure 1-1: Chemical structure of PBDEs

There are three commercial products on the market; Decabromodiphenylether (DeBDE), Octabromodiphenylether (OcBDE) and Pentabromodiphenylether (PeBDE). The DeBDE product consists to 97-98% of the congener BDE-209 and some low levels of Nona-BDE. The OcBDE contains the congener 183 and some of the congener 153 and 154 as main substances. PeBDE mainly consists of congener 99

and congener 47, to a lower extent of congener 100 and some traces of congener 28 and 17 (European Chemicals Bureau, 2000, 2002, 2003 and Alaee et al., 2003).

Annual production of PBDEs was around 70'000 metric tons in 2003. About 56'000 tons thereof was Deca-BDE (Hites, 2004). The use of PeBDE and OcBDE was banned in the European Union from 2006 onward in the EU Directive on the Restriction of the use of certain Hazardous Substances in E&E Equipment (RoHS) (European Commission, 2003). Deca-BDE was exempted from the legislation based on the results of risk assessment reports (European Commission, 2005). Deca-BDE is less toxic and less bioaccumulative than other PBDEs. Though, Deca-BDE can be degraded into lower brominated congeners and thus cause harm to organisms in the environment. The extent of debromination in the environment is therefore crucial and it will thus be part of this work to include debromination in order to investigate the amount of lower brominated congeners formed from higher brominated ones in various media. Despite restrictions on the production of PBDEs, large amounts are present in materials in use and thus PBDEs will be released for years to come (Darnerud et al., 2001).

Several studies have investigated the environmental fate of brominated flame retardants (Wania and Dugani, 2003; Palm et al., 2002; Gandhi et al., 2006; Raff an Hites, 2007). These studies increase knowledge about environmental processes influencing the partitioning between various media and the lifetimes therein. Thus, they provide a part of the environmental and health risk assessment for these chemicals with high production and use worldwide.

However, knowledge about the environmental fate is still limited and there remain many uncertainties in the modeling studies performed so far. This is partly due to limited research on chemical properties and thus uncertain property data for many PBDE congeners. For some congeners data are even missing and must be extrapolated from other congeners. Models are not magic machines that can predict something from nothing. Or, to say it with the famous aphorism in computer sciences: *garbage in, garbage out*. The model output is not better than the model input. Building a model is thus just one part, the other equally important part is choosing what data are fed into the model. Many parameters needed for environmental fate models are uncertain and even their level of uncertainty is unknown. Furthermore, parameters describing the environmental processes are often not specific for the modeled environment.

In Lake Thun abnormal malformations of gonads in whitefish were detected in year 2000. A possible correlation between endocrine disrupting chemicals and the observed adverse biological effects are being investigated in an interdisciplinary research project, called FLEET (brominated flame retardants and other endocrine disrupting chemicals in the ecosystem of Lake Thun).

This diploma thesis was performed in collaboration with Christian Bogdal, PhD student at the Swiss Federal Laboratories for Materials Testing and Research (Empa) under supervision of Prof. Konrad Hungerbühler (ETHZ). His thesis is part of the FLEET project and included sampling and analytics of brominated flame retardants and other toxic and persistent chemicals at Lake Thun.

All measured data from Lake Thun were obtained directly from Christian Bodgdal via personal communication[1]. Part of the data has been published already (Bogdal 2007a, Bogdal, 2007b). All other data will be published soon or are available from Christian Bogdal upon request.

Christian Bogdal performed extensive measurements of various persistent organic pollutants in and around Lake Thun. Samples were taken from lake water, tributaries, air, fish and sediment. In the water, the dissolved and the particle bound chemicals were analyzed, in the air, gas and particle bound phase were analyzed and furthermore, air deposition of the chemicals was measured. Investigated chemicals included the polybrominated diphenyl ethers (PBDE) and hexabromocyclododencanes (HBCD) – both flame retardants, and polychlorinated biphenyls (PCB) and polychlorinated naphtalenes (PCN). Pioneering work has been performed regarding sampling and analytics of the water phase. Thus, a high quantity of high quality measured data is available, which is a good basis for building a model that can be compared with the different data series.

In this diploma thesis a model to assess the environmental fate of chemicals in a lake was developed. The principal purpose of the model was to examine the mass balance for the case study about PBDEs in Lake Thun in order to give further insight into which processes determine measured levels in various environmental media. However, the model code is completely independent of the environment and the chemicals modeled and it can thus easily be applied to other compounds and to other lakes.

A focus is put on property data and environmental data. Besides trying to find the parameters that best suit to the modeled environment, their uncertainty will also be assessed as good as possible in order to obtain sound model output uncertainties.

This diploma thesis addresses flame retardants present in the environment and therefore it focuses on the adverse side of these chemicals. Nevertheless, it should be mentioned here that these compounds are produced to increase safety, namely in preventing and limiting fires and in this way, flame retardants can safe lives and prevent damages. In many products it might even be necessary to add flame retardants in order to meet fire safety regulations. Therefore, a comprehensive and accurate assessment of environmental risks is important in order to provide decision makers a basis to weigh pros and contras of these chemical products.

It is the motivation for this diploma thesis to contribute to the knowledge about the behavior of flame retardants in the environment and thus to help assess the environmental risks associated with them.

The following objectives are addressed:

- Develop a lake model for the examination of the environmental fate of PBDEs in Lake Thun, which could serve as a basis for further assessments with other chemicals and/or other lake ecosystems.

[1] Data obtained from Christian Bogdal by personal communication has been referenced with 'Bogdal, 2007' in the text.

- Find and analyze chemical property and environmental data in order to have confidence in model input parameters.
- Calculate PBDE concentrations in various media in and around the lake with the model and compare with measurements.
- Investigate the mass balance in detail in order to discover major sinks and sources of PBDEs and to determine the major processes that influence the chemicals' distribution.
- Perform sensitivity and uncertainty analysis in order to identify the most important parameters and to show confidence intervals of model outputs.

Chapter 2 deals with the property data of PBDEs.

Chapter 3 gives a short overview of the Lake Thun environment and presents some important meteorological data.

Chapter 4 describes the model set up, including detailed information about the compartments used, the partition equilibria and transfer processes.

Chapter 5 shortly deals with the mathematical background to solve the mass balance equation systems set up in the model.

Chapter 6 covers the methods used to perform the sensitivity analysis and the uncertainty propagation.

Chapter 7 presents the results of the steady-state and the dynamic solution. Modeled values are compared with the measured values. Sensitivity of parameters is shown and residence times are calculated.

Chapter 8 summarizes the main findings of the study and gives some recommendations for further research.

2. Compound properties

The model was principally developed for the investigation of PBDEs. For further evaluation of the model, PCBs were used, and therefore for both substance classes property data are needed. PCBs are similar to PBDEs in their partitioning behavior and consequently the model is likely to have similar accuracy for both types of chemicals. For both chemical groups, measurements of prominent congeners in various media in and around Lake Thun are available, which gives a good basis for comparison of model results.

The model needs partition constants, inner energies of phase transition and degradation rates for the chemicals as well as concentrations in the atmosphere and inflowing rivers as inputs. These data are easily exchangeable in the model input files and thus additional model runs for further chemicals would be possible.

This chapter addresses partition data of PBDEs and PCBs. Degradation rates are included in chapter 4.5 and input concentrations for the Lake Thun case study are provided in chapter 4.7.

2.1. PBDE properties

2.1.1. Selection of congeners

There are 209 possible PBDE congeners from mono- up to deca-brominated diphenyl ethers. For simplicity not individual congeners, but homologues were used in the model. 9 groups were built, each group representing those PBDEs with the same number of bromine substitutions (2-10 bromines). Mono-BDE were not included due to low property data availability.

The reason for this approach is the easier handling of degradation reaction in the model. Since PBDEs can undergo debromination, lower brominated PBDEs can be formed by degradation of higher brominated congeners in the environment. There is some lack of knowledge about the path of this debromination, which results in high uncertainty regarding which congeners are formed by a debromination step. By aggregating congeners to homologue groups the uncertainty can be reduced, since only the percentage of debromination needs to be known and information about which congeners are formed can be neglected.

In each homologue group (containing the same number of bromines) a main congener was defined. Basically those congeners were included, that are found in the environment the most frequently. These include those who are contained in the commercial products and those who are mainly formed by debromination reactions. Congener 154 was not included due to low property data availability. BDE-15 was chosen as the representative for Di-BDE, BDE-28 as the representative of Tri-BDE. Both have been detected as debromination products (Sanchez-Prado et al., 2005, Keum and Li, 2005 and Law et al. 2006) and properties are frequently measured for these two congeners. Finally, the congeners chosen as representatives for the homologue groups were:

- Di-BDE-15
- Tri-BDE-28
- Tetra-BDE-47
- Penta-BDE-99
- Penta-BDE-100
- Hexa-BDE-153
- Hepta-BDE-183
- Deca-BDE-209

For Penta-BDEs, the average of property values for congener 99 and congener 100 was built. Property data for Octa-BDE and Nona-BDE were extrapolated with linear regressions (see below).

2.1.2. Literature research

Values for properties have been compiled from various literature sources. Data have been searched for partition constants (air-water, octanol-water and octanol-air) and for vapor pressure and aqueous solubility. Furthermore, inner energy (or enthalpy) data for phase transitions and solubilities have been searched.

Some values were omitted, either if they were only estimated and not measured or if the source of the value was unclear. The average value of the remaining set built the 'literature derived values'. These values were used in the least-squares adjustment method by Schenker et al. (2005) in order to obtain data for all properties that are in consistency with each other. Data gaps were filled with calculations from other properties by applying thermodynamic constraints (further explained below). The values obtained after the least-squares adjustment and after calculations from other properties are denoted as 'final values'.

An overview of the found literature values is shown in Table 2-1. All literature derived values together with references are listed in *Appendix II – PBDE property data*. Values for the enthalpy of solution in octanol and for the enthalpy of octanol-water phase exchange were not found. Except for the air-water partition constant (K_{aw}) of congener 183, measured values have been found for all partition constants and all congeners considered. Data on enthalpies are more limited, except for the enthalpy of vaporization only one source was found for each property.

Table 2-1: Number of independent literature values found for a specific congener and property listed separately for those directly measured in laboratory experiments and those extrapolated or calculated from other congeners or other properties.

	Measured								Calculated/Extrapolated							
	BDE-15	BDE-28	BDE-47	BDE-99	BDE-100	BDE-153	BDE-183	BDE-209	BDE-15	BDE-28	BDE-47	BDE-99	BDE-100	BDE-153	BDE-183	BDE-209
P	3	3	3	3	2	3	1	1	2	3	4	4	2	2	2	4
S_w	2	1	2	3	2	2	1	2	3	2	4	4	3	3	3	5
K_{aw}	4	5	5	4	4	1	0	1	3	3	3	3	3	3	3	1
K_{ow}	2	2	4	4	3	4	2	2	3	3	5	5	4	4	2	5
K_{oa}	1	1	1	1	1	1	1	1	0	1	2	3	4	5	6	7
K_{oc}	0	0	0	0	0	0	0	0	1	1	1	1	1	1	1	1
ΔU_{vap}	2	1	2	2	1	2	1	0	0	0	0	0	0	0	0	1
ΔU_w	1	0	1	1	0	1	0	0	0	0	0	0	0	0	0	0
ΔU_{aw}	0	1	1	1	1	1	0	1	0	0	0	0	0	0	0	0
ΔU_{oa}	0	1	1	1	1	1	1	0	0	0	0	0	0	0	0	0

2.1.3. Data adjustment

The least-squares adjustment procedure was applied (as described in Schenker et al., 2005) for the measured data in order to get values that are internally consistent. The adjustment procedure is based on the following thermodynamic constraints.

$$\text{Log}(S_A) - \log(S_w) - \log(K_{aw}) = w_1 \quad (2\text{-}1)$$
$$\text{Log}(S_A) - \log(S_o) - \log(K_{oa}) = w_2 \quad (2\text{-}2)$$
$$\text{Log}(S_w) - \log(S_o) - \log(K_{ow}^*) = w_3 \quad (2\text{-}3)$$

K_{aw}	Air-water partition constant	m^3/m^3
K_{oa}	Octanol-air partition constant	m^3/m^3
K_{ow}*	Dry octanol-water partition constant[2]	m^3/m^3
S_A	Solubility in air = P/(R·T) (P = vapor pressure (Pa), R = universal gas constant (8.314 J K^{-1} mol^{-1}, T =Temperature (K)	mol/m^3
S_w	Solubility in water	mol/m^3
S_o	Solubility in octanol	mol/m^3
w_1, w_2, w_3	Misclosure errors	

The misclosure errors are 0 if the data set is consistent. Additional misclosure errors can be defined by combining the equations 1-3. The adjustment procedure

[2] K_{ow} can be converted into K_{ow}* with the equation (given in Schenker et al., 2005): $\log K_{ow}^* = 1.36 \cdot \log K_{ow} - 1.6$

adjusts the property values in a certain way so that the errors become 0. (For detailed explanations consider Schenker et al., 2005).

Properties, whereof no measured data was available, were derived from other properties by the same thermodynamic constraints.

Wania and Dugani (2003) state in their review of literature values that the values for the higher brominated congeners (especially the Deca-BDE) for vapor pressure and water solubility are extremely low and the values for K_{oa} and K_{ow} are extremely high and therefore likely to lie beyond the reliability of measurement methods. They suggest using extrapolated values (by linearly extrapolation versus molar mass) rather than measured and believe that this leads to better values. Palm et al. (2002) applied a similar approach and also used extrapolated data obtained through linear regressions in their PBDE modeling study.

If there was no measured value available, values obtained from linear extrapolations were included into the literature derived data set. However, especially for some properties the linear regression is not very good. One reason might be that the number of bromines in ortho-position have a certain influence on the result. Wong et al. (2001) takes this into account by deriving individual linear regression equations for non- mono- and Diortho PBDEs for vapor pressure data. Cetin and Odabasi (2005) also mention a possible influence of the number of ortho-bromines to the Henry's law constant and refer to another study (Bamford et al. 2000) which found a significant variation of the Henrys' law constant with the number of orthochlorines in PCBs. Consequently, values obtained by linear regressions were only used if it was not possible to derive the value from other property data as described above.

For every property the relative variance was defined as needed in the least-squares adjustment. This relative variance is a relative measure, which defines how big the adjustments for the individual property should be in relation to the adjustments of the other properties. Initially all relative variances were set to 3. According to the scheme presented here, the variance was then set to 4 (+1) or to 2 (-1) under certain conditions:

The relative variance was set to 4 (+1) if:

- There was only one measured value available

or

- If the different values of the measurements of a given property differed by more than 1 logarithmic (base 10) unit.

The variance was set to 2 (-1) if:

- There were 2 measured values and more, and the values differed by less than ¼ logarithmic (base 10) unit

or

- There were 3 measured values and more, and the values differed by less than ½ logarithmic (base 10) unit

Previously ejected values were not considered for the determination of the relative variance.

The relative variance for inner energy values was defined slightly different. It was set to 3 if there was more than one measurement and to 4 if there was only one measurement.

2.1.4. Result of adjustment

An adjustment of the partitioning data was possible for all congeners except for congener 209. For congener 209 a full set of values was derived by applying the thermodynamic constraints, but no adjustment was possible, and thus the final values represent the literature derived values.

Figure 2-1 shows the misclosure errors for the literature derived partitioning data. The definition of the misclosure errors has been shown above (equations 2-1 to 2-3). The misclosure errors w_2 and w_3 were not possible to calculate since we did not have values for solubility in octanol. But by combining equations 1-3, two additional misclosure errors are defined (w_4, w_5) that can be determined with our data set.

$\log(S_A) - \log(S_w) - \log(K_{aw}) = w_1$ (2-4))
$\log(K_{aw}) + \log(K_{oa}) - \log(K_{ow}^*) = w_4$ (2-5)
$\log(S_a) - \log(S_w) + \log(K_{oa}) - \log(K_{ow}^*) = w_5$ (2-6)

Note, that for congener 183 only w_5 could be calculated and for congener 209 no misclosure error could be calculated.

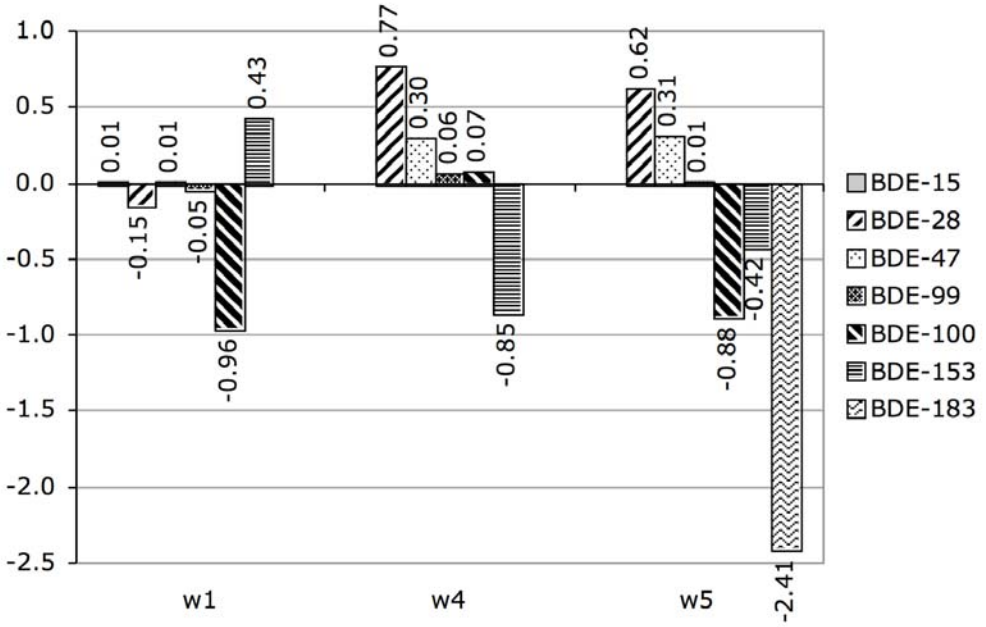

Figure 2-1: Misclosure errors (w1, w4 and w5) for the literature derived data.

The misclosure errors show some trend from the lower brominated to the higher brominated ones, which implies that there is a systematic error in the measured data.

Figure 2-2 shows the misclosure error for the inner energy data. Misclosure errors for inner energy data can be defined in the same way as for partition constants. However, due to limited data, it was only possible to calculate one misclosure error, which is defined as:

$$\Delta U_a - \Delta U_w - \Delta U_{aw} = w_I \quad (2\text{-}7)$$

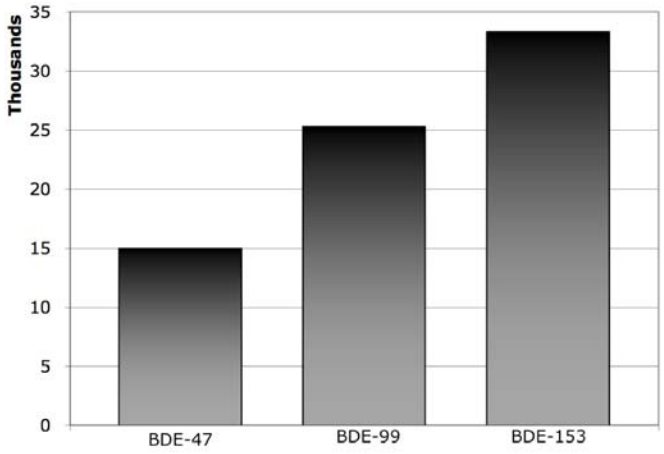

Figure 2-2: Misclosure error (w_I) for the literature derived inner energy data (J mol^{-1})

Only for three congeners sufficient data was available to calculate a misclosure error and consequently it was only possible for those three congeners to adjust the values. With only three data values for the misclosure error it is not possible to derive a clear trend as seen in the misclosure errors for partitioning data.

2.1.5. Final adjusted values

Table 2-2 summarizes all final values, which will be used in the model. The bold values were adjusted from literature values by the least-squares adjustment method. The non-bold ones are values that could not be adjusted because not enough data was available and are therefore the same as the literature derived values. Values that were calculated by the thermodynamic constraints are also shown in non-bold style.

As seen in Table 2-2, no values for ΔU_{OW} have been found in literature, and other ΔU are also missing for some congeners. Consequently, not all inner energy values could be defined either from literature values or by the thermodynamic constraints. Since inner energies are not highly variable between congeners, the use of average values seemed to be appropriate where no other values were available. The least variability between congeners has been observed with ΔU_{AW} and ΔU_{OA}. For these two the average was built where necessary (indicated with asterisk(*) in table) and the other properties (ΔU_{OW}, ΔU_O, ΔU_W) were calculated based on these average values when necessary (indicate with a cross(+).

Table 2-2: Final values. Bold values are values that could be adjusted, non-bold ones are values that have been calculated from other properties and values with an asterisk (*) represent default values (Only occurs in inner energy data. No literature data was available and therefore the value was set to the average of the other values.). A plus (+) means that the value was calculated based on these default (*) values.

	P (Pa)	S_w (mol/m³)	S_o (mol/m³)	Log K_{aw}	Log K_{ow}	Log K_{oa}
BDE-15	**1.37E-02**	**1.07E-03**	6.83E+02	**-2.29**	**5.44**	8.09
BDE-28	**2.11E-03**	**4.27E-04**	1.22E+03	**-2.70**	**5.92**	**9.16**
BDE-47	**2.40E-04**	**1.26E-04**	2.38E+03	**-3.12**	**6.53**	**10.39**
BDE-99	**3.92E-05**	**3.70E-05**	3.08E+03	**-3.37**	**7.00**	**11.29**
BDE-100	**6.01E-05**	**1.45E-04**	4.42E+03	**-3.78**	**6.68**	**11.26**
BDE-153	**4.33E-06**	**8.29E-06**	2.12E+03	**-3.68**	**7.36**	**12.08**
BDE-183	**1.87E-06**	**1.45E-05**	2.75E+03	-4.28	**7.26**	**12.56**
BDE-209	9.03E-08	**2.33E-06**	2.12E+06	**-4.81**	**9.97**	16.77
	ΔU_A	**ΔU_W**	**ΔU_O**	**ΔU_{AW}**	**ΔU_{OW}**	**ΔU_{OA}**
BDE-15	70321	20900	-21946+	49421	-42846+	-92267*
BDE-28	**77221**	**15501**	4421	**61720**	-11080	**-72800**
BDE-47	**86730**	**20354**	-10270	**66376**	-30624	**-97000**
BDE-99	**94768**	**12304**	3668	**82464**	-8636	**-91100**
BDE-100	99521	42873	-5479	56648	-48351	-105000
BDE-153	**97242**	**20506**	-958	**76736**	-21464	**-98200**
BDE-183	115521	49944+	26021	65577*	-23923+	-89500
BDE-209	145022	79345	52755+	65677	-26590+	-92267*

Since the availability of enthalpy (or inner energy) data is limited, Wania and Dugani (2003) did not use measured enthalpy values in their modeling study. They therefore used default values of -80 kJ mol^{-1} for octanol-air phase transfer, 60 kJ mol^{-1} for air-water phase transfer and -20 kJ mol^{-1} for octanol water phase transfer. The values are close to the measured values used here.

The values for congener 183 do not fit very well into the data set. The water solubility is higher than for congener 153 and the K_{ow} is lower than for congener 153. In both cases the value does not fit into the general trend. As mentioned above, the Koa for congener 183 is possibly too low. The value for S_w is possibly too high, as seen in Figure 2, which is caused by the high value measured for 183 by Tittlemier et al. (2002). These facts influence the correction of the K_{ow}. As a consequence, a higher uncertainty for properties of congener 183 should be assumed in the multimedia models.

2.1.6. Values for homologues

As mentioned above, homologue groups of PBDE congeners were built for the modeling case study. In Table 2-3 the final values for the homologues are summarized. Included are the values for Octa- and Nona-BDEs, which were obtained by linear extrapolation from the other values. The linear regression for the solubility in octanol is not so good. However, the solubility in octanol is approximately constant over all congeners and therefore the values obtained are still usable. The values for S_o are not that important anyway, because they are not

directly used in the model. All other regressions are good as shown with the R^2 measure.

Table 2-3: Final values for partition constants of homologues including values for the Octa- and Nona- BDEs obtained by linear regression.

BDE	log P	log S_w	log S_o	log K_{aw}	log K_{ow}	log K_{oa}
Di-	-1.86	-2.97	2.83	-2.29	5.44	8.09
Tri-	-2.68	-3.37	3.09	-2.70	5.92	9.16
Tetra-	-3.62	-3.90	3.38	-3.12	6.53	10.29
Penta-	-4.31	-4.14	3.57	-3.57	6.84	11.28
Hexa-	-5.36	-5.08	3.33	-3.68	7.36	12.08
Hepta-	-5.73	-4.84	3.44	-4.28	7.26	12.56
Deca-	-7.04	-5.63	6.33	-4.81	9.97	16.77
Extrapolated values						
Octa-	-6.17	-5.20	4.73	-4.36	8.48	14.29
Nona-	-6.83	-5.54	5.11	-4.68	9.01	15.33
Linear regression parameters						
R^2	0.97	0.92	0.74	0.97	0.94	0.99
Slope	-0.66	-0.34	0.38	-0.32	0.53	1.04
Intercept	-0.88	-2.47	1.72	-1.80	4.26	5.95

Table 2-4 shows the values for inner energies of homologues. The correlations for the inner energies are all bad except for the inner energy of vaporization. Therefore the average values as defined above were used for Octa- and Nona-BDEs.

Table 2-4: Final values for inner energies of homologue groups. An asterisk (*) represent default values (Only occurs in inner energy data. No literature data was available and therefore the value was set to the average of the other values.). A plus (+) means that the value was calculated based on these default (*) values.

BDE	ΔU_A	ΔU_W	ΔU_O	ΔU_{AW}	ΔU_{OW}	ΔU_{OA}
Di-	70321	20900	-21946+	49421	-42846+	-92267*
Tri-	77221	15501	4421	61720	-11080	-72800
Tetra-	86730	20354	-10270	66376	-30624	-97000
Penta-	97144	27588	-905	69556	-28494	-98050
Hexa-	97242	20506	-958	76736	-21464	-98200
Hepta-	115521	49944+	26021	65577*	-23923+	-89500
Deca-	145022	79345	52755+	65677	-26590+	-92267*
Extrapolated values						
Octa-	123'729	58151+	31462+	65577*	-26689+	-92267*
Nona-	133'039	67462+	40773+	65577*	-26689+	-92267*
Linear Regression parameters						
R^2	0.98					
Slope	9'311					
Intercept	49'244					

2.2. PCB properties

Only those congeners measured in the samples taken at Lake Thun were considered, which include PCB-28, PCB-52, PCB-101, PCB-138, PCB-153 and PCB-180 (structure and substitution pattern is included in *Appendix I – Substances*). Values for partition constants and inner energies were taken from Schenker et al. (2005), who applied their least-squares-adjustment procedure to a data compilation by Li et al. (2003).

Table 2-5: PCB properties, final adjusted values from Schenker et al. (2003).

PCB	log K_{aw}	log K_{ow}	log K_{oa}	ΔU_{aw}	ΔU_{ow}	ΔU_{oa}	ΔU_a	ΔU_w
Tri-CB-28	-1.93	5.66	7.86	51822	-26556	-78378	77100	25278
Tetra-CB-52	-1.96	5.95	8.22	53800	-27500	-81300	77700	23900
Penta-CB-101	-2.08	6.38	8.83	65182	-19265	-84447	84118	18935
Hexa-CB-138	-1.97	7.19	9.67	64707	-22161	-86868	93900	29193
Hexa-CB-153	-2.13	6.86	9.45	68227	-26561	-94788	91800	23573
Hepta-CB-180	-2.51	7.15	10.17	69033	-26148	-95181	94100	25067

3. The Lake Thun environment

3.1. Lake Thun properties

Lake Thun is a pre-alpine lake in the Berner Oberland region of Switzerland. The lake has a total surface area of 47.69 km^2, a mean depth of 136m and a volume of 6.42 km^3 (Laboratory of Soil and Water Protection Bern, 2007). The main tributary is the Aare, which is an outflow of Lake Brienz. The second largest tributary is the Kander including the water from Simme, which is discharged into Kander shortly before the Kander enters Lake Thun. 90% of the water input is allotted to those two rivers. The Kander carries about 85% of the particle load into the lake. The Aare carries less than 1%. 15% are brought by some additional small streams. (Sturm and Matter, 1972) The nutrient load and biomass production is low compared to other Swiss lakes. Oxygen is available in the whole water column (Laboratory of Soil and Water Protection Bern, 2007). The upper sediment is aerobic (Kohler, M; personal communication). The Lake Thun basin is characterized by steep slopes on the shore and a flat bottom with low inclination towards the south-east end.

3.2. Meteorological and hydrological data

Meteorological data are available from meteorological stations located around the lake. Highly resolved data is available from the MeteoSwiss automatic weather station in Interlaken (Data from MeteoSwiss, 2007), located at the main inflow in the south-east of the lake. Measured data include temperature, precipitation, wind and solar radiation. Average rainfall data are also available from MeteoSwiss for stations in Hondrich and Thun (Data from MeteoSwiss, 2007). A privately operated weather station in Thun also provides data from the 10th of June 2006 onwards on an hourly basis. (Data from weather station Thun, 2007).

Hydrological data from gauging stations are available for the tributaries Aare in Interlaken, Kander in Hondrich and Simme in Latterbach (Data from BAFU, hydrology division, 2007). A pollutants measuring station including measurement of aerosols (PM10) is located in Thun (Data from Canton Bern, pollutant measuring, 2007). The location of the meteorological and hydrological measurement stations are shown in Figure 3-1 .

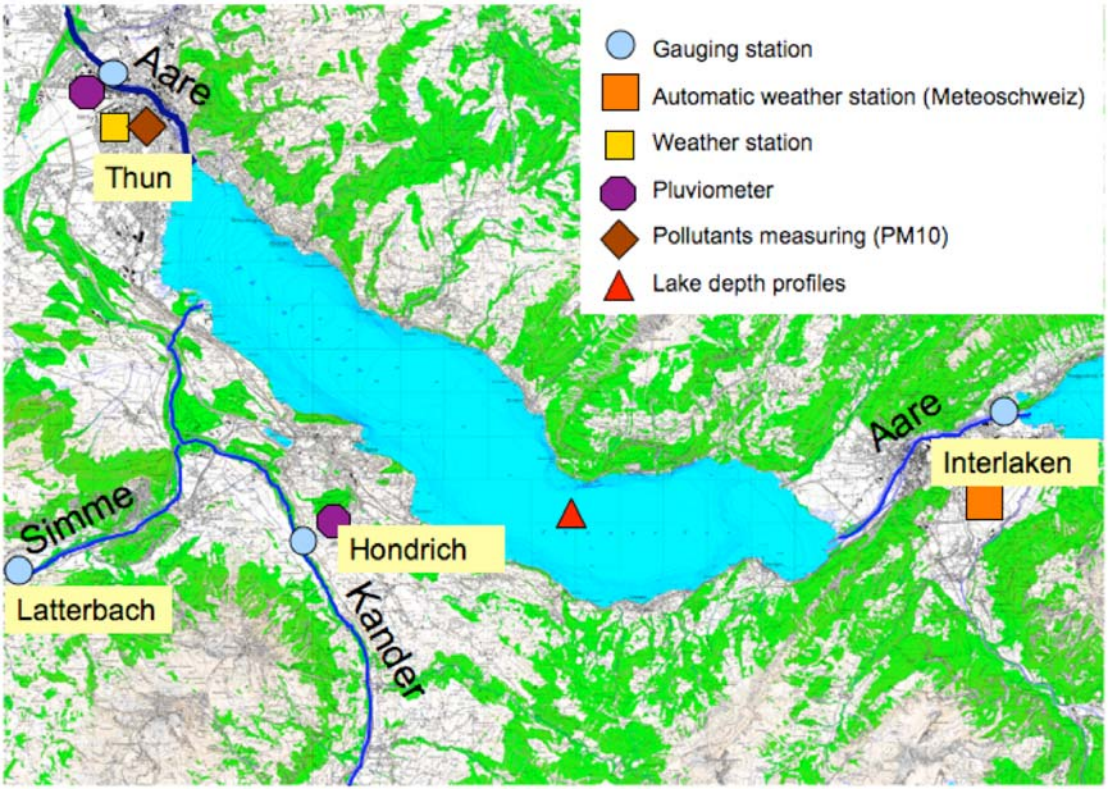

Figure 3-1: Meteorological, hydrological and pollutants measuring stations around Lake Thun.

The standard model run is performed for the period from January 2006 until July 2007, because all measurements took place within this period. Meteorological and hydrological data were compiled for this period. The model was run with a monthly time resolution. For parameters listed in Table 3-1 values for each month were assessed and used in the model. All other parameters are constant over time.

Table 3-1: Sources for variable meteorological and hydrological parameters.

Parameter	Location	Source
Air temperature	Weather station Interlaken	MeteoSwiss
Lake surface temperature	Lake Thun, deepest point.	Canton Bern, Laboratory of Soil and Water Protection
OH-radical concentration	Zonal average (for latitude of Lake Thun)	Spivakovsky et al. (2000)
Solar radiation	Weather station Interlaken	MeteoSwiss
Wind speed	Weather station Interlaken	MeteoSwiss
Precipitation	Weather station Interlaken	MeteoSwiss
Runoff from lake	Gauging station Thun	BAFU, Hydrology division

A list of the input values used for these parameters (time period January 2006 until August 2007) is included in *Appendix IV – Variable parameters*.

3.2.1. Temperature

Temperature is important since it has an influence on many parameters, especially on partitioning and on biodegradation rates.

Figure 3-2 shows monthly average data for precipitation and air temperature at the MeteoSwiss weather station Interlaken and the lake surface temperatures measured at the deepest point of Lake Thun.

As seen in Figure 3-2, temperatures in air and water are approximately identical from March until October 2006. During the winter months the lake temperatures tend to be about 5° higher than the atmospheric temperature. The mean temperature of the air during the year 2006 was 8.5°. The mean temperature of the surface water was 11.2°.

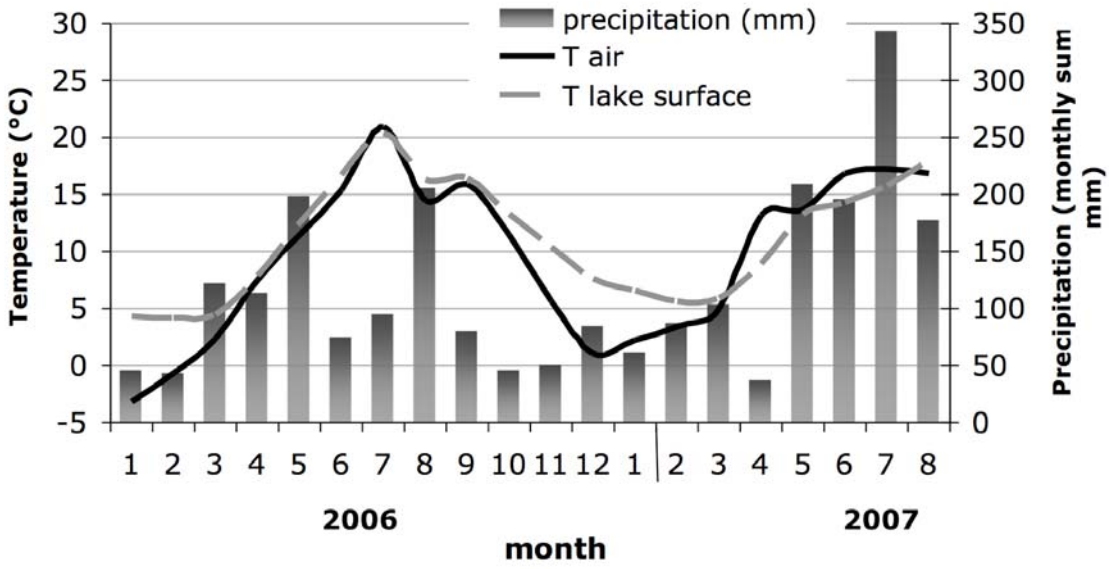

Figure 3-2: Monthly averaged values for precipitation and air temperature for the period January 2006 until August 2007 at weather station Interlaken. Lake surface temperatures at the deepest point in Lake Thun.

Unusual for the year 2006 were the months June and July with low precipitation and the month August with exceptional high precipitation and low temperatures. The summer 2007 was characterized by even higher precipitation in summer, especially in July, which was caused by heavy thunderstorms.

3.2.2. Precipitation

The precipitation values obtained from the station in Interlaken were compared with other measurements around the lake in order to assess spatial variability. Precipitation measurements near the lake are also carried out in Thun and Hondrich by MeteoSwiss. Averaged data for the period from 1961-1990 are shown in Figure 3-3. It can be seen that Interlaken is close to the average and the difference in the data measured at the stations is up to 30%. Especially the values for the station Thun are much lower than the values in Interlaken during the winter months. This variability will be taken into account in the uncertainty analysis

(chapter 6). When comparing with Figure 3-2, it can be seen that the precipitation for the months June-August 2006 deviates from the long-term average and that August 2007 highly exceeds the long-term average for that month.

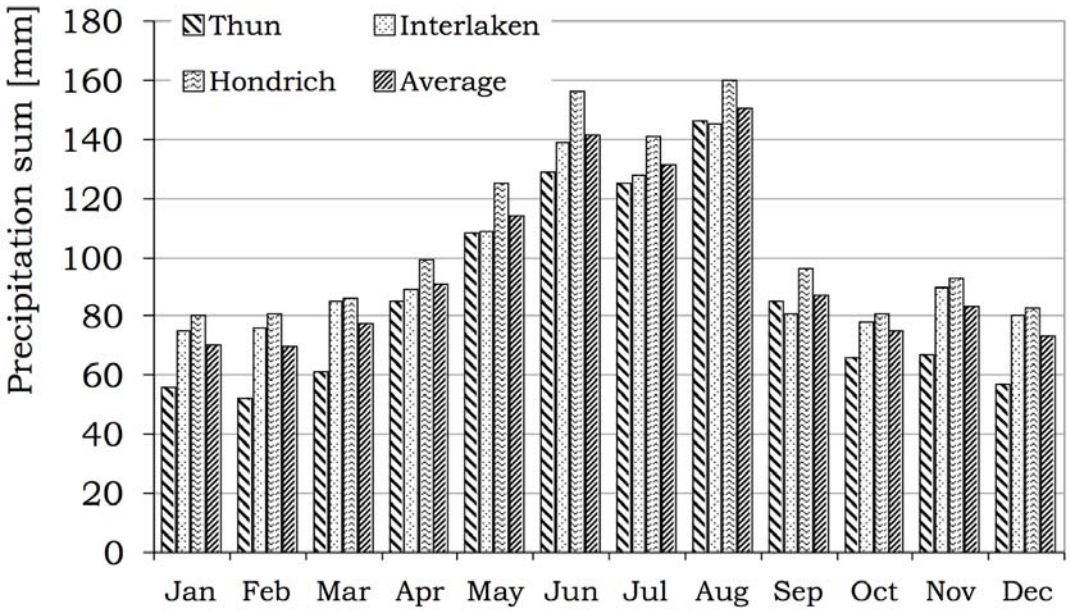

Figure 3-3: Precipitation data for stations around Lake Thun. Annual average values for the time period 1961-1990.

3.2.3. Solar radiation

Solar radiation influences the degradation rates for direct photolysis. OH-radical induced photodegradation is also dependent on the radiation intensity, since more OH-radicals are built with higher radiation intensity. However, OH-radical formation is not modeled, since it depends on many factors and available values from literature were considered to be sufficient (see also chapter 4.5 on degradation).

Solar radiation is measured at the weather station in Interlaken. Figure 3-4 shows the monthly average values for solar radiation in Interlaken. The low value for August 2006 compared to other months also reflects the weather conditions already observed in the precipitation profile. The high value for April 2007 corresponds with low precipitation for that month, while the high precipitation in summer 2007 is reflected in low solar radiation data for these months.

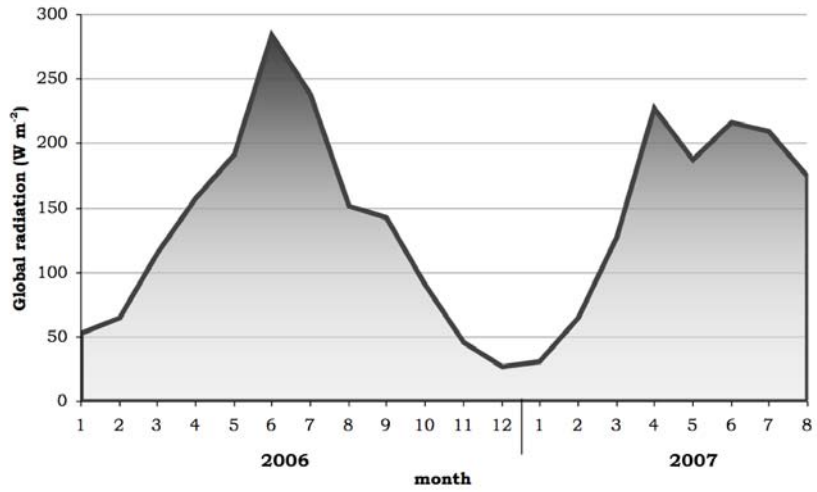

Figure 3-4: Solar radiation in W m^{-2} at the weather station Interlaken. Shown are monthly averaged values.

3.2.4. Wind

Wind determines the amount of air entering the Lake Thun region per time and thus wind influences the amount of chemicals carried to the lake environment as well as leaving the atmospheric compartment. This is the only effect, where the influence of wind has been considered in the model. Other effects are mentioned here qualitatively but not included in the model. A trend for higher wind speeds in summer compared to winter month is visible in Figure 3-5. However, the variability in wind is generally low over the year and the processes influenced by wind (mainly diffusion) have low importance and therefore it is justified to use average wind speeds (except for input and output into/from the atmospheric compartment).

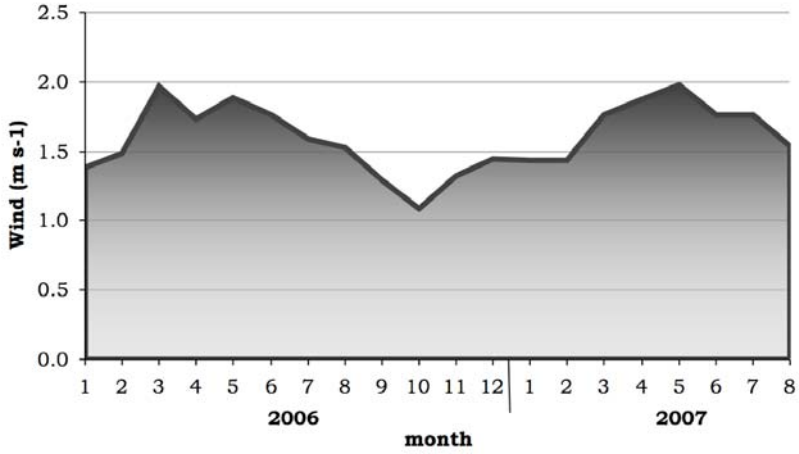

Figure 3-5: Monthly averaged scalar wind speed in Interlaken

Wind influences air-water diffusion by changing the air and water-side diffusion depths. Higher wind speed reduces the diffusion depth, which increases diffusive transport.

Wind has an influence on the aerosol distribution over the lake. Wind from the west and north-west will bring higher aerosol and probably higher PBDE loads from

the higher populated areas around Bern and Thun, while the wind from east and south east is coming from mountainous and less populated areas and carries less aerosols and less PBDEs. An assessment of wind directions showed that for about the equal number of days the wind comes from west and north-west as from south and south-west.

Furthermore, wind affects the mixing of the water body. Western winds create a flow of the water in counter direction of the water flow and thus trigger upwelling close to the lake outflow, while eastern winds are in the same direction as the water flow and upwelling is lower. This effect is reflected in the temperature of the Aare downstream of Lake Thun. During western winds, the outflow is fed with colder water from the bottom of the Lake. The influence of the wind is shown schematically in Figure 3-6.

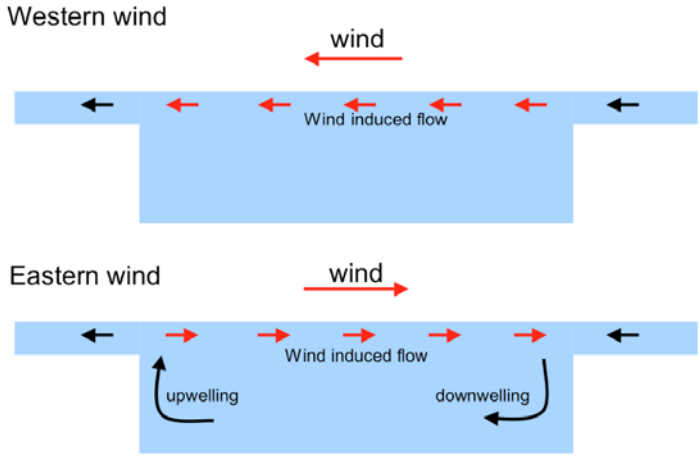

Figure 3-6: Influence of wind direction to water flows in Lake Thun.

4. Model development

The model consists of three bulk compartments; atmosphere, lake water and lake sediment. Each of the bulk compartments is composed of various phases. The atmospheric compartment includes the free gas phase and aerosols. The lake water compartment includes free water, suspended particles and fish and the sediment includes solid sediment and pore water. All compartments are treated as well-mixed boxes.

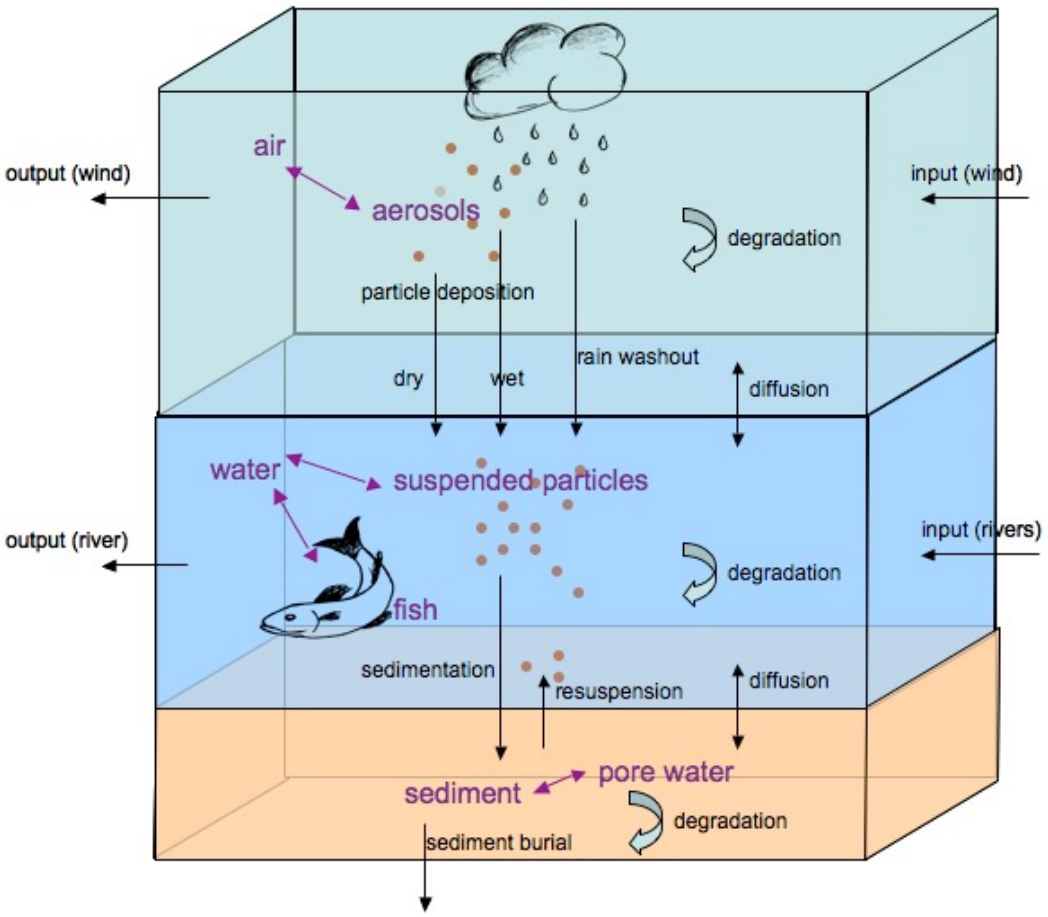

Figure 4-1: Lake model: compartments and processes

All compartments and modeled processes are shown in Figure 4-1. Mass balance equations for each compartment are set up, which include transport processes between the compartments, inputs into and outputs from the system as well as degradation processes. Kinetic processes between the phases of the same compartment (e.g. air and aerosol) are neglected and equilibrium is assumed, which is based on the assumption that these kinetic processes are much faster than the other processes in the model.

The model was developed in two different solution modes. Modus 1 is the three box model just described. Compounds enter into the system via wind into the atmospheric compartment and via rivers into the lake water compartment.

For modus 2, the model is reduced to a two box model, including lake water compartment and sediment compartment as well-mixed boxes. Concentrations in

the atmosphere are used as an input parameter, and transport processes from atmospheric to the lake water compartment are modeled based on these concentrations. However, a mass balance for the atmospheric compartment is still set up separately, but solved for the input mass flow (or concentration in the input) instead of the concentration in the atmosphere. Potential feedback processes from water to atmosphere (diffusion) are considered in this mass balance for the atmosphere. The mass balance for the atmospheric compartment is used to calculate the hypothetic concentration needed in the air input (wind) to reach the given concentration.

4.1. Compartment dimensions and properties

For the compartment sizes, the surface area of the lake together with individual compartment heights (respectively depths) were chosen. The lake surface area is 47'670'000 m^2. The compartments are modeled as cuboids. Since Lake Thun has a trough form with steep slopes at the shore and a quite flat part in the middle, this approximation should be justified. The sediment-water interface area is assumed to be the same as the water air interface. This assumption neglects the processes concerning the lateral surfaces of the hypothetical water body cuboid. Especially for deposition of particles in the water, this approximation is good, since the deposition flux is rectangular to the horizontal surface area.

For the water compartment the average depth of the lake, 136m, is used. The atmosphere compartment height is determined by the height that an air parcel can reach during its flow over the Lake Thun with a maximum vertical uplift. This mixing height was determined with a formula used by another multi-media chemical fate model (CalTOX), where the height is calculated with $0.22 \cdot ((\text{Area})^{1/2})^{0.8}$ if the area is smaller than $6 \cdot 10^8$ m^2 (McKone et al., 1997). Inserting the surface area of Lake Thun (47.6km^2) leads to a height of 260m.

Only the part of the sediment which is in interaction with the water compartment was included. This part is about 4cm high (see chapter 4.1.3). The shape of the lake surface was approximated with a rectangle of 3'000 m width and 15'890 m length.

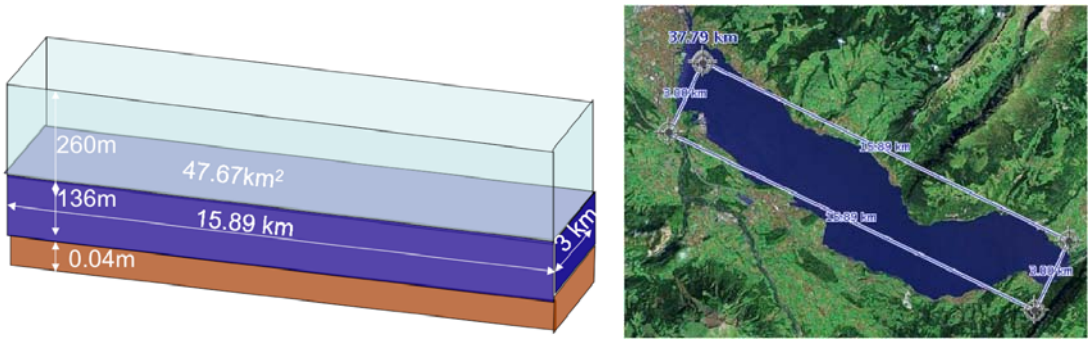

Figure 4-2: Compartment dimensions

4.1.1. Atmosphere

The atmospheric compartment consists of air and aerosols. The aerosol composition and size distribution are highly variable and depend on the sources of

the aerosols and on weather conditions. Differences in aerosol composition are shown in Figure 4-3. The data presented is based on a data collection of aerosol measurements at various sites in Europe (Putaud et al, 2004). Dry and wet particle deposition, the processes that transport aerosols into the lake, are also aerosol size dependent. Due to these differences it makes sense to divide the aerosols up into size classes. Two classes were chosen, fine aerosols with a diameter up to 2.5 µm and coarse aerosols with a diameter between 2.5 µm and 10 µm. These two fractions, also called PM2.5 and PM10-PM2.5 are usually measured in the environment. Particles above 10 µm are not taken into account since the total volume of these particles is very low in the atmosphere compared to the smaller particles.

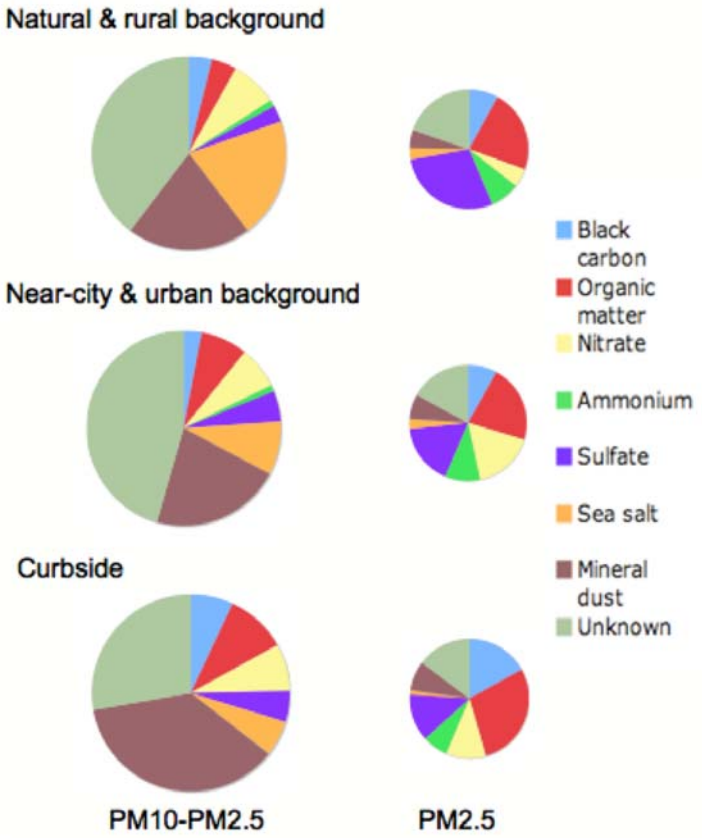

Figure 4-3: Typical aerosol composition at various sites in Europe (Putaud et al., 2004)

Aerosol concentrations can be estimated from measurements of particulate matter and from models. A measurement station for PM 10 is installed in Thun (Data from Canton Bern, pollutant measuring, 2007). The concentrations are influenced by activities in the city, namely traffic and house heatings, and therefore aerosol concentrations would be higher than the mean concentrations over the lake. The Swiss Federal Office of Environment (BAFU) carried out a study where aerosol immissions are modeled based on emission estimations and wind patterns (BAFU, 2003). Figure 4-4 shows the results of the model study for the Lake Thun area.

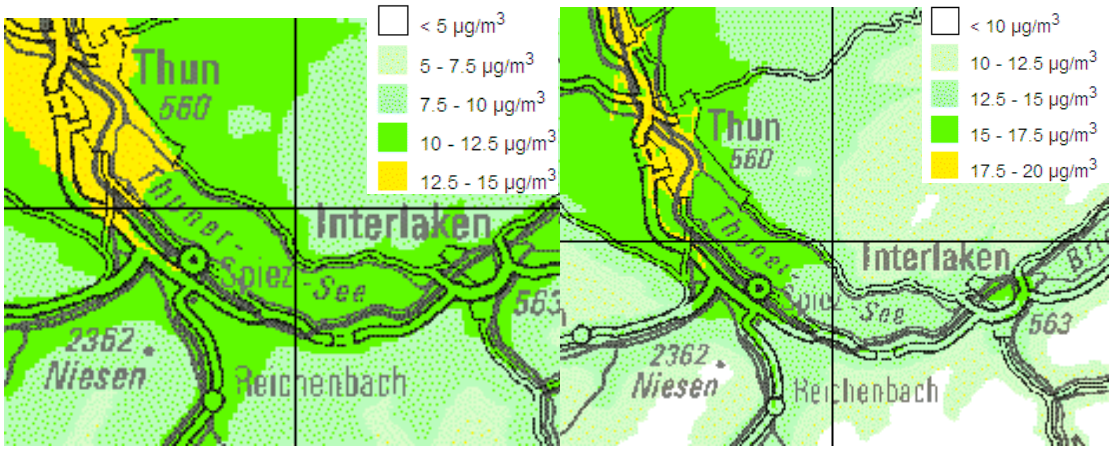

Figure 4-4: Aerosol immission modeled for the Lake Thun area (BAFU, 2003), PM2.5 in the left, PM 10 in the right figure.

Aerosol concentrations are higher in the north-western part of the Lake due to higher population density and impacts from roads.

Based on the maps shown in Figure 4-4, a Lake Thun average aerosol concentration was estimated for both aerosol size fractions. The average was calculated by weighting the zones with different aerosol concentrations according to their contribution to the whole lake area.

Table 4-1: Aerosol concentrations above Lake Thun

	PM 2.5 (< 2.5 µm)		PM 10 (< 10 µm)	
Size class (mean) µg/m³	**Percentage of lake surface**	**Contribution to average concentration µg/m³**	**Percentage of lake surface**	**Contribution to average concentration µg/m³**
10-12.5 (11.25)	88%	9.90		
12.5-15 (13.75)	12%	1.65	48%	6.60
15-17.5 (16.25)	-	-	50%	8.13
17.5-20 (18.75)	-	-	2%	0.38
Total		**11.6**		15.1
				-11.6
		Coarse fraction (PM 10 – PM2.5)		**3.6**

The values obtained with this calculation were compared with aerosol measurements performed at various sites in Switzerland (Hueglin et al., 2005) and measured with deposition samplers in Faulensee (Bogdal, 2007). A list of measured data is presented in Table 3.

Table 4-2: Aerosol concentration measurements. (µg/m³)

Fraction measured	Site	Value	Ref.
PM 10	Curbside, Bern	40.2	Hueglin, 2005
PM 2.5	Curbside, Bern	24.6	Hueglin, 2005
PM 10	Rural, Payerne	13.7	Hueglin, 2005
PM 2.5	Rural, Chaumont, altitude 1000 m (no value available for Payerne)	7.7	Hueglin, 2005.
PM total	Faulensee, Lake Thun July 2006	24.2 (min: 12.3, max: 66.7)	Bogdal, 2007
PM total	Faulensee, Lake Thun March 2007	24.9 (min: 10.4, max: 50.5)	Bogdal, 2007

The values obtained by the approximation above (Table 4-1) are close to the ones measured at the rural site in Payerne and Chaumont. Towns, roads and railway around Lake Thun might lead to slightly higher aerosol concentrations than expected for a rural site. A difference to the measured concentrations in Payerne and Chaumont should be expected. The measurements in Faulensee, where air and deposition of the chemicals were measured are significantly higher. They are closer to the one measured at a curbside location in the city of Bern. This reflects the fact that the measurement station in Faulensee is close to a road. The site might therefore not be representative for Lake Thun. This should be kept in mind when analyzing chemical concentrations in air and aerosol and deposition mass flux. However, the concentrations of chemicals in aerosols must not necessarily differ from the average over the lake, but the total mass is likely to differ when using aerosol concentrations from Faulensee instead of aerosol concentrations representative for Lake Thun.

Aerosol concentrations vary over time, influenced by different weather conditions and emission patterns. Rain events reduce aerosols, while typical inversions during wintertime increase aerosol concentrations due to capping. Figure 4-5 shows the monthly averaged aerosol (PM 10) concentrations at the station Thun (Data from Canton Bern, pollutant measuring, 2007) for the period January 2006 until July 2007. There is a trend to higher concentrations in winter compared to summer months visible. This might be a result of typical winter weather conditions as mentioned above and additional emissions caused by house heatings. The average over one year (2006) is 23.6 µg/m³. The station is located in the middle of Thun at an urban site and therefore higher than expected for Lake Thun. This value is slightly higher than the value indicated in the map above (Figure 4-4). One reason is the unusual high value for January 2006. The range of the values for the other months matches the values of the map quite well.

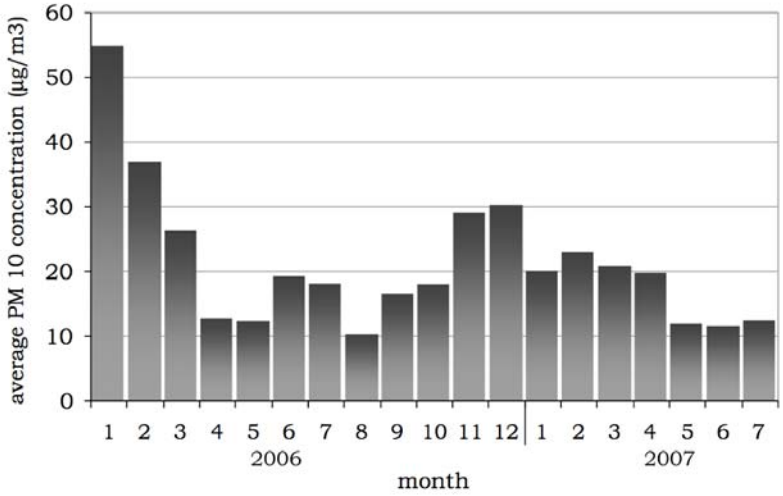

Figure 4-5: Monthly averaged PM 10 concentrations at the measurement station Thun.

Seasonal variability in aerosol concentrations is not included in the model. The values from Table 4-1 are used as annually averaged input values in the model.

The vertical distribution of aerosols is characterized by an exponential decrease. This can be described by (Seinfeld and Pandis, 1998)

$$C_{PM,z} = C_{PM,0} \cdot \exp(-\frac{z}{h_s}) \quad (4\text{-}1)$$

$C_{PM.z}$	Concentration of particulate matter (aerosols) at height z	µg m^{-3}
$C_{PM.0}$	Concentration of particulate matter (aerosols) at the surface	µg m^{-3}
z	Height	m
h_s	Scaling height. 730 m for remote continental areas (Seinfeld and Pandis, 1998)	m

For dry deposition, the aerosol concentration at ground should be taken, since the deposition flux into the lake is influenced only by the aerosol concentration at ground level. For wet deposition, an average aerosol concentration up to the height of clouds could be used, which represents the travel distance of raindrops that are incorporating particulate matter. The cloud base is typically between 200 and 400m. According to equation (5-12) a factor of 0.77 – 0.87 could be used to correct PM concentrations. For simplicity, no correction was included in the model because for the Lake Thun case study, the modeled height is only 260m and uncertainties in wet deposition parameterization would outweigh this improvement.

4.1.2. Lake water

The lake compartment consists of water, suspended particles and fish. The amount of suspended particles was estimated from the measurements of total non-

dissolved substances at various depths in the Lake performed twice a year in February and October by the Water and Soil Protection Laboratory of the Canton of Bern. Data were available from October 2003 until February 2007. Since measurement points were not evenly distributed over the lake depth, weighted average with the vertical height were calculated. This approach neglects, that the cross-section in the lake decreases with increasing lake depth. However, since Lake Thun has a quite flat bottom and since the particle concentrations did not vary much with depth, this approach should still lead to a reasonable value.

	Particle concentration in Lake Thun[3]. Average (Standard deviation)	
February	0.34 (0.26)	mg l^{-1}
October	1.04 (1.29)	mg l^{-1}
Average	**0.65 (0.89)**	**mg l^{-1}**

The amount of fish in the lake is difficult to estimate. The average of the caught amount over the last 5 years was 50 t/y (Inspectorate of fisheries, Canton Bern, 2007; Küng, C., personal communication). Most of the fish are whitefish (Thunerseefelchen). It is assumed that about 1/3 of the inventory is caught, which gives 150t of fish in the lake (Küng, C., personal communication).

This value can be explained by taking growth and mortality of fish into consideration. It was assumed that about 2/3 of the 50t caught fish are 3 year old fish, which is the average age of caught fish. (Küng, C. personal communication). It is also assumed that 2/3 of the 3 year old fish are caught. This means, that about 50t 3 year old fish exist, and 17t thereof remain in the lake.

It was assumed that a 3 years old fish weighs 300g, a two years old fish about 225g and a 1 year old fish about 75g (based on Kirchhofer, 1990[4]). This means a 300% growth between 1 and 2 years old and a 33% growth between 2 and 3 years.

The amount of 2 years old fish needed to produce 50t of 3 years old fish can be calculated by taking into account a mortality rate of 0.5 (Küng, C., personal communication) and a growth of about 33%, which leads to 75t (37.5 t will survive and an increase of 33%=12.5t will give 50t).

With the same approach, 50t of 1 year old fish are obtained (25t will survive and 300% growth will lead to 75t 2 year old fish.)

A total of 142t (50t + 75t + 17t) falls on 1-3 year old fish. Taking into account that some older fish are present, this value can be rounded up to 150t. Figure 4-6 illustrates this approach.

[3] Values below detection limit (<0.2 mg/l) were treated as half detection limit (0.1 mg/l)

[4] The fish weight for a specific age was calculated with the formulas given by Kirchhofer (1990), which are determined for Lake Brienz whitefish:

$$l(t) = L_{\infty} \cdot (1 - e^{K \cdot (t - t0)}),$$

where l(t) is the length of the fish at time t (y), L_{∞} is the maximal length, K is a population specific growth coefficient and t0 is the hypothetic point where length is zero. The mass can be calculated with the following empirical relationship found by Kirchhofer (1990):

$$M = 0.000005 \cdot l^{3.111}$$

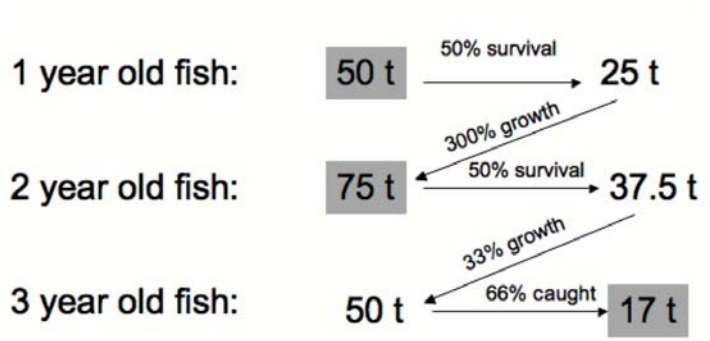

Figure 4-6: Fish growth scheme. The shaded values are the fish present in the lake.

Assuming a density of 1000 kg/m^3 for a fish, a total volume of 150 m^3 fish are present in the lake, which represents a volume fraction in the lake of about $2.3 \cdot 10^{-8}$. This is about two orders of magnitude lower than the generic value used by Mackay (1992) of $1 \cdot 10^{-6}$. However, since Lake Thun is not a highly productive lake, it is reasonable that the amount of fish is lower than the value used by Mackay (1992).

4.1.3. Sediment

Only the uppermost part of the sediment is included into the model, which is called the surface mixed sediment layer (SMSL). It is assumed that this part is in interaction with the lake water compartment by resuspension of particles and via diffusion between pore water and open water. A height of 4 cm has been taken from the description of the SMSL in Schwarzenbach et al. (2003, P.1074).

The sediment compartment consists of solid sediment and pore water. Solid sediment is composed of the settled particles. However, the organic content of the sediment is lower than in particles, since organic matter is decomposed during particle settling and in the sediment.

The pore water is connected to the open water and diffusive exchange is possible between the two water bodies. The porosity of sediment (= the fraction of pore water in sediment) was set to 0.8. The value in Schwarzenbach et al. (2003; P.1074) is 0.85, Mackay (1992) uses 0.8 and 0.67 is used in Mackay (2001, Ch.4,P.8.)

4.2. Partitioning

Equilibrium is assumed between the different phases in each compartment. Partition coefficients are needed to determine the concentrations in each media. Partitioning between the various phases are based on three different partition constants, namely the air-water partition constant (K_{aw}), the octanol-water partition constant (K_{ow}) and the octanol-air partition constant (K_{oa}). Values for these constants have been measured in laboratory experiments. A literature review of available partitioning data was performed and best available values were determined by choosing those values with high reliability and by adjusting them with a procedure based on thermodynamic constraints (see chapter 2).

4.2.1. Partition constants and coefficients

Partitioning between two well-defined phases (air, water, octanol) is described by a partition constant. For phases such as aerosols, fish and sediment the term partition coefficient is used. There are various empirical relationships between partition coefficients and partition constants, usually including some parameters describing the phases which are represented with the partitioning coefficient.

Table 4-3 summarizes all partition constants and coefficients. The approach to calculate the different partition coefficient will be presented in the following paragraphs.

Table 4-3: Partition constants and coefficients for PBDEs used in the model (at 25°)

BDE	log K_{aw}	log K_{ow}	log K_{oa}	log K_p	log K_p	log K_{sw}	log K_{pw}	Log K_{wf}
	m^3/m^3	m^3/m^3	m^3/m^3	$m^3/\mu g$	$m^3/\mu g$	m^3/m^3	m^3/kg	m^3/m^3
Di-	-2.29	5.44	8.09	-5.41	-4.93	3.64	0.26	4.22
Tri-	-2.70	5.92	9.16	-4.34	-3.87	4.12	0.74	4.70
Tetra-	-3.12	6.53	10.29	-3.21	-2.73	4.73	1.35	5.30
Penta-	-3.57	6.84	11.28	-2.22	-1.75	5.04	1.66	5.62
Hexa-	-3.68	7.36	12.08	-1.41	-0.94	5.56	2.18	6.14
Hepta-	-4.28	7.26	12.56	-0.94	-0.46	5.46	2.08	6.04
Octa-	-4.36	8.48	14.29	0.79	1.27	6.68	3.30	7.26
Nona-	-4.68	9.01	15.33	1.83	2.31	7.21	3.83	7.79
Deca-	-4.81	9.97	16.77	3.27	3.74	8.17	4.79	8.75

4.2.2. Aerosol - air partitioning

The aerosol-air partition coefficient is based on a linear relationship to K_{oa} (based on Harner and Bidleman, 1998 and Götz et al., 2007a).

$$K_p = 1.22 \cdot 10^{-12} \cdot K_{oa} \cdot f_{OM} \cdot \frac{M_O}{M_{OM}} \cdot \frac{\gamma_O}{\gamma_{OM}} \qquad (4\text{-}2)$$

K_p	Aerosol - air partition coefficient	$m^3/\mu g$
K_{oa}	Octanol – air partition constant	m^3/m^3
f_{OM}	Mass fraction of organic matter in aerosol	kg/kg
M_O, M_{OM}	Molar mass of octanol or organic matter respectively M_O = 130 g/mol, M_{OM} = 500 g/mol (Götz et al., 2007a). M_O/M_{OM}=0.26	g / mol
γ_O, γ_{OM}	Activity coefficient of chemical in octanol or organic matter respectively $\frac{\gamma_O}{\gamma_{OM}} = 1$	-

The organic mass fraction for fine aerosols was set to 0.3, the mass fraction for coarse aerosols to 0.1 (based on measured data by Putaud et al., 2004.)

Inserting the data for K_{oa} into equation (4-2) leads to values for K_p presented in Table 4-3.

4.2.3. Water – suspended particles partitioning

The partition coefficient between water and sediment and between water and suspended particles is defined with the same approach. For the hydrophobic compounds considered here it is assumed that most of the sorption is associated with organic matter. The partitioning can therefore be described with the water organic carbon partition coefficient (K_{oc}) and the fraction of organic carbon in the particles or sediment respectively. K_{oc} values are usually reported in units of L water per kg organic carbon, which results in the factor 1/1000 in formula (4-3) in order to convert L/kg to m^3/kg.

$$K_{sw} = f_{OC} \cdot K_{OC} \cdot \frac{1}{1000} \qquad (4\text{-}3)$$

K_{pw}	Partition coefficient between particles (or sediment) and water	m^3/ kg
K_{OC}	Partition coefficient between organic carbon and water	l/kg
f_{OC}	Organic carbon fraction in the suspended particle (or sediment)	kg/kg

Since organic matter has similar properties as octanol, relationships of the form

$$K_{OC} = a \cdot K_{OW}{}^{b} \qquad (4\text{-}4)$$

have been developed. A compilation of different relationships valid for different substance classes is provided by Schwarzenbach et al. (2001, P. 303). Note that the relationship includes a unit conversion from m^3/m^3 to L/kg. Values for the coefficients a and b have been determined for various substances and Kow ranges, but no literature data for PBDE were found.

Seth et al. (1999) derived a K_{oc} to K_{ow} correlation from a set of hydrophobic chemicals. The correlation parameters suggested to use are a = 0.33 (lower limit: 0.14 and upper limit: 0.89) and b = 1. Consequently, there is some high uncertainty in the correlation leading to a high uncertainty range in K_{oc} values.

Organic carbon was measured in lake water samples from Lake Thun at the Empa (Bogdal, C. personal communication) Unfortunately the values for particulate organic carbon were below the detection limit of 2 mg/l. Therefore a generic value of 20% (foc = 0.2) organic carbon (Mackay, 1992) on particles have been used. For the sediment, an OC content of 2% (foc = 0.02) was measured in Lake Thun (Kohler, M., personal communication).

The partition coefficient for water-sediment was defined on a volume (m^3/m^3) basis in the model. Consequently the density of sediment needs to be included in equation (4-3).

Generic density values were obtained from Mackay (1992) and are 2400 kg/m³ for the sediment and 1500 kg/m³ for the suspended particles.

4.2.4. Water – fish partitioning

The partition coefficient between water and fish is calculated with the K_{ow} partition constant. Partitioning of hydrophobic chemicals into fish is mainly associated with the fish lipids. By assuming that octanol is a good approximation for the fish lipids, only the lipid content of the fish is needed as a parameter.

$$K_{FW} = L \cdot K_{OW} \quad (4\text{-}5)$$

K_{FW}	Partition coefficient between fish and water	m³ water/m³ fish
K_{OW}	Octanol-water partition constant	m³ water/m³ octanol
L	Lipid content of the fish	m³/m³

The average lipid mass fraction of fish in Lake Thun was 5.7% (Bogdal, 2007 and Naef, M., personal communication). Earlier measurements were similar, with 5.6% (Zennegg et al., 2003). The mass fraction was used as lipid content by taking the assumption that lipids have the same density as the whole fish.

Since results will be presented in mol/g lipid weight, it is not so important to know the lipid content exactly. It only influences the inventory of substances in the fish, which is small compared to the total lake compartment and therefore has a small effect to the overall fate of the chemicals.

4.3. The fugacity approach

The model is based on the fugacity approach. This method has been described extensively by Mackay (2001). The fugacity approach has some advantages in the algebraic solution, since the fugacity is equal for phases that are in equilibrium with each other.

$$f = \frac{c}{Z} \ (1) \quad (4\text{-}6)$$

The fugacity is related to the concentration by the fugacity capacity (Z). The fugacity in the gas phase is equal to vapor pressure, and thus:

$$Z_{air} = \frac{1}{RT} \ (4\text{-}7) \qquad \text{and} \ f_{air} = \frac{\frac{p}{RT}}{\frac{1}{RT}} = p \qquad (4\text{-}8)$$

The fugacity capacities of the other phases are calculated by using partition coefficients between air and the respective phase.

At equilibrium: $\frac{c_{air}}{c_{water}} = \frac{Z_{air}}{Z_{water}} = K_{aw}$ (4-9) and therefore: $Z_{water} = \frac{Z_{air}}{K_{aw}} = \frac{1}{RT} \cdot \frac{1}{K_{aw}}$ (4-10)

All z-values are listed in Table 4-4.

Table 4-4: Z-values for all phases in the model.

Air	$Z_a = \frac{1}{RT}$	(4-7)
Aerosol	$Z_p = \frac{1}{RT} \cdot \frac{1}{K_p}$	(4-11)
Water	$Z_w = \frac{1}{RT} \cdot \frac{1}{K_{aw}}$	(4-10)
Suspended particle	$Z_{sp} = \frac{1}{RT} \cdot \frac{1}{K_{wp}} \cdot \frac{1}{K_{aw}}$	(4-12)
Sediment	$Z_s = \frac{1}{RT} \cdot \frac{1}{K_{ws}} \cdot \frac{1}{K_{aw}}$	(4-13)
Fish	$Z_f = \frac{1}{RT} \cdot \frac{1}{K_{wf}} \cdot \frac{1}{K_{aw}}$	(4-14)

In order to quantify mass flows of the intercompartmental processes shown in Figure 4 based on fugacities, D-values are used, which are defined as:

$D = \frac{N}{f}$ (4-15) and respectively: $N = D \cdot f$ (4-16)

D	D-value	mol Pa^{-1} h^{-1}
N	Mass flow	mol h^{-1}
f	Fugacity	Pa
Z	Fugacity capacity	dependent on the unit of 'c'

The term 'D · f' is equal to the term 'k · c', where k is a rate constant and c the concentration.

4.4. Transport processes

Transport processes include the processes which move compounds from one compartment to another as well as across the system boundaries.

The processes between the atmospheric and water compartment are wet and dry particle deposition and deposition of gas phase compounds by dissolution in rain and diffusion. The processes between water and sediment are particle sedimentation from water to sediment, resuspension from sediment into the water and diffusion between the open water and the pore water. There are no direct processes between the atmosphere and the sediment.

Input of chemicals is considered into the atmospheric compartment by wind containing the compounds and into the water by the tributaries to Lake Thun. No direct input into the sediment from outside of the system is assumed.

4.4.1. Dry deposition

Dry deposition of particles is dependent on the amount of particles in the atmosphere and the velocity at which the particles deposit into the lake. The deposition of the observed chemicals by dry deposition further depends on the partitioning between air and aerosols (chapter 4.2.2). The total amount of chemical depositing in the lake is calculated by multiplying the deposition flux with the lake surface area. The D-value is thus:

$$D_{dd} = A_{aw} \cdot k_{dry} \cdot C_{PM} \cdot Z_p \quad (4\text{-}17)$$

D_{dd}	D-value for dry deposition	mol Pa^{-1} h^{-1}
A_{aw}	Interface area between atmosphere and lake compartment = lake surface area	m^2
k_{dry}	Dry deposition velocity	m h^{-1}
C_{PM}	Aerosol concentration in air	µg / m^3
Z_p	Fugacity capacity of aerosol	mol μg^{-1} Pa^{-1}

The dry deposition velocity (k_{dry}) is influenced by Brownian diffusion and gravitation. Brownian diffusion is important for smaller particles (<1µm), while for larger particles (>1µm) gravitation becomes more important (BAFU, 2003). Deposition velocities can be calculated for a particle of a certain diameter by taking into account these two acting forces. In the model average deposition rates for fine aerosols (<2.5 µm) and coarse aerosols (2.5-10 µm) are needed. Therefore, a weighted average of aerosol deposition velocities for different diameters depending on their share on the total aerosol fraction needs to be calculated. The weighted average values for aerosol deposition velocities are taken from an aerosol concentration model for Switzerland (BAFU, 2003) for the Lake Thun case study.

Table 4-5: Dry deposition velocities for fine and coarse aerosol fractions.

Parameter	value	unit	Ref.
Dry deposition velocity for fine aerosols	3.6	m h^{-1}	BAFU, 2003
Dry deposition velocity for coarse aerosols	18	m h^{-1}	BAFU, 2003

4.4.2. Wet deposition

Wet deposition includes rain washout by dissolution of the chemicals in the raindrops and wet particle deposition.

Dissolution of the chemicals in the raindrop is dependent on the partitioning between air and raindrops. During a rain event there are many raindrops in the atmosphere and single raindrop has therefore only a limited air volume available. Therefore an upper limit for $Z_{raindrop}$ is set by taking into account the air volume accessible for a raindrop. $Z_{raindrop}$ is thus calculated by:

$$Z_{raindrop} = \frac{Z_{air}}{K_{aw} + \frac{V_w}{V_a}} \quad (4\text{-}18)$$

The ratio (V_w/V_a) is the raindrop to air volume ratio. A generic value of $6 \cdot 10^{-8}$ was suggested by Jolliet and Hauschild (2005) based on the assumption of a drop speed of 7 m/s and a rain intensity of $4 \cdot 10^{-7}$ m/s. The D-value for rain washout is calculated by:

$$D_{rw} = k_r \cdot A_{aw} \cdot Z_{raindrop} \qquad (4\text{-}19)$$

D_{rw}	D-value for rain washout	mol Pa^{-1} h^{-1}
A_{aw}	Interface area between atmosphere and lake compartment = lake surface area	m^2
k_r	Rainfall rate	m h^{-1}
$Z_{raindrop}$	Fugacity capacity of raindrop (consider formula 4-18)	mol m^{-3} Pa^{-1}

The rainfall rate is dependent on the season. The monthly rainfall data used are shown in Figure 3-2 and listed in *Appendix IV – Variable parameters.*

Compounds adsorbed to particles are removed from the atmosphere by wet particle deposition. The amount of particles deposited by rain depends on the volume a raindrop passes through during its fall. Assuming a cloud height of 200 m and a raindrop diameter of 1mm, a raindrop falls trough 200'000 times its own volume, which is called the scavenging ratio (Mackay, 2001). Taking into account that raindrops cannot take up all aerosols when falling through the air, a scavenging efficiency is included, which quantifies the percentage of aerosols that are incorporated into an aerosol of the aerosols that are present in the volume where a raindrop falls through (Götz et al., 2007b). The D-value for wet particle deposition is thus calculated by:

$$D_{wp} = k_r \cdot A_{aw} \cdot Q \cdot E \cdot C_{PM} \cdot Z_p \qquad (4\text{-}20)$$

D_{wp}	D-value for wet particle deposition	mol Pa^{-1} h^{-1}
A_{aw}	Interface area between atmosphere and lake compartment = lake surface area	m^2
k_r	Rainfall rate	m h^{-1}
Q	Scavenging ratio	m^3/m^3
E	Scavenging efficiency	-
C_{PM}	Aerosol concentration in air	µg / m^3
Z_p	Fugacity capacity of aerosols	mol μg^{-1} Pa^{-1}

The aerosol concentrations in air were addressed in chapter 4.1.1. Scavenging efficiencies of 0.01 for fine fraction and 0.5 for coarse fraction have been used (Seinfeld and Pandis, 1998).

The model includes the intermittent rainfall approach (Götz et al. 2007b). This approach leads to more realistic wet deposition mass fluxes since it takes into account that rainfall is intermittent rather than continuous. When rainfall is modeled continuously, the model erroneously assumes that there is rainfall all the time with a low rainfall rate. This approach leads to an overestimation of wet deposition flux, since it assumes that the chemical load in the atmosphere is

constant, though in reality during rain events the chemical load in the atmosphere is dramatically reduced and finally chemicals can actually be completely washed out during rain events. The intermittent rainfall approach takes this fact into account by setting an upper limit to the wet deposition flux, which is set based on the assumption that during a rain event the chemical (gas phase and particle bound) is completely washed out. The upper limit is thus dependent on a minimum residence time of the chemical in the atmosphere, which can be described by the average durations of rain events and dry periods.

The minimum residence time can be described as (Götz et al., 2007b):

$$\tau_{air}^{\min} = \frac{t_{dry}}{2} \cdot \frac{t_{dry}}{t_{wet} + t_{dry}} \quad \text{or} \quad k_{wet}^{\max} = \frac{2}{t_{dry}} \cdot \frac{t_{wet} + t_{dry}}{t_{dry}} \qquad (4\text{-}21)$$

The maximal D-value for wet deposition including rain washout and wet particle deposition is thus:

$$D_{wet}^{\max} = V_a \cdot \frac{2}{t_{dry}} \cdot \frac{t_{wet} + t_{dry}}{t_{dry}} \cdot Z_{bulk,a} \qquad (4\text{-}22)$$

with

$$Z_{bulk,a} = Z_a + Z_{p,coarse} \cdot C_{PM,coarse} + Z_{p,fine} \cdot C_{PM,fine} \qquad (4\text{-}23)$$

$\tau_{air}^{\min}$	Minimal residence time in the atmosphere	h
$k_{wet}^{\max}$	Maximal removal rate from atmosphere by wet deposition	h^{-1}
t_{dry}	Average duration of dry period	h
t_{wet}	Average duration of wet period	h
$D_{wet}^{\max}$	Maximal D-value for wet deposition	mol Pa^{-1} h^{-1}
V_a	Volume of atmospheric compartment	m^3
$Z_{bulk,a}$	Bulk fugacity capacity in atmosphere	mol m^{-3} Pa^{-1}
Z_a	Fugacity capacity of air	mol m^{-3} Pa^{-1}
$Z_{p,coarse}$	Fugacity capacity of coarse aerosols	mol μg^{-1} Pa^{-1}
$Z_{p,fine}$	Fugacity capacity of fine aerosols	mol μg^{-1} Pa^{-1}
$C_{PM,coarse}$	Coarse aerosol concentration in air	$\mu g\ m^{-3}$
$C_{PM,fine}$	Fine aerosol concentration in air	$\mu g\ m^{-3}$

The wet deposition D-value is set to the minimum of the D^{max}-value (Equation 4-22) and the sum of the D-values for rain washout and wet particle deposition (Götz et al., 2007b)

$$D_{wet,total} = \min\left[D_{wet}^{\max}; D_{rw} + D_{wp}\right] \qquad (4\text{-}24)$$

The duration of rain events and the duration of dry periods are highly variable through the year. Furthermore, a single rain event can be characterized by rainfall of different intensities following each other. It can also be shortly interrupted by no rainfall for several minutes or hours and then continue. Hence, it must be defined how long it should not rain until a starting rainfall is regarded as a new event.

For the Lake Thun case study, precipitation data on an hourly basis for the year 2006 was analyzed. First, it was defined for each hour if it belongs to a wet or dry period. An hour was counted as wet period if there was rain in this particular hour, in the hour before or the hour thereafter. A dry period thus starts when there is more than one hour without rain. As a fact of the definition for the wet period, the dry periods stop one hour before the rain starts.

The durations of dry and wet periods are approximately log-normal distributed. The geometric mean was thus calculated for both. A summary of the analysis is presented in Table 4-6.

Table 4-6: Summary of dry and wet periods analysis for the year 2006 in Interlaken.

Total rain events	135
Average duration of wet period	6.2 h
Average duration of dry period	11.5 h
Maximal duration of wet period	68 h
Maximal duration of dry period	413 h

4.4.3. Air-Water diffusion

Chemicals can be transferred between the atmosphere and the lake by diffusion. The air-water interface is described by a air-side layer and a water side layer, where only molecular diffusion occurs. Within these layers a concentration gradient is present leading to a directed diffusion. At the boundary between the air phase and water phase the concentrations in the two media are in equilibrium. The diffusion flux can be described by (adapted from Schwarzenbach et al., 2003 P.891):

$$F_{a\to w} = k_{aw} \cdot \left(c_w^{eq} - c_w\right) \quad (4\text{-}25)$$

with,

$$c_w^{eq} = \frac{c_a}{K_{aw}} \quad \text{and} \quad k_{aw} = \frac{1}{\frac{1}{k_w} + \frac{1}{k_a \cdot K_{aw}}} \quad (4\text{-}26)$$

The D-value can be determined based on these equations. By using equation (4-6) and (4-26) Equation (4-25) can be transformed to:

$$F_{a\to w} = \frac{1}{\frac{1}{k_w} + \frac{1}{k_a \cdot \frac{Z_a}{Z_w}}} \cdot \left(f_a \cdot Z_a \cdot \frac{Z_w}{Z_a} - f_w \cdot Z_w\right) \quad (4\text{-}27)$$

Rearrangement (factor out Z_w and cancel out Z_w in the k_{aw} expression) leads to:

$$F_{a\to w} = \frac{1}{\frac{1}{k_w \cdot Z_w} + \frac{1}{k_a \cdot Z_a}} \cdot \left(f_a - f_w\right) \qquad (4\text{-}28)$$

The D-value is obtained by multiplying $F_{a\to w}$ with the air-water surface area in order to become a total mass flow and applying equation (4-11):

$$D_{awd} = \frac{1}{\frac{1}{k_w \cdot Z_w} + \frac{1}{k_a \cdot Z_a}} \cdot A_{aw} = \frac{1}{\frac{1}{k_w \cdot Z_w \cdot A_{aw}} + \frac{1}{k_a \cdot Z_a \cdot A_{aw}}} \qquad (4\text{-}29)$$

Note, that this D-value needs to be multiplied by the difference of fugacities in air and water $\left(f_a - f_w\right)$. This has the advantage that two theoretic diffusive transports can be calculated, one for the diffusion from air to water ($D_{aw} \cdot f_a$) and one for the diffusion from water to air ($D_{aw} \cdot f_w$). The splitting of the diffusive transport to those two parts is advantageous for the set up of mass balance equations.

$F_{a\to w}$	Flux from atmosphere to water	mol m^{-2} h^{-1}
k_{aw}	Total exchange velocity	m h^{-1}
c_w^{eq}	Theoretic concentration in water in equilibrium with atmosphere	mol m^{-3}
c_w	Concentration in water	mol m^{-3}
K_{aw}	Partition constant between air and water	m^3/m^3
k_w	Air side diffusive exchange velocity	m h^{-1}
k_a	Water side diffusive exchange velocity	m h^{-1}
D_{awd}	D-value for diffusive exchange	mol Pa^{-1} h^{-1}
A_{aw}	Interface area between atmosphere and lake compartment = lake surface area	m^2

Depending on K_{aw} , the air side exchange (k_a) or the water side exchange (k_w) dominates k_{aw}. The critical K_{aw} is equal to $\frac{k_w}{k_a}$ ~ 10^{-3}. At this K_{aw}, the two velocities become equal. The ratio between the two velocities is approximately equal to the ratio of densities of the two media, which results in the factor of 10^{-3}. K_{aw} for PBDEs are in the range of critical K_{aw}. Up to Tri-BDE the exchange is dominated by the water side exchange velocity, while congeners with four and more bromines are dominated by air side exchange velocity.

The diffusion velocity can be determined by:

$$k_{diff} = \frac{D^*_i}{\delta} \quad (4\text{-}30)$$

k_{diff}	Diffusion velocity	m h^{-1}
D^*_i	Diffusivity of compound i. The * is used to distinguish between Diffusivity and D-values.	m^2 h^{-1}
δ	Diffusion path length	m

Diffusivity in water was estimated with the empirically derived formula given by Schwarzenbach et al. (2003, P.810):

$$D^*_{iw} = \frac{13.26 \cdot 10^{-5}}{\eta^{1.14} V_i^{0.589}} \quad (4\text{-}31)$$

D^*_{iw}	Diffusivity in water	cm^2 s^{-1}
η	Viscosity of water	g m^{-1} s^{-1}
V_i	Molar volume of the chemical	cm^3 mol^{-1}

At the average temperature of the water surface (11.2° C), the viscosity is 1.27 g m^{-1} s^{-1}. The McGowan molar volume was calculated according to the method presented by Schwarzenbach et al. (2003, P. 149).

Diffusivity in air was estimated with the empirically derived formula given by Schwarzenbach et al (2001, P.801)

$$D^*_{ia} = 10^{-3} \frac{T^{1.75}\left[(1/M_{air}) + (1/M_i)\right]^{1/2}}{p\left[\overline{V}_{air}^{1/3} + V_i^{1/3}\right]^{1/2}} \quad (4\text{-}32)$$

D^*_{ia}	Diffusivity in air	cm^2 s^{-1}
T	Absolute temperature	K
M_{air}	Average molar mass of air	28.97 g mol^{-1}
M_i	Molar mass of chemical i	g mol^{-1}
p	Gas phase pressure	atm
$\overline{V}_{air}$	Average molar volume of the gases in air	~20.1 cm^3 mol^{-1}
V_i	Molar volume of chemical i	cm^3 mol^{-1}

The average temperature in air (8° C) and a gas phase pressure of 1 atm has been used. Diffusion path length for air (0.3 cm) and water (0.02 cm) were taken from Schwarzenbach et al. (2003, P.908). The results for diffusivities and diffusion velocities is shown in Table 4-7.

Table 4-7: Diffusivities and diffusion velocities for PBDEs in air and water

BDE	Molar volume	Diffusivity in water	Diffusion velocity in water	Diffusivity in air	Diffusion velocity in air
		$cm^2\ s^{-1}$	$m\ h^{-1}$	$cm^2\ s^{-1}$	$m\ h^{-1}$
15	173	4.85E-06	0.009	0.054	6.53
28	191	4.58E-06	0.008	0.052	6.20
47	208	4.35E-06	0.008	0.049	5.93
99	226	4.15E-06	0.007	0.047	5.69
100	226	4.15E-06	0.007	0.047	5.69
153	243	3.97E-06	0.007	0.046	5.48
183	261	3.81E-06	0.007	0.044	5.29
209	313	3.42E-06	0.006	0.040	4.83
average		**4.16E-06**	**0.007**	**0.048**	**5.70**

Since no distinction is made in the model for different PBDEs the average values were used.

Diffusion velocities are dependent on the wind velocity. Various relationships between wind velocity and diffusion velocity in air and water have been developed. A compilation of the methods can be found in Schwarzenbach et al. (2003, P. 915). However, the dependence of diffusivities on wind velocity was not included in the model, since it was observed that diffusion plays a minor role in the air – water exchange and wind velocities are quite low at the Lake Thun and have low variability.

4.4.4. Output with wind

Most of the compounds entering the atmospheric compartment are passing directly through the compartment and leave the system again with the wind. The output of chemicals with wind is dependent on the concentration in the air and aerosols, since both leave the atmospheric compartment with the outflowing wind.

The D-value is described as:

$$D_{a,out} = q_a \cdot Z_a + q_a \cdot Z_{p,fine} \cdot C_{PM,fine} + q_a \cdot Z_{p,coarse} \cdot C_{PM,coarse} \quad (4\text{-}33)$$

$D_{a,out}$	D-value for output with wind	$mol\ Pa^{-1}\ h^{-1}$
q_a	Wind output	$m^3\ s^{-1}$
Z_a	Fugacity capacity of air (gas phase)	$mol\ m^{-3}\ Pa^{-1}$
$Z_{p,fine}$ $Z_{p,coarse}$	Fugacity capacity of fine and coarse aerosols respectively	$mol\ \mu g^{-1}\ Pa^{-1}$
$C_{PM,fine}$ $C_{PM,coarse}$	Concentration of fine and coarse aerosols respectively	$\mu g\ m^{-3}$

4.4.5. Sedimentation

Chemicals are removed from the lake water by sedimentation of the particle bound fraction. Sedimentation is modeled in the same way as atmospheric particle deposition.

$$D_{sed} = A_{ws} \cdot k_{sed} \cdot C_{SP} \cdot Z_{SP} \quad (4\text{-}34)$$

D_{sed}	D-value for sedimentation of suspended particles	mol Pa^{-1} h^{-1}
A_{ws}	Interface area between lake and sediment compartment	m^2
k_{sed}	Sedimentation velocity	m h^{-1}
C_{SP}	Concentration of suspended particles	kg m^{-3}
Z_{sp}	Fugacity capacity of suspended particles	mol kg^{-1} Pa^{-1}

The interface area between water and sediment would be bigger than the lake surface area, but in the Lake Thun case study it is set equal to the surface area. However, since the sedimentation flux is vertical to the lake surface, it makes sense to use a horizontal surface to calculate the total sedimentation mass flow.

Sedimentation velocities can be calculated in a similar way as the dry deposition velocity in the atmosphere. The settling velocity can be described by Stokes Law (Schwarzenbach et al., 2003, P 1061):

$$k_{sed} = \alpha \cdot B \cdot r^2 \quad (4\text{-}35) \quad \text{with} \quad B = \frac{2 \cdot g \cdot \left(\rho_{sp} - \rho_w\right)}{9 \cdot \eta} \quad (4\text{-}36)$$

k_{sed}	Sedimentation velocity	m h^{-1}
α	Form factor, = 1 for spheres	-
r	Particle radius	m
g	Gravity constant	9.81 m s^{-2}
ρ_{sp}	Density of suspended particles	kg m^{-3}
ρ_w	Density of water	kg m^{-3}
η	Viscosity of water	kg m^{-1} s^{-1}

With given density and diameter of particles the settling velocity can be calculated. Particles in the water have different diameters (in the range of a few µm) and densities (around 1000 kg m^{-3} for organic particles and 2500 kg m^{-3} for mineral particles). However, it was difficult to find exact data on the particle size distribution and therefore it was not considered to calculated sedimentation velocities by using the equations (4-35) and (4-36).

Mackay (2001) assumes a sedimentation velocity of 1 m/d (or 0.04 m/h). Assuming an average density of 1500 kg m^{-3} for particles and assuming that particles can be regarded as spheres, the formulas above lead to an average particle radius of about 3.4 µm.

Sedimentation in Lake Thun for organic particles is expected to take about 1 week to 2 months (Bogdal, C., personal communication). This is equal to a

sedimentation velocity of 0.09 – 0.8 m/h. Mineral particles would even settle faster. This sedimentation velocity is significantly higher than the one assumed by Mackay et al. (2001).

4.4.6. Resuspension

Part of the solid sediment material is resuspended into the lake water. The D-value for this transfer can be described by:

$$D_{res} = A_{ws} \cdot k_{res} \cdot \phi_s \cdot Z_s \quad (4\text{-}37)$$

D_{res}	D-value for resuspension of sediments	mol Pa^{-1} h^{-1}
A_{ws}	Interface area between lake and sediment compartment	m^2
k_{res}	Resuspension velocity	m h^{-1}
ϕ_s	Volume fraction of solids in sediment	m^{-3} solids / m^{-3} bulk sediment
Z_s	Fugacity capacity of solid sediment	mol m^{-3} Pa^{-1}

Resuspension can be determined by a fraction of the mixed sediment layer that is resuspended per year. Schwarzenbach et al. (2003) suggest a value of 10% per year in their description of the SMSL model.

The resuspension rate can be calculated by:

$$k_{res} = f_{res} \cdot h_s \quad (4\text{-}38),$$

where f_{res} is the fraction resuspended (=0.1 y^{-1}) and h_s is the sediment height (=0.04m).

The value obtained for k_{res} is $4.6 \cdot 10^{-7}$ m h^{-1}. Another generic value is provided by Mackay et al. (2001): $1.1 \cdot 10^{-8}$ m h^{-1}, which is almost 9 times slower than the value calculated here.

4.4.7. Sediment burial

Sediment burial is the actual accumulating mass in the sediment. The parameterization can be performed with site specific data on sediment accumulation. These can be obtained from sediment cores by measuring the thickness of a layer that represents one year. The D-value can be determined by:

$$D_{sb} = A_{ws} \cdot k_{sb} \cdot \phi_s \cdot Z_s \quad (4\text{-}39)$$

The sediment accumulation is related to the sediment burial velocity by:

$$Ac = k_{sb} \cdot \rho_{sed} \cdot \phi_s \qquad k_{sb} = \frac{Ac}{\rho_{sed} \cdot \phi_s} \quad (4\text{-}40)$$

D_{sb}	D-value for sediment burial	mol Pa^{-1} h^{-1}
A_{ws}	Interface area between lake and sediment compartment	m^2
k_{sb}	Sediment burial velocity	m h^{-1}

ϕ_s	Volume fraction of solids in sediment	m^{-3} solids / m^{-3} bulk sediment
Z_s	Fugacity capacity of solid sediment	mol m^{-3} Pa^{-1}
ρ_{sed}	Sediment density	kg m^{-3}
Ac	Sediment accumulation	kg m^{-2} h^{-1}

Sediment accumulation data are shown in Table 4-8. The data represents the accumulation for year 2004. With equation (4-40) the sediment burial velocity for the three sediment core sampling sites was calculated. A sediment density of 2'400 kg m^{-3} and a solid sediment volume fraction of 0.2 was used.

Table 4-8: Sediment accumulation measured in Lake Thun

Sediment core location	Sediment accumulation	Calculated k_{sb}
Därligen	3.18 kg m^{-2} y^{-1}	$7.6 * 10^{-7}$ m h^{-1}
Beatenbucht	1.88 kg m^{-2} y^{-1}	$4.5 * 10^{-7}$ m h^{-1}
Dürrenast	1.95 kg m^{-2} y^{-1}	$4.6 * 10^{-7}$ m h^{-1}

A generic burial rate of $3.4 \cdot 10^{-8}$ m h^{-1} was used by Mackay (2001). As with the resuspension velocity, this rate is again lower than the Lake Thun specific rate based on sediment accumulation measurements.

4.4.8. Mass balance for particles and sediment

Sedimentation, resuspension and sediment burial are dependent on each other. A mass balance can be set up for the SMSL. Since organic matter is degraded in the sediment, it is useful to set up the mass balance for the mineral content only. It is assumed that the organic mass is two times the organic carbon mass. The mass balance equation is thus:

$$k_{sed} \cdot C_{sp} \cdot \left(1 - 2 \cdot f_{OC,p}\right) - k_{res} \cdot \rho_{sed} \cdot \phi_s \cdot \left(1 - 2 \cdot f_{OC,s}\right) - k_{sb} \cdot \rho_{sed} \cdot \phi_s \cdot \left(1 - 2 \cdot f_{OC,s}\right) = 0 \quad (4\text{-}41)$$

Values for all three rates have been derived in the previous chapters. The mass balance equation can be used to find a set of velocities that fulfill the mass balance and at the same time lie between the range of the values found in literature. Sediment burial and resuspension velocities are given less uncertainty. The sediment burial velocity because it is Lake Thun specific and based on direct measurement in the lake and the resuspension velocity because the range of found values is lower than for the sedimentation velocities. Sedimentation velocities are then calculated based on the other two. This results in sedimentation velocities ranging from 0.5 m h^{-1} to 1.4 m h^{-1} with an average of 0.9 m h^{-1} calculated based on the geometric mean of the three sediment accumulation values and the average for the two independently obtained resuspension velocities. It seems that the average sedimentation value is quite high when compared to the values indicated above for sedimentation velocities. However it is still in the range indicated and regarded as the best available value. The final values used for the Lake Thun case study are shown in Table 4-9.

Table 4-9: Velocities for the water-sediment transfer processes used for the Lake Thun case study.

	Velocity	Value	Unit
k_{res}	Resuspension velocity	$2.3 \cdot 10^{-7}$	m h^{-1}
k_{sb}	Sediment burial velocity	$5.6 \cdot 10^{-7}$	m h^{-1}
k_{sed}	Sedimentation velocity	0.9	m h^{-1}

4.4.9. Lake water-pore water diffusion

Diffusion between lake water and pore water can be described by a simple diffusion process since it does not involve phase transition as in the air water diffusion process.. The D-value can be described by:

$$D_{wsd} = k_{ws} \cdot A_{ws} \cdot Z_w \quad (4\text{-}42)$$

D_{wsd}	D-value for diffusion between sediment pore water and lake water	mol Pa^{-1} h^{-1}
A_{ws}	Interface area between lake and sediment compartment	m^2
k_{ws}	Pore water – lake water diffusion velocity	m h^{-1}
Z_w	Fugacity capacity of water	mol m^{-3} Pa^{-1}

Note, that this D-value needs to be multiplied with the fugacity difference between open water and pore water to obtain the net mass flow.

The diffusivities and diffusion velocities in water are listed in Table 4-10. A diffusion path length of 0.0005 m for Lake Superior was found in literature (Schwarzenbach et al. (2001, P-1074) and is used here. The diffusion velocity is calculated with formula (4-28). Since the diffusion velocity is independent of the congener in the model an average value of 0.004 has been used in the model.

Table 4-10: Diffusivity and diffusion velocity for lake water – pore water diffusion.

Congener	Diffusivity (D*)	Unit	Diffusion velocity sediment-water (k_d)	Unit
15	0.0551	$cm^2\ s^{-1}$	0.00458	$m\ h^{-1}$
28	0.0523	$cm^2\ s^{-1}$	0.00433	$m\ h^{-1}$
47	0.0500	$cm^2\ s^{-1}$	0.00411	$m\ h^{-1}$
99	0.0480	$cm^2\ s^{-1}$	0.00392	$m\ h^{-1}$
100	0.0480	$cm^2\ s^{-1}$	0.00392	$m\ h^{-1}$
153	0.0462	$cm^2\ s^{-1}$	0.00375	$m\ h^{-1}$
183	0.0446	$cm^2\ s^{-1}$	0.00360	$m\ h^{-1}$
209	0.0407	$cm^2\ s^{-1}$	0.00323	$m\ h^{-1}$

4.4.10. Output with runoff

Chemicals leave the lake with the Aare, the river flowing out of Lake Thun. The mass flux is dependent on the volumetric water flow and the concentration in the lake. In the model it was assumed, that fish do not leave the lake. The D-value can be described by:

$$D_{wa,out} = q_w \cdot Z_w + q_w \cdot Z_{sp} \cdot C_{SP} \quad (4\text{-}43)$$

$D_{w,out}$	D-value for output with water	$mol\ Pa^{-1}\ h^{-1}$
q_w	Water output	$m^3\ h^{-1}$
Z_w	Fugacity capacity of water (dissolved phase)	$mol\ m^{-3}\ Pa^{-1}$
Z_{sp}	Fugacity capacity of suspended particles	$mol\ kg^{-1}\ Pa^{-1}$
C_{SP}	Concentration of suspended particles	$kg\ m^{-3}$

4.5. Degradation

Three different degradation reactions are considered, namely direct photolysis, reaction with OH radicals and biodegradation.

A D-value for each degradation pathway (biodegradation, OH-reaction and photolysis) and in each media can be defined. The general equation is:

$$D_{\mathrm{deg},i,j} = k_{\mathrm{deg},i,j} \cdot Z_i \cdot \phi_i \quad (4\text{-}44)$$

$D_{deg,I,j}$	D-value for degradation in media i by reaction j	$mol\ Pa^{-1}\ h^{-1}$
Z_i	Fugacity capacity of media i	various
$k_{deg,I,j}$	degradation rate in media i for reaction j	h^{-1}
ϕ_i	Mass or volume fraction of the media i (compared to whole compartment). This depends on the definition of Z	various

The D-values for all media and for each reaction need to be summed up in order to get the overall D-value.

$$D_{\mathrm{deg}} = \sum_{j=1}^{m}\left(\sum_{i=1}^{n} k_{\mathrm{deg},i,j}\cdot Z_i \cdot \phi_i\right) \quad (4\text{-}45)$$

with m = 3 (different reactions) and n = number of media in the compartment for which D_{deg} is defined. Some of these D-values are zero, since not all reactions take place in all media.

4.5.1. Photolysis

Photolytic degradation has been measured in various media. Eriksson et al. (2004) measured 15 PBDE congeners with four to ten bromine substitutions in a 80:20 methanol water mixture, 9 congeners in methanol and 4 congeners in tetrahydrofuran (THF). Da Rosa et al. (2003) measured degradation of Deca-BDE in toluene and investigated the development of Nona-, Octa- and Hepta-BDE and their decay and therewith derived degradation rates for Deca-BDE and the Nona-, Octa- and Hepta- homologues. Zetzsch et al. (2004) measured BDE-153 adsorbed to aerosols made of fused silica and thus showed that photolysis on aerosol is possible. Peterman et al., 2003 investigated photolytic decay of 39 different PBDE congeners. Since all congeners were exposed together to sunlight, only for the highest brominated (congener 183) a degradation rate could be derived from the measurements, since for the lower ones it was not possible to distinguish between degradation and formation from higher brominated congers. Degradation of Deca-BDE is of high interest due to its high production volume and the therewith connected concerns of the potentially building of lower brominated congeners from Deca-BDE, which have higher toxicity and therefore several studies have been addressing photolytic decay of Deca-BDE. Photolytic degradation rates of Deca-BDE were measured by Bezares-Cruz et al. (2004) in hexane, by Palm et al. (2004) adsorbed on silicon dioxide in an aqueous suspension, by Gerecke (2006) adsorbed on kaolinite, and by Söderström et al. (2004) on toluene, silica gel, sand, sediment and soil. One recent study (Raff and Hites, 2007) determined photolysis rates for various congeners in air based on their adsorption spectra and quantum yield measurements of Di-BDE3 and Tri-BDE-7. They derived a linear regression (R^2 = 0.838) for their calculated photolysis lifetimes. All data compiled are shown in Figure 4-7. The original literature data are included in *Appendix III – PBDE degradation data.*

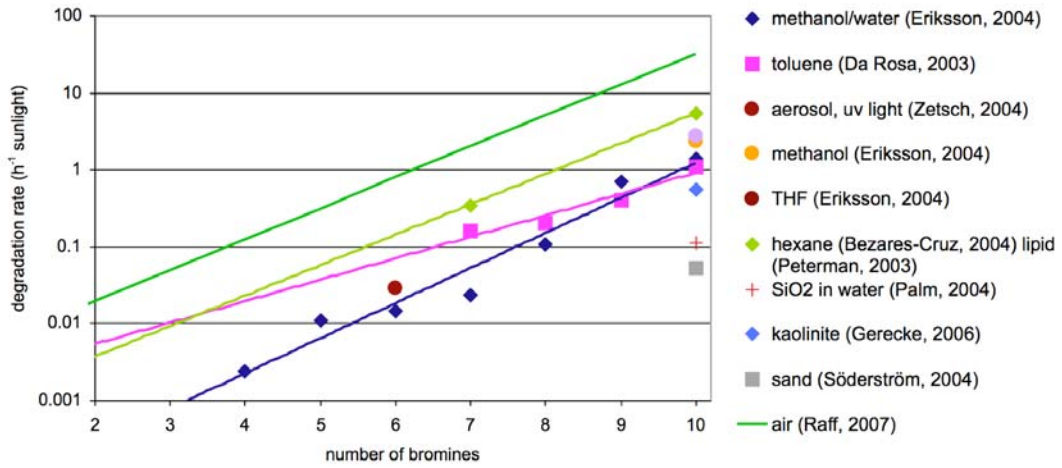

Figure 4-7: Literature values of measured photolysis rates in various matrices with individual linear regressions for toluene, hexane-lipid and methanol-water measurements. Source indicated in legend. All values are listed in *Appendix III – PBDE degradation data.*

Direct photolysis is assumed to take place in the atmosphere both in the free gas phase and in aerosols. For the gas phase, the values from Raff and Hites (2007) were used. For the aerosol phase, an average slope of the 4 linear regressions in Figure 4-7 was used (slope = 0.88). The intercept was adapted to Deca-BDE by taking an average of SiO_2, hexane and kaolinite (average degradation rate for Deca-BDE = 0.7).

Photolysis in water is calculated by taking light attenuation in the water column into consideration. The light intensity is exponentially decreasing in the water column:

$$I_z = I_0 \cdot e^{K_0 \cdot (-z)} \quad (4\text{-}46)$$

I_z	Light intensity at depth z	W m^{-2}
I_0	Light intensity at the surface	W m^{-2}
K_o	Light attenuation coefficient	m^{-1}
z	Depth in the lake	m

K_0 is dependent on particles and solutes in the water. Hence, it is a lake specific parameter and can change seasonally. During algae blooms higher attenuation must be expected. Finger et al., 2006 provide a value for K_0 in Lake Thun of 0.19 in winter (Oct-Apr) and 0.25 in summer (May-Sept) and an annual mean of 0.21. No seasonal variation was included since uncertainties in photolytic decay rates and in K_0 seem to outweigh the seasonal variation.

In order to get a photolytic decay rate over the whole water column, an average intensity in the water needs to be calculated.

$$\overline{I_{0-z}} = I_0 \cdot \alpha \quad (4\text{-}47)$$

Where $\overline{I_{0-z}}$ is the average light intensity between the depth z and the surface. α can be calculated by integrating equation 5-40:·

$$\alpha = \frac{1}{z} \cdot \int_0^z e^{K_0 \cdot (-z)} = \frac{1}{z} \cdot \frac{1}{-K_0} \cdot \left(e^{-K_0 \cdot z} - e^{-K_0 \cdot 0} \right) = \frac{1}{K_0 \cdot z} \left(1 - e^{-K_0 \cdot z} \right) \qquad (4\text{-}48)$$

Inserting 0.21 for K_0 and 136 m for z (mean depth of Lake Thun) into equation (4-48), results in an α of 0.035.

Dependence on solar radiation

Photolysis is dependent on solar radiation intensity. A correction for the measured photolysis rates is therefore needed in order to obtain photolysis rates in the environment. The photolytic decay for a specific wavelength is linearly dependent on the solar radiation intensity of that wavelength. The assumption has been made that the solar radiation intensity of a particular wavelength is linearly dependent on the overall solar radiation over all wavelength[5]. This assumption would be true, if adsorption by gases and clouds in the atmosphere were independent of wavelength and all were adsorbed to equal proportions. This approximation seemed to be appropriate in order to get radiation dependent photolytic decay rates without performing extensive calculations. Limited availability of solar radiation intensity data for individual wavelengths would even make it difficult to apply a better approach.

Photolytic decay rates were divided by the solar radiation intensity present at the time of measurement. In the model, these photolytic decay rates are multiplied with solar radiation intensity of a particular month to obtain the photolytic decay rate in the environment. With this approach varying photolytic rates for different seasons can be taken into consideration.

The solar radiation intensity present at the time of measurement alters for the different measurements. The data from Gerecke (2006) were measured in Dübendorf (Switzerland, latitude 47°) on Sept 21, 2005, beginning at 12:32 (Gerecke, A., personal communication). The data from Raff and Hites (2007) represent annual averages at 48° latitude. Palm et al. (2004) determined photolytic decay rates for June at 50° latitude and Bezares-Cruz et al. (2004) measured on July 2nd, 2.50-3.10 pm and October 23 1:44-2.39 pm at Purdue University (West Lafayette, latitude 40°)[6]. The degradation rates from Gerecke (2006) are close to the mean used (0.55 vs. 0.7 as defined above) for Deca-BDE and since solar radiation data was available for this location and time, it was chosen to use his measurement for the calculation of solar radiation dependence. This approach should be justified also for the photolytic rates in the gas phase (data from Raff and Hites, 2007), since September 21 (measurement by Gerecke, 2006) should be a good approximation for an annual average and the longitude is approximately the same (Gerecke, 2006: 47°, Raff and Hites, 2007: 48°).

Solar radiation data for September 21st, 2005, was obtained from MeteoSwiss for the stations Zurich-MeteoSwiss and Zurich-Kloten, which both are close to

[5] The overall solar radiation is described by 'solar radiation' in chapter 3.2.3.

[6] The degradation rate in Figure 4-7 from Bezares-Cruz represents the average of the two measurements in July and October.

Dübendorf (place of measurement). Deviation of these two measurement stations was about 10%. The average of the two stations during the period of measurement was 680 Wm^{-2}. All photolytic rates were thus divided by this value.

For simplicity, the degradation rate in water was calculated based on the degradation rate on aerosol and the factor α as defined above. This neglects potential differences in photolytic rates for chemicals dissolved in water to the chemicals dissolved/adsorbed in SiO_2(in water), hexane and kaolinite, that were used as proxy for an aerosol. The final photolytic decay rates for the gas phase, aerosol phase and water phase are shown in Table 4-11.

Table 4-11: Photolytic decay rates in the gas phase, adsorbed to aerosols and in the water phase divided by the solar radiation.

BDE	Gas phase	Aerosol	Water	Unit
Di-BDE	1.11E-05	3.72E-07	1.30E-08	$m^2\ W^{-1}\ h^{-1}$
Tri-BDE	2.80E-05	8.96E-07	3.13E-08	$m^2\ W^{-1}\ h^{-1}$
Tetra-BDE	7.08E-05	2.16E-06	7.56E-08	$m^2\ W^{-1}\ h^{-1}$
Penta-BDE	1.79E-04	5.21E-06	1.82E-07	$m^2\ W^{-1}\ h^{-1}$
Hexa-BDE	4.53E-04	1.26E-05	4.39E-07	$m^2\ W^{-1}\ h^{-1}$
Hepta-BDE	1.15E-03	3.03E-05	1.06E-06	$m^2\ W^{-1}\ h^{-1}$
Octa-BDE	2.90E-03	7.30E-05	2.55E-06	$m^2\ W^{-1}\ h^{-1}$
Nona-BDE	7.33E-03	1.76E-04	6.16E-06	$m^2\ W^{-1}\ h^{-1}$
Deca-BDE	1.86E-02	4.24E-04	1.48E-05	$m^2\ W^{-1}\ h^{-1}$

4.5.2. OH radical reaction

OH-radical reaction rates were calculated with AOPWIN software[7], which is based on a structure activity relationship (SAR) introduced by Atkinson (1986). Raff and Hites (2007) used the same underlying SAR methods to derive OH-reaction lifetimes. Reaction rates were measured for 3 Mono- and 4 Di-BDE by Raff and Hites (2006) in the gas phase in a small reaction chamber and by Zetzsch et al. (2004) for BDE154 adsorbed to aerosols in an aerosol smog chamber. All estimated values and measured values mentioned are presented in Figure 4-8. The geometric mean for the values of different congeners from Raff and Hites (2006) were built. Zetzsch (2004) estimated the uncertainty to be about 50%. Uncertainty for the values from Raff and

[7] AOPWIN Version 1.92. OH-radical reaction estimation tool. Part of the EPI Suite Software package provided by the United States Environmental Protection Agency. The estimation program is based on the structure – activity relationship (SAR) methods developed by Atkinson (1986). Various findings following the publication by Atkinson (1986) have been included into the model, among these the review by Kwok and Atkinson (1995). Details about the underlying predictive methods can be found on the EPA website (http://www.epa.gov/opptintr/exposure/pubs/episuite.htm) and in the help files for the program (download on the same page).

Hites (2006) were calculated with formula (6-4)[8] (see chapter 6.2) by considering the confidence intervals for the values of individual congeners.

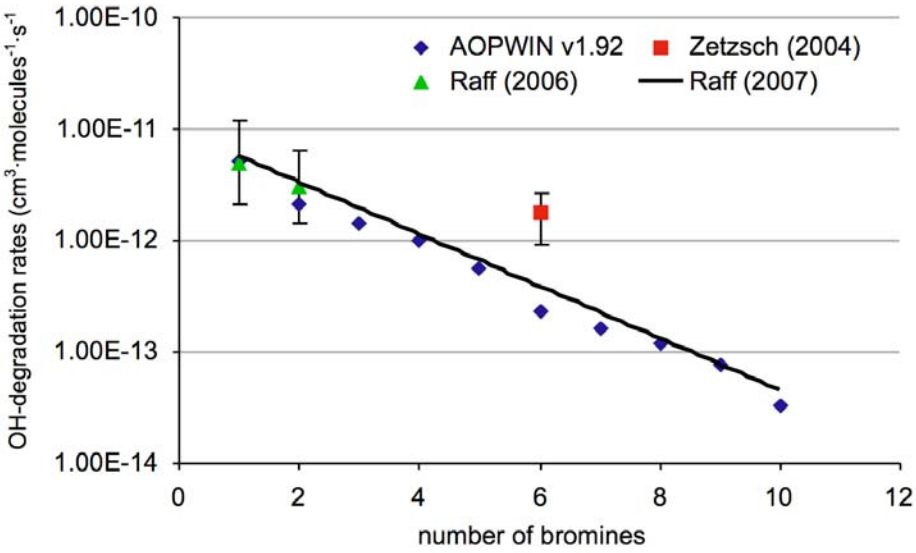

Figure 4-8: OH reaction rates obtained from AOPWIN estimation software, measurements by Zetzsch et al. (2004), Raff and Hites (2006) and including the SAR relationship equation presented by Raff and Hites (2007).

The OH-reaction rates obtained from AOPWIN were used for the model. The values are shown in Table 4-11.

OH-concentrations from Spivakovski et al. (2000) were used. The data provided in the paper for 44° and 52° were linearly interpolated to obtain a value for 47,6° (latitude for Lake Thun) and the data for missing months were linearly interpolated too. The resulting OH-concentrations are shown in Table 4-13.

[8] The sensitivity of a single value to the geometric mean of all values can be calculated by:

$$S = \frac{\Delta O / O}{\Delta I / I} = \frac{\frac{O \cdot cf^{1/n} - O}{O}}{\frac{I \cdot cf - I}{I}} = \frac{cf^{1/n} - 1}{cf - 1}$$, where S is the sensitivity, O is the geometric mean (output), I is the single value (Input), cf is the confidence factor for the single value, and n are the number of values for which the geometric mean is built.

Table 4-12: OH-reaction rates used in the model

BDE	OH-reaction rate
	cm^3 / (molecules h^{-1})
Di-BDE	7.7E-09
Tri-BDE	5.1E-09
Tetra-BDE	3.6E-09
Penta-BDE	2.0E-09
Hexa-BDE	8.3E-10
Hepta-BDE	6.0E-10
Octa-BDE	4.2E-10
Nona-BDE	2.7E-10
Deca-BDE	1.2E-10

Table 4-13: OH-concentrations used in the model (derived from Spivakovski et al. (2000).

month	OH-concentration
	10^5 molecules / cm^3
January	0.6
February	2.1
March	3.6
April	5.2
May	6.9
June	8.6
July	10.2
August	8.0
September	5.7
October	3.5
November	2.5
December	1.6

4.5.3. Biodegradation

Biodegradation rates were estimated with the software BIOWIN[9]. 7 different outputs are generated (BIOWIN_1-7), which are based on different methods. The program however does not calculate biodegradation rates directly, but only probabilities of degradation and timeframes for the rapidness, which are based on quantitative structure biodegradability relationships and surveys of expert opinions.

Two options have been considered to convert BIOWIN outputs to biodegradation rates. The first option is to use the Biowin_4 output, which gives a figure for the primary (first reaction step) biodegradation timeframe. A value between 1 and 5 is given in the output. As indicated in the BIOWIN output, the scale can be attributed to half-lives as follows: 5 = hours, 4 = days, 3 = weeks, 2 = months, 1 = longer.

Therefore, a direct translation of these values is possible by using a linear regression of the BIOWIN-4 output versus ln(half-life) and assuming that 4.5 represents a half-life of 1 day, 3.5 represents 1 week (7 d), 2.5 represents one month (30 d) and 1.5 represents 1 year (365 d). The regression obtained is:

[9] BIOWIN Version 4.10. Biodegradation rates estimation tool, part of the EPI Suite Software package provided by the United States Environmental Protection Agency. Estimates are based on fragment constants that were developed by multiple linear and non-linear regressions determined with a set of chemicals with experimental data on biodegradation. Details about the underlying predictive methods can be found on the EPA website (http://www.epa.gov/opptintr/exposure/pubs/episuite.htm) and in the help files for the program (download on the same page).

$$\ln\left(t_{1/2}(d)\right) = -1.92 \cdot \text{BIOWIN\_4} + 8.56$$

The second approach was to use the linear regressions derived by Arnot et al. (2005) for BIOWIN outputs 1,3,4 and 5. Arnot et al. (2005) derived these regressions by using a training set of chemicals with empirical data on biodegradation rates. The equations from Arnot et al. (2005) are shown in Table 4-14.

Table 4-14: Linear regressions from Arnot et. al (2005)

Regression	R^2	Maximum half life
$\ln\left(t_{1/2}(d)\right) = -1.32 \cdot \text{BIOWIN\_1} + 2.24$	0.72	BIOWIN_1<-0.95: 3300 days (9 years)
$\ln\left(t_{1/2}(d)\right) = -1.07 \cdot \text{BIOWIN\_3} + 4.20$	0.77	BIOWIN_3<0.85: 2190 days (6 years)
$\ln\left(t_{1/2}(d)\right) = -1.46 \cdot \text{BIOWIN\_4} + 6.51$	0.78	BIOWIN_4<2: 3650 days (10 years)
$\ln\left(t_{1/2}(d)\right) = -1.86 \cdot \text{BIOWIN\_5} + 2.23$	0.58	BIOWIN_5<-0.7: 3650 days (10 years)

Arnot et al. (2005) excluded extremely recalcitrant compounds from calibration and therefore maximum half-lives are defined for BIOWIN outputs that are lower than a certain threshold (indicated in Table 4-14). These maximum half-lives are not very accurate, but for the purpose of multimedia modeling they are still useful, since for such slowly degrading compounds other removal processes will be more important and a degradation rate with high accuracy is not needed.

The geometric mean of the four half-lives obtained with the equations from Arnot et al. (2005) was built. The degradation rates for PBDEs calculated with the two approaches are listed in Table 4-15.

Table 4-15: Biodegradation half-lives for PBDEs obtained from BIOWIN and with regressions from Arnot et al. (2005)

BDE	BIOWIN direct	Arnot et al (2005) Geometric mean
	t ½ (d)	t ½ (d)
Di-BDE	13	57
Tri-BDE	21	104
Tetra-BDE	35	192
Penta-BDE	59	353
Hexa-BDE	99	653
Hepta-BDE	163	880
Octa-BDE	457	1295
Nona-BDE	273	1069
Deca-BDE	759	1581

The values obtained from Arnot et al. (2005) were chosen for the Lake Thun case study, since it seemed to be appropriate to be on the conservative side regarding degradation rates in the environment.

4.5.4. Debromination

PDBEs can be debrominated to lower brominated congeners by photolytic degradation and by biodegradation. The fraction of debromination on total degradation could only be estimated.

The response curve shown in Da Rosa et al. (2002) for congeners formed by photolytic decay of Deca-BDE was estimated to be about 80% of the degradation of Deca-BDE. From the response curve of the photolysis of a Tetra-BDE shown by Palm et al. (2004) a formation of about 50% of Tetra-BDE from Penta-BDE can be estimated. Rayne et al. (2006) mention that the formation of other products such as dibenzo-furans has mainly been observed for lower brominated congeners. This fact suggest to use a higher debromination fraction for the higher brominated congeners than for lower brominated congeners. In the Lake Thun case study, a fraction of 0.5 was therefore assumed for Di-, Tri-, Tetra-, and Penta-BDE and a fraction of 0.8 was assumed for Hexa-, Hepta-, Octa- and Nona-BDE.

Gerecke et al. (2005) measured anaerobic degradation of Deca-BDE in sewage sludge and found that at least 5% of the Deca-BDE was transformed to Nona-BDE. The actual fraction was estimated to be somewhat higher than 0.05 since in such experiments never all degradation products can be identified. In the Lake Thun case study finally a fraction of 0.1 was used and applied for all congeners since no information about the influence of the degree of bromination has been found.

4.6. Degradation rates of PCBs

PCB degradation is possible by OH-reaction in the atmosphere or by biodegradation in lake water and sediment. There are no direct photolytic reactions.

OH-reaction rates were obtained from Anderson and Hites (1996), who assessed OH-reaction rates for some PCBs and derived a linear regression of OH-reaction rate with number of chlorine substitutions. The biodegradation rates were obtained from Wania and Daly (2002), who estimated half-lives of seven PCB congener. No value was available for Hexa-PCB138. Since mainly the degree of chlorination influences the degradation rate, the rates for Hexa-PCB153 was used for Hexa-PCB138.

Table 4-16: OH reaction rate and biodegradation half-lives in water and sediment collected for PCBs.

PCB	OH-reaction rate[1)]	Biodegradation in water[2)]	Biodegradation rate in sediment[2)]
	cm^3 / molecules h^{-1}	half life (h)	half life (h)
Tri-CB-28	1.2E-12	5500	17'000
Tetra-CB-52	7.4E-13	10'000	55'000
Penta-CB-101	4.5E-13	31'000	55'000
Hexa-CB-138	2.7E-13	55'000	170'000
Hexa-CB-153	2.7E-13	55'000	170'000
Hepta-CB-180	1.6E-13	55'000	170'000

1) from linear regression provided by Anderson and Hites (1996)
2) from Wania and Daly (2002)

4.7. Transport processes into the system

The observed chemicals enter the model system by wind into the atmospheric compartment and by the rivers into the lake water compartment. These two mass flows need to be provided as inputs for the model, except for the alternative calculation modus (see chapter 5.2.2).

4.7.1. Atmospheric input

General aspects

The input into the atmosphere above the lake is dependent directly on the wind velocity, its direction and the concentration level of the chemical in the atmosphere where the wind comes from. Wind velocity data were taken from the weather station Interlaken. For the concentration, the air measurements carried out in Faulensee (Bogdal, 2007) were used. Although the location of air measurements does not represent the air where the wind comes from, it provides a good estimate of this concentration since degradation and removal processes are slow compared to the time needed for the air to travel from outside the modeled system to the location of measurement. By taking this approach, the model is calibrated to the concentration in the atmosphere and consequently modeled and measured concentration levels in the atmospheric compartment will be close to each other.

Other multimedia box models use emission estimates for the input into the different compartments of the modeled system. The calculation of emissions is performed by summing up the emissions occurring in the production, use and disposal of products containing the compound of interest. These emissions can be estimated by taking into account production levels and emission factors. However, for the model presented here such an approach is hardly possible, since the concentration in the air adjacent to the lake is not only dependent on emissions but also on long-range transport of these compounds and partitioning of the chemical in the environment adjacent to the lake. A quantification of the concentration level by taking into account these factors would require an extension of the model to a

bigger geographic area. Probably, the model would need an extension to the global scale, but the accuracy of such a model would also be low since global scale models have a low resolution and cannot provide a result that would be Lake Thun specific. However, global scale multimedia models could be used to provide a concentration profile in the atmosphere over time and use this as an input for the Lake Thun model. This would especially be advantageous to perform analysis of different emission scenarios where emissions in various regions of the world are changing differently.

Fraction of chemicals on aerosols

In the atmosphere, gas phase and particle bound concentrations were measured. These were compared with the gas-particle partitioning model presented in chapter 4.2.2 based on K_{oa}. In Figure 4-9 a comparison between the model and the measurements of the fraction on particles is shown. The fraction on particles of measurements is defined as:

$$\phi_{\text{measurement}} = \frac{1}{1+\frac{c_a}{c_p}\cdot\frac{1}{C_P}} \quad (4\text{-}49)$$

The fraction on particles based on the partition coefficient as defined in chapter 4.2.2 is:

$$\phi_{\text{model}} = \frac{1}{1+\frac{1}{K_p}\cdot\frac{1}{C_P}} \quad (4\text{-}50)$$

For the K_p calculation an organic matter content of 20% was used. The different points in Figure 4-9 represent different measurements. K_p (and Φ_{model}) was adapted to the temperature at the day of measurement. This leads to different points for Φ_{model} for the same homologue group (same number of bromines).

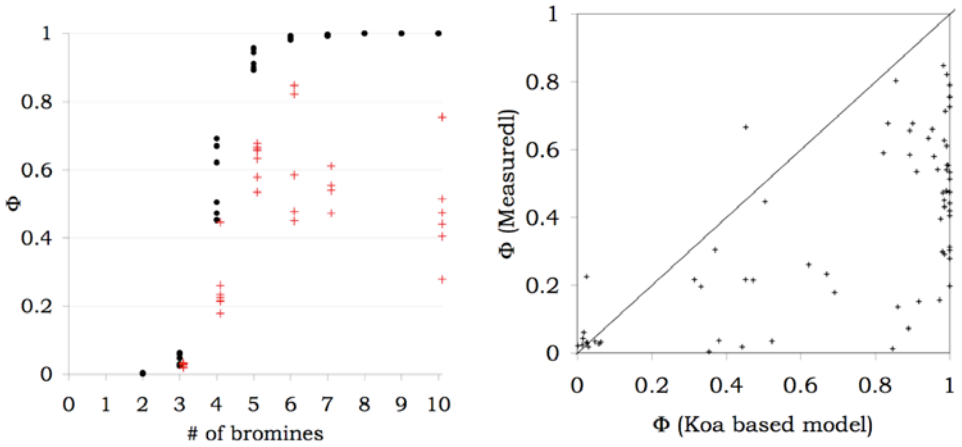

Figure 4-9: Left figure: Comparison of fraction on aerosol (Φ) measured (red crosses) and calculated with the Koa based model (Equation 4-2) (black points). Right: Comparison of the same data by showing modeled fractions versus measured fractions.

Measured aerosol concentrations are generally too low compared to what would be expected by assuming thermodynamic equilibrium with the measured gas phase concentration. This fact is very pronounced for Deca-BDE, where the K_{oa} based model calculates a Φ close to 1, while measurements show a Φ between 0.3 and 0.75. The disagreement between Φ_{model} and $\Phi_{measurement}$ for 4-6 bromine substituted congeners is not as bad as it seems. When Φ is around 0.5, a small change in concentration (e.g. a measurement error) leads to a high change in Φ, whereas for Φ close to 1, a change in concentration has a low effect. This shows that there seems to be an error in the Deca-BDE measurements. The Φ_{model} and $\Phi_{measurement}$ for Tri-BDE are corresponding well, shown by the points in the lower-left corner of the right plot in Figure 4-9.

This fact might lead to an underestimation of the deposition mass flux into the lake and finally to too low concentrations in the lake and in sediment.

Approach to determine seasonal dependent input concentrations

Concentrations in the atmosphere vary seasonally. First, the partitioning between aerosols and air is temperature dependent, whereas in colder season the fraction of PBDEs on aerosols is higher. This effect is shown in Figure 4-10, which show the measurements of air samples at Lake Thun. Second, the bulk air concentration is expected to be higher in summer, because emissions are higher since more chemicals can evaporate from PBDE containing products at warmer temperatures. Third, bulk air concentrations are lower in colder season, since more PBDE are bound to soils, while during warmer periods more PBDE are evaporating from soils or vegetation. Additional seasonal variation can be observed due to snow pack in winter and increasing vegetation volume in summer, which both can absorb PBDEs. This fact can lead to multiple peaks in the atmospheric concentrations as observed by Gouin et al. (2002).

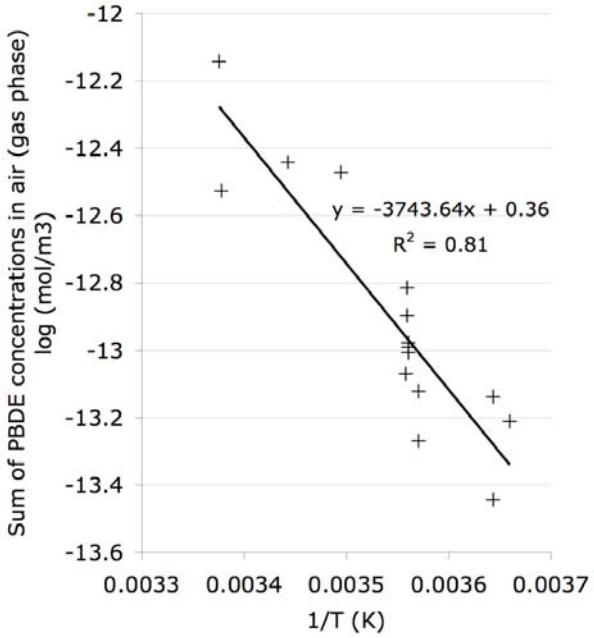

Figure 4-10: Gaseous concentrations in air samples from Lake Thun. Plotted vs temperature at the day of measurement[10].

In the Lake Thun case study, the seasonal variation in input concentration was determined by considering the empirical data. It was assumed that the major effect influencing the bulk concentration (gaseous + particle bound concentration) of the atmosphere is the temperature. Hence, input concentrations as a linear function of temperature have been determined based on the concentrations in air samples. Figure 4-11 shows the bulk concentrations versus temperature of the individual air measurements. A confidence factor of 3 (see chapter 6.2.1) has been assumed for the input concentrations. The range defined with the confidence factor should include 95% of the values, which can be shown in the figures.

[10] The slope of the linear regression should be equal to $\Delta U_{oa}/(2.303 \cdot 8.314)$, where the factor 2.303 comes from conversion of log(10) to ln and 8.314 is the universal gas constant. The empirical data thus imply a ΔU_{oa} of -72'000 J mol^{-1} which corresponds well with the data presented in Table 2-4.

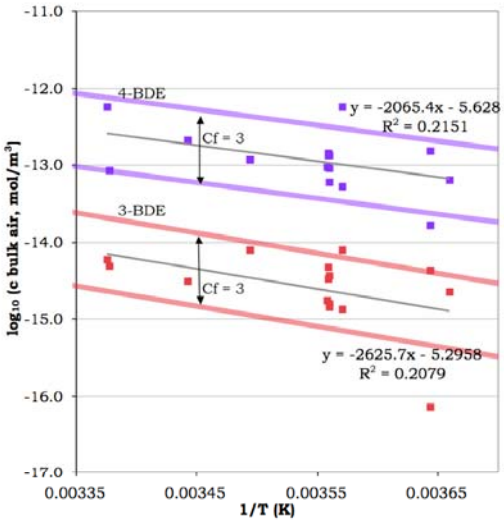

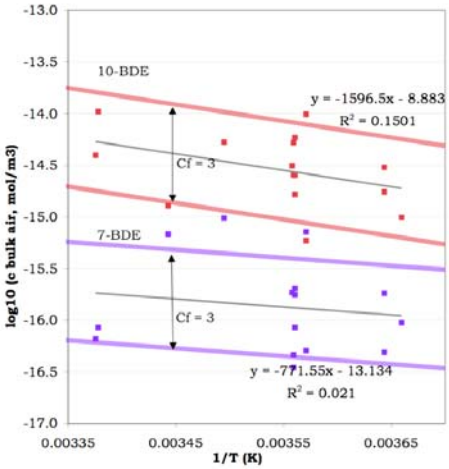

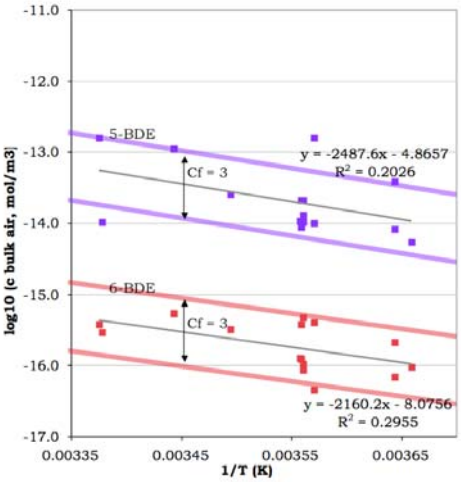

Summary of linear regressions:

	Slope (a)	**Intercept (b)**
Tri-BDE	-2626	-5.3
Tetra-BDE	-2065	-5.6
Penta-BDE	-2488	-4.9
Hexa-BDE	-2160	-8.1
Hepta-BDE	-772	-13.1
Deca-BDE	-1597	-8.9

$$\log C_{air,bulk,i} = a \cdot \frac{1}{T} + b \quad (4\text{-}51)$$

$C_{air,\ bulk,\ I}$ is the bulk concentration in air (mol/m³). T is the air temperature (K).

Figure 4-11: Bulk air concentration at Lake Thun as a function of temperature. Plots show empirical data with (individual measurements).

The input in the lake can then be calculated by:

$$q_{a,i} = c_{air,bulk,i} \cdot \text{wind} \cdot (h \cdot w) \quad (4\text{-}52)$$

$q_{a,i}$	Input mass flow for chemical i into the atmospheric compartment	mol h^{-1}
$c_{air,bulk,i}$	Bulk concentration in air	mol/m³
wind	Wind speed	m h^{-1}
h	Height of atmospheric compartment	m
w	Width of atmospheric compartment	m

The same analysis was performed for PCBs. The resulting slopes and intercepts are given in Table 4-17.

Table 4-17: Linear regressions of bulk atmospheric concentration versus temperature for PCB measurements at Lake Thun

	Slope (a)	Intercept (b)
Tri-CB-28	-3259	-2.4
Tetra-CB-52	-3094	-2.8
Penta-CB-101	-3256	-2.4
Hexa-CB-138	-3447	-2.0
Hexa-CB-153	-3241	-2.8
Hepta-CB-180	-2999	-4.2

4.7.2. Input by rivers

The input by rivers was estimated from measurements in the Aare and Kander, the two main tributaries to Lake Thun. Together they provide about 90% of the water input. In Table 4-18 a hydrological balance for Lake Thun is provided. The river Simme discharges into the river Kander before the Kander discharges into Lake Thun. Input by rain directly to the surface is low compared to the input by tributaries. Neglected in the water balance are additional tributaries and evaporation from lake surface which cause the gap between input and output in the balance presented.

Table 4-18: Hydrological balance for Lake Thun. Average values for year 2006 used (in m^3/s)

		average 2006 m^3/s
INPUT	Rain	1.8
	Aare	59.6
	Kander	18.9
	Simme	22.5
	Sum	102.7
OUTPUT	Aare Thun	112

Unfortunately, the sampling and analytics for the water phase is still not elaborated enough to provide exact data. For many congeners the measurements were below detection limit, i.e. below 5 times the blank value. However, the samples taken were the only basis on which input by rivers could be estimated.

For the Lake Thun case study weighted average concentration (60% Aare, 40% Kander) were used, which are then multiplied with the seasonal volumetric flow of the Aare in Thun (outflow) in the model. It is thus assumed that all inflows are equal to the outflow, which neglects evaporation. No seasonal variation of the input concentration was included, since no data was available to observe such an effect.

Table 4-19: Input concentrations in the tributaries used in the Lake Thun case study

	Aare mol/m³	Kander mol/m³	Weighted average mol/m³
Tri-CB-28	6.2E-12	8.2E-12	7.0E-12
Tetra-CB-52	1.1E-11	1.1E-11	1.1E-11
Penta-CB-101	1.0E-11	1.2E-11	1.1E-11
Hexa-CB-138	1.0E-11	1.6E-11	1.2E-11
Hexa-CB-153	1.1E-11	1.7E-11	1.4E-11
Hepta-CB-180	1.4E-11	2.0E-11	1.7E-11
Di-BDE	0	0	0
Tri-BDE	2.2E-13	3.8E-13	2.8E-13
Tetra-BDE	1.1E-11	2.3E-11	1.6E-11
Penta-BDE	1.5E-12	4.5E-12	2.7E-12
Hexa-BDE	0	1.8E-13	7.0E-14
Hepta-BDE	2.8E-13	1.1E-12	6.0E-13
Octa-BDE	0	0	0
Nona-BDE	0	0	0
DEca-BDE	1.0E-11	3.5E-11	2.0E-11

4.8. Temperature dependence of partitioning

Partition coefficients are temperature dependent and consequently fugacity capacity change with temperature.

The general equation for the temperature dependence of a partition constant is:

$$\ln K(T_2) = \ln K(T_1) - \frac{\Delta U}{R} \cdot \left(\frac{1}{T_2} - \frac{1}{T_1} \right) \quad (4\text{-}53)$$

where K is the partition constant at temperature T_1 and T_2 respectively, ΔU is the inner energy of phase transition (in J mol^{-1}) that is described with the partition constant, R is the universal gas constant (8.314 J K^{-1} mol^{-1}) and T is the temperature (K).

If partition coefficients are linearly dependent on their underlying partition constants, the adaptation of the partition coefficient to the ambient temperature can be carried out with the inner energy of phase transition of the corresponding partition constant. For instance, the aerosol-air partition coefficient at standard temperature can be converted to the aerosol-air partition coefficient at ambient temperatures by applying equation (4-44) and the energy of phase transition from octanol to air.

A problem arises in assessing partitioning in the environment, because phases might have different temperatures. Particularly lake water temperatures deviate from air temperatures. In this case, inner energy of dissolution for the two phases need to be considered in order to derive a partition constant for phases with

different temperatures. With the example of the air-water partition constant (K_{aw}) , the temperature dependence can be calculated by:

$$K_{aw}(T_{a,2},T_{w,2}) = \frac{S_a(T_{a,2})}{S_w(T_{w,2})} = \frac{S_a(T_1)\cdot\exp\left[-\frac{\Delta U_a}{R}\cdot\left(\frac{1}{T_{a,2}}-\frac{1}{T_1}\right)\right]}{S_w(T_1)\cdot\exp\left[-\frac{\Delta U_w}{R}\cdot\left(\frac{1}{T_{w,2}}-\frac{1}{T_1}\right)\right]} \quad (4\text{-}54)$$

$$= K_{aw}(T_1)\cdot\exp\left[\frac{1}{R}\cdot\left(\Delta U_w\cdot\left(\frac{1}{T_{w,2}}-\frac{1}{T_1}\right)-\Delta U_a\cdot\left(\frac{1}{T_{a,2}}-\frac{1}{T_1}\right)\right)\right]$$

where S_a is the solubility in air, S_w is the solubility in water, ΔU_a the inner energy of vaporization, ΔU_w the inner energy of dissolution in water, $T_{a,2}$ and $T_{w,2}$ the ambient temperatures of air and water respectively and T_1 the temperature where K_{aw} is known (usually 298.15 K).

The problem remains, which temperature in a specific media should be chosen. In the air compartment, temperatures do not differ very much with height, at least not within the 260m, which was used as atmospheric compartment height in the Lake Thun case study. In the lake however, temperature differences between surface and bottom water are high. While surface water temperatures reach 20° in summer in Lake Thun, the bottom water temperature remains between 4-5° throughout the year.

There is some trade-off in choosing the appropriate temperature for the water compartment. The surface temperature would be the correct one to describe air-water diffusion exchange, while an average temperature in the lake water would be needed to describe an average fugacity capacity and thus to correctly describe the water-suspended particles partitioning, while finally for the sediment pore-water, the bottom water temperature at the lake bottom would be appropriate.

It was therefore decided to calculate two different K_{aw} in the model, one with the surface temperature (T_s) and one with the bottom lake temperature (T_b). The $K_{aw}(T_a,T_b)$ is used to calculate Z_{pw}, the $K_{aw}(T_a,T_s)$ is used to calculate Z_w. Hence, Z_w, which defines the fugacity capacity of the (whole) lake water, is defined with the surface temperature. This was assumed to be most appropriate in order to correctly quantify the diffusive transport between the atmosphere and the lake water. This approach makes also sense with regard to the comparison of the model with measurements, which have been taken at the lake surface.

For the calculation of the temperature dependence of K_{sw} (particle-water partition coefficient) and K_{fw} (fish-water partition coefficient), the average between surface and bottom water temperatures was used.

These simplifications in calculating the temperature dependence of partition coefficients will cause some errors. However, these could only fully be omitted, if the lake water compartment is divided up into multiple individual boxes, for which partition coefficients (and fugacity capacities) are calculated individually.

5. Algebraic solution

Mass balance equations for each compartment are set up by the following principle:

$$\Delta M = Input - Output \quad (5\text{-}1),$$

where the change of the mass in a compartment is defined by the difference of inputs and outputs. Inputs include the input into the system from outside and the inputs from the other compartments. The inputs from the other compartments are dependent on the fugacity in these compartments. The outputs are the output out of the system and the mass flows into the other compartments.

Mass balance equations can be formulated by differential equations for each compartment.

The equations result in a differential equation system, which can be written in the matrix form:

$$\begin{pmatrix} \dot{m}_a \\ m_w \\ m_s \end{pmatrix} = \begin{pmatrix} D_a & D_{wa} & D_{sa} \\ D_{aw} & D_w & D_{sw} \\ D_{as} & D_{ws} & D_s \end{pmatrix} \cdot \begin{pmatrix} f_a \\ f_w \\ f_s \end{pmatrix} + \begin{pmatrix} q_a \\ q_w \\ q_s \end{pmatrix} \quad (5\text{-}2)$$

or:

$$\dot{\underline{M}} = \underline{\underline{D}} \cdot \underline{f} + \underline{q} \quad (5\text{-}3)$$

M is the vector for the total masses in the three different compartments, f is the vector of fugacities in the three compartments and q is the vector of inputs into the three compartments from outside of the system.

The D-matrix is set up with the different D values as in equation (5-1) and as defined in the transport processes in chapter 4.

$D_a = - (D_{deg,a} + D_{dd} + D_{wet,total} + D_{awd} + D_{a,out})$

$D_{wa} = D_{awd}$

$D_{sa} = 0$ (no direct flow from sediment into air)

$D_{aw} = D_{dd} + D_{wet,total} + D_{awd}$

$D_w = - (D_{deg,w} + D_{awd} + D_{sed} + D_{wsd} + D_{wout})$

$D_{sw} = D_{res} + D_{wsd}$

$D_{as} = 0$ (no direct flow from air to sediment)

$D_{ws} = D_{sed} + D_{wsd}$

$D_s = - (D_{deg,s} + D_{res} + D_{wsd} + D_{sb})$

5.1. Multi-chemical mass balance

Equation (5-2) can only be used for individual chemicals. However, for the assessment of PBDEs, formation of chemicals from other chemicals needs to be

included, since by debromination lower brominated congeners can be formed from the higher brominated ones. In the case of PBDEs, 9 homologues are considered and consequently the equation (5-2) can be written 9 times leading to 27 differential equations. By setting up the equations in matrix form below each other, it is possible to include the terms for formation of compounds by degradation of others.

$$\begin{pmatrix} \dot{\underline{M}}_1 \\ \dot{\underline{M}}_2 \\ \dots \\ \dot{\underline{M}}_n \end{pmatrix} = \begin{pmatrix} \underline{\underline{D}}_1 & \underline{\underline{B}}_{12} & \dots & \underline{\underline{B}}_{1n} \\ \underline{\underline{B}}_{21} & \underline{\underline{D}}_2 & & \\ \dots & & \dots & \\ \underline{\underline{B}}_{n1} & & & \underline{\underline{D}}_n \end{pmatrix} \cdot \begin{pmatrix} \underline{f}_1 \\ \underline{f}_2 \\ \dots \\ \underline{f}_n \end{pmatrix} + \begin{pmatrix} \underline{q}_1 \\ \underline{q}_2 \\ \dots \\ \underline{q}_n \end{pmatrix} \quad (5\text{-}4)$$

where B_{ij} represent 3x3 matrices and are defined as:

$$B_{ij} = R_{ij}^{bio} \cdot \begin{pmatrix} D\deg(a,bio,j) & 0 & 0 \\ 0 & D\deg(w,bio,j) & 0 \\ 0 & 0 & D\deg(s,bio,j) \end{pmatrix} + R_{ij}^{photo} \cdot \begin{pmatrix} D\deg(a,photo,j) & 0 & 0 \\ 0 & D\deg(w,photo,j) & 0 \\ 0 & 0 & D\deg(s,photo,j) \end{pmatrix} \quad (5\text{-}5)$$

and R_{bio} and R_{photo} are defined by:

$$R = \begin{pmatrix} r(c1 \to c1) & r(c2 \to c1) & \dots & r(cn \to c1) \\ r(c1 \to c2) & & & \\ \dots & & & \\ r(c1 \to cn) & & & r(cn \to cn) \end{pmatrix} \quad (5\text{-}6)$$

R_{ij} represents the element in row i and column j of the R matrix and $r(c_j \to c_i)$ is the fraction of debromination on the total degradation. Two separate R-matrices are defined, one for biodegradation and one for photodegradation, since both degradation pathways might include debromination.

Equation (5-3) can be written as:

$$\dot{\underline{M}}^* = \underline{\underline{A}} \cdot \underline{f}^* + \underline{q}^* \quad (5\text{-}7),$$

where the superscript(*) has been introduced in order to distinguish between equation (5-7) and equation (5-3). Note, that $\underline{f}^*$ in equation (5-7) is a vector with 27 elements (3 compartments and 9 compounds), while $\underline{f}$ in equation (5-3) is a vector of 3 elements.

5.2. Level III solution

The level III solution is defined by solving the mass balance equations for steady state conditions (see Mackay, 2001, for detailed explanation of the terms level I – level IV for multimedia models).

In the model presented here two different solving approaches were established; one if all the input concentrations are known and one if the concentration in the atmosphere and input concentration in river is known.

5.2.1. Solution for known input concentration

Steady state conditions mean that there is no change in mass in a compartment with time. The mass derivative in equation (5-7) becomes zero. Then, one can solve the right side of the equation to obtain the fugacity vector f.

$$0 = \underline{\underline{A}} \cdot \underline{f^*} + \underline{q^*}$$

$$\underline{f^*} = -A^{-1} q^* \qquad (5\text{-}8)$$

Since fugacities of phases in equilibrium are equal by definition, the fugacity for bulk compartments is identical to the fugacity of the phases within these compartments.

Concentrations of compounds within the phases are then calculated by applying equation (4-6) and using the fugacity of the corresponding bulk compartment and the fugacity capacity of the respective phase.

5.2.2. Solution for known compartment concentration

For the second solution modus, the solution of the mass balance becomes slightly more complicated, because for some mass balance equations the input term (q) is known, while for others, the fugacity (f) is known.

To solve the mass balance equation system, the equations need to be separated. Equation system (5-9) only contains the mass balances for the water and the sediment compartment. Intercompartmental processes involving the air are added to the q vector. The mass flow from air to water is represented by D_{aw} and f_a, which both are known. D_{as} is zero since there is no direct mass flow from the atmosphere to the sediment. However it is included here for completeness, because this approach can also be used for mass balance equation systems representing other compartments and media.

$$\begin{pmatrix} \dot{m}_w \\ m_s \end{pmatrix} = \begin{pmatrix} D_w & D_{sw} \\ D_{ws} & D_s \end{pmatrix} \cdot \begin{pmatrix} f_w \\ f_s \end{pmatrix} + \begin{pmatrix} q_w + D_{aw} \cdot f_a \\ q_s + D_{as} \cdot f_a \end{pmatrix} \qquad (5\text{-}9)$$

For the Level III solution the mass derivatives are again set to zero. The equation system can then be solved for the fugacity vector since all other terms are known.

$$\begin{pmatrix} f_w \\ f_s \end{pmatrix} = -\begin{pmatrix} D_w & D_{sw} \\ D_{ws} & D_s \end{pmatrix}^{-1} \cdot \begin{pmatrix} q_w + D_{aw} \cdot f_a \\ q_s + D_{as} \cdot f_a \end{pmatrix} \qquad (5\text{-}10)$$

The calculated fugacity in water and sediment can then be used to calculate the input into the air compartment (q_a). The mass balance for the air compartment just needs to be solved for q_a, which is shown by equations (5-11a) and (5-11b)

$$\dot{m}_a = D_a \cdot f_a + D_{wa} \cdot f_w + D_{sa} \cdot f_s + q_a \qquad \text{(5-11a)}$$

$$q_a = -(D_a \cdot f_a + D_{wa} \cdot f_w + D_{sa} \cdot f_s) \qquad \text{(5-11b)}$$

This approach is extendable for multi-chemical mass balances, which is:

$$\begin{pmatrix} \dot{\underline{M}}_1^{\times} \\ \dot{\underline{M}}_2^{\times} \\ \dots \\ \dot{\underline{M}}_n^{\times} \end{pmatrix} = \begin{pmatrix} \underline{\underline{D}}_1^{\times} & \underline{\underline{B}}_{12}^{\times} & \dots & \underline{\underline{B}}_{1n}^{\times} \\ \underline{\underline{B}}_{21}^{\times} & \underline{\underline{D}}_2^{\times} & & \\ \dots & & \dots & \\ \underline{\underline{B}}_{n1}^{\times} & & & \underline{\underline{D}}_n^{\times} \end{pmatrix} \cdot \begin{pmatrix} \underline{f}_1^{\times} \\ \underline{f}_2^{\times} \\ \dots \\ \underline{f}_n^{\times} \end{pmatrix} + \begin{pmatrix} \underline{q}_1^{\times} + \underline{N}_1 \\ \underline{q}_2^{\times} + \underline{N}_2 \\ \dots \\ \underline{q}_n^{\times} + \underline{N}_n \end{pmatrix} \qquad \text{(5-12)}$$

where,

$$\underline{N}_i = \begin{pmatrix} D_{aw,i} \cdot f_{a,i} \\ D_{as,i} \cdot f_{a,i} \end{pmatrix} \quad \underline{M}_i^{\times} = \begin{pmatrix} m_{w,i} \\ m_{s,i} \end{pmatrix} \quad \underline{D}_i^{\times} = \begin{pmatrix} D_{w,i} & D_{sw,i} \\ D_{ws,i} & D_{s,i} \end{pmatrix}$$

$$B_{ij} = R_{ij}^{bio} \cdot \begin{pmatrix} D_{\deg(w,bio,j)} & 0 \\ 0 & D_{\deg(s,bio,j)} \end{pmatrix} + R_{ij}^{photo} \cdot \begin{pmatrix} D_{\deg(w,photo,j)} & 0 \\ 0 & D_{\deg(s,photo,j)} \end{pmatrix}$$

The equation system (5-12) can be written in short form as:

$$\dot{\underline{M}}^{\times} = \underline{\underline{A}}^{\times} \cdot \underline{f}^{\times} + \underline{q}^{\times} + \underline{N}^{\times} \qquad \text{(5-13)}$$

This equation system can easily be solved for f^{x}.

$$0 = \underline{\underline{A}}^{\times} \cdot \underline{f}^{\times} + \underline{q}^{\times} + \underline{N}^{\times}$$

$$\underline{f}^{\times} = -\left(\underline{\underline{A}}^{\times}\right)^{-1}\left(\underline{q}^{\times} + \underline{N}^{\times}\right) \qquad \text{(5-14)}$$

and again, the calculated fugacity vector can be used to calculate the q vector in the air compartment mass balance.

The mass balance for the air compartment including degradation of compounds into other compounds is:

$$\begin{pmatrix} \dot{m}_{a,1} \\ m_{a,2} \\ \dots \\ m_{a,n} \end{pmatrix} = \begin{pmatrix} D_{\deg,a,1} \cdot f_{a,1} + D_{wa,1} \cdot f_{w,1} + D_{sa,1} \cdot f_{s,1} \\ D_{\deg,a,2} \cdot f_{a,2} + D_{wa,2} \cdot f_{w,2} + D_{sa,2} \cdot f_{s,2} \\ \dots \\ D_{\deg,a,n} \cdot f_{a,n} + D_{wa,n} \cdot f_{w,n} + D_{sa,n} \cdot f_{s,n} \end{pmatrix} +$$

$$\left(\begin{pmatrix} r(c1 \to c1) & r(c2 \to c1) & \dots & r(cn \to c1) \\ r(c1 \to c2) & \dots & & \\ \dots & & \dots & \\ r(c1 \to cn) & & & r(cn \to cn) \end{pmatrix}^{PHOTO}_{\bullet} \cdot \begin{pmatrix} D_{\deg,a,photo,1} & D_{\deg,a,photo,2} & \dots & D_{\deg,a,photo,n} \\ D_{\deg,a,photo,1} & \dots & & \\ \dots & & \dots & \\ D_{\deg,a,photo,1} & & & D_{\deg,a,photo,n} \end{pmatrix} \right) \cdot \begin{pmatrix} f_{a,1} \\ f_{a,2} \\ \dots \\ f_{a,n} \end{pmatrix} + \begin{pmatrix} q_{a,1} \\ q_{a,2} \\ \dots \\ q_{a,n} \end{pmatrix}$$

(5-15)

The term $D_{deg,a,photo.i}$ is the D-value for photodegradation in the atmosphere. The point after the R-matrix represents an array multiplication. An array operation is processing the operation element by element, which means in this case that the first element in the R matrix is multiplied with the first element of the D_{deg} matrix and so on. Both matrices have the same dimensions and the result is again a matrix with the same dimensions.

The R-matrix specifies the ratio of debromination to total degradation as defined above.

The equation can also be written in short form:

$$\underline{\dot{M}_a} = \underline{\underline{N_a}} + \left(\underline{\underline{R_{photo}}}_{\bullet} \cdot \underline{\underline{D_{\deg,photo}}} \right) \cdot \left(\underline{f_a} \right) + \underline{q_a} \qquad (5\text{-}16)$$

Since biodegradation does not take place in the atmosphere, it was not included. However, if the equation is applied to other phases biodegradation needs to be included, which is done by the following way.:

$$\underline{\dot{M}_a} = \underline{\underline{N_a}} + \left(\underline{\underline{R_{photo}}}_{\bullet} \cdot \underline{\underline{D_{\deg,photo}}} + \underline{\underline{R_{bio}}}_{\bullet} \cdot \underline{\underline{D_{\deg,bio}}} \right) \cdot \left(\underline{f_a} \right) + \underline{q_a} \qquad (5\text{-}17)$$

The solution for Level III is then:

$$\begin{aligned} 0 &= \underline{\underline{N_a}} + \left(\underline{\underline{R_{photo}}}_{\bullet} \cdot \underline{\underline{D_{\deg,photo}}} + \underline{\underline{R_{bio}}}_{\bullet} \cdot \underline{\underline{D_{\deg,bio}}} \right) \cdot \left(\underline{f_a} \right) + \underline{q_a} \\ \underline{q_a} &= -\left(\underline{\underline{N_a}} + \left(\underline{\underline{R_{photo}}}_{\bullet} \cdot \underline{\underline{D_{\deg,photo}}} + \underline{\underline{R_{bio}}}_{\bullet} \cdot \underline{\underline{D_{\deg,bio}}} \right) \cdot \left(\underline{f_a} \right) \right) \end{aligned} \qquad (5\text{-}18)$$

5.3. Level IV solution

The level IV solution represents the dynamic solution of the differential mass balance equations. Three different solutions for the level IV model have been included.

- Analytical solution of differential equation system
- Numerical solution 1, with MATLAB ODE Solver
- Numerical solution 2, self-programmed, with small iterative steps

An analytical solution developed for the CliMoChem model has been used (Scheringer et al., 2000). The analytical solution has the advantage to be very fast and mathematically accurate. However, a major drawback is, that no parameters can be changed unless the analytical solution has to be recalculated. The mathematical accuracy of the analytical solution can therefore be outweighed by the fact that environmental parameters that have determined the solution are not representative for the whole period of time for which the analytical solution has been calculated. Due to this fact, the analytical solution has to be calculated again for each season when parameters are changed. If the model wants to be used in high time resolution for environmental parameters (e.g. daily temperature values), the high number of analytical recalculations could make the program slow.

Since computers nowadays are able to perform large number of iterations in short time, numerical solutions are a good option to solve differential equation

systems. The advantage of numerical solutions are the possibilities to change parameters at any time. It is thus easier to perform calculations which have a high time resolution. MATLAB has integrated solvers for ordinary differential equations (ODEs), which are based on different methods. The solvers and underlying methods are described in the MATLAB help files. There are 7 ODE Solvers implemented in MATLAB. It was observed that the differential equations set up in the model are stiff, which means that some numerical solutions are unstable unless an extremely small time step is chosen. Therefore the solver ODE23s provided by MATLAB was used which can handle stiff differential equations.

The third solution alternative has the advantage that it can be modified easily in the program code. The solution integrates the differential equations for small time-steps (Δt) assuming that the fugacity within these steps are constant. Thus, a fugacity change (Δf) is obtained which can be added to the fugacity at time t to obtain the fugacity at time $t+\Delta t$. Δt was set to 0.01 h in the Lake Thun case study, which approved to result in stable solutions.

The differential equation system needs to be reformed in order to get the derivative for the fugacity. This is done by dividing both sides of the differential equation system presented in the previous chapter by ($V \cdot Z_b$), where V is the volume vector containing the volumes of all compartments and Z_b is the bulk fugacity vector containing the bulk fugacity of all compartments. The bulk fugacity for the atmosphere is calculated with formula (4-23), the bulk fugacity capacity for the other compartments is calculated in analogue way.

The transformation is shown the example of equation (5-3):

$$\dot{\underline{M}} = \underline{\underline{D}} \cdot \underline{f} + \underline{q} \qquad (5\text{-}3)$$

Division by ($V \cdot Z_b$) leads to:

$$\begin{aligned} \frac{\dot{\underline{M}}}{\underline{V} \cdot \underline{Z_b}} &= \frac{\underline{\underline{D}}}{\underline{V} \cdot \underline{Z_b}} \cdot \underline{f} + \frac{\underline{q}}{\underline{V} \cdot \underline{Z_b}} \\ = \dot{\underline{f}} &= \frac{\underline{\underline{D}}}{\underline{V} \cdot \underline{Z_b}} \cdot \underline{f} + \frac{\underline{q}}{\underline{V} \cdot \underline{Z_b}} \end{aligned} \qquad (5\text{-}19)$$

5.4. Model outputs

The model can be applied to calculate concentrations (or mass) in different media either under steady state conditions or dynamic as a function of time. This is of particular interest in order to compare results with measurements. With the equations presented in chapter 4 for transport processes, the intercompartmental mass flows can be calculated. The model outputs will thus comprise concentrations in all media, mass in each media and intercompartmental mass flows as well as mass flows across the system boundary. All these outputs are obtained for the whole set of chemicals.

6. Sensitivity analysis and model uncertainty

6.1. Sensitivity of individual parameters

Model results are dependent on various parameters and hence on their uncertainty. Calculating a model output by using mean values for all parameters does not tell anything about the uncertainty of the results.

The sensitivity of the model results was therefore assessed with a sensitivity analysis, where each parameter was changed and the influence on the model results observed.

For each parameter, minimum and maximum value were defined with a confidence factor (Cf). The confidence factor for a parameter value X is defined as follows:

$$probability\left\{\frac{\mu}{Cf} < X < Cf \cdot \mu\right\} = 0.95 \qquad (6\text{-}1)$$

Meaning that the confidence interval (95%) goes from μ/Cf to μ·Cf, when μ is the expectation of X.

With consecutive model runs, each parameter was varied separately by setting the parameter to its minimum for one model run and then setting the parameter to its maximum for the next model run.

Two different sensitivity indicators were computed; relative sensitivity and sensitivity index. Relative sensitivity is defined as the change of an output value in relation to the output value. The sensitivity index is defined as the relative sensitivity in relation to the relative change of the parameter.

$$Sr = \frac{\Delta O}{O} \qquad (6\text{-}2) \qquad\qquad S = \frac{\frac{\Delta O}{O}}{\frac{\Delta I}{I}} \qquad (6\text{-}3)$$

Sr	relative sensitivity
S	sensitivity index
O	model output value
I	parameter (model input value)

The relative sensitivity is an indicator of how much the result will change as a result of changing an input parameter. By contrast to the sensitivity index, it takes the variance of input parameters into account. It thus includes both factors (influence of the input parameter and variance of the input parameter) that have affect output value. Relative sensitivity informs best about where improvements in the model parameterization would be advantageous. Those parameters with a high relative sensitivity should be considered first, since they either have high variance and/or high influence on the result.

The sensitivity index is a normalized indicator and does only tell us something about the influence of a parameter on the result but nothing about the input

parameter uncertainty. It is the advantage of the sensitivity index that it is independent of the uncertainty of input parameters (namely the Cf of parameters). For many parameters the Cf's are based on assumptions and might be over- or underestimated which then can lead to too high or too low relative sensitivities (Sr) but do not affect the sensitivity index (S).

6.2. Model output uncertainty

In order to assess the uncertainty of model outputs the propagation of uncertainties in input parameters through the model needs to be addressed. Two different approaches were considered in this work:

- Analytical uncertainty propagation method according to MacLeod et al. (2002)
- Monte Carlo simulation

6.2.1. Analytical uncertainty propagation method

A method to analyze uncertainty of model outputs was proposed by MacLeod et al. (2002). The approach is based on the assumptions that there exist linear relationships between input parameters and model outputs, independence of input parameters and log-normal distribution of input parameters.

These assumptions may cause some error in the calculated uncertainty. There are non-linear mathematical operations in the model, as for instance the calculation of temperature dependence of partition constants (with inner energies and temperature) and not all parameters are independent, as for example the partition constants. Log normal distribution is likely to be a good choice when the exact shape of the parameter distribution is not known (MacLeod et al., 2002). However, here it is important that input parameters are provided in a form where log-normal distribution is expected. Partition constants should therefore be used in the input in a non-logarithmic form, since the logarithm of the partition constant is expected to be normal distributed. Temperature values should be provided in absolute temperature (Kelvin) rather than units of Celsius, since log-normal distribution can only include positive numbers.

For each parameter two indicators need to be known; the sensitivity index and the confidence factor. The sensitivity index is calculated as described above (equation 6-3) where the input parameter modification is set to 0.1% ($\Delta I/I=0.001$) as proposed by MacLeod et al. (2002). The confidence factor of input parameters (Cf_i) is defined above.

A confidence factor for a specific output can then be calculated with

$$Cfo_j = \exp\left[S_{I_1,j}^2 \left(\ln Cf_{I_1}\right)^2 + S_{I_2,j}^2 \left(\ln Cf_{I_2}\right)^2 + ... + S_{I_1,j}^2 \left(\ln Cf_{I_n}\right)^2 \right]^{1/2} \qquad (6\text{-}4)$$

where Cfo_j is the confidence factor for the model output j, $S_{I,j}$ is the sensitivity index for parameter I to the output j and Cf_I is the confidence factor of the parameter I.

Definition of confidence factors

As described in chapter 2.1.3, a relative variance on a scale from 2-4 was attributed to the partition constants. The relative variance was set to 2, if 2 or more values were within ¼ log unit or 3 or more values within ½ log unit. It was thus assumed that the confidence interval for values with a relative variance of 2 is less than +/- 1 log unit. On the other hand it was assumed that the confidence interval for values with a relative variance of 3 is a more than +/- 1 log unit. Therefore a confidence factor of 10 (1 log unit) was attributed to a relative variance of 2.5. The confidence factor can thus be calculated from the relative variance by:

$$Cf = 10^{\left(2\cdot\sqrt{\alpha\cdot \text{rel.variance}}\right)} \quad (6\text{-}5)$$

where α is the conversion factor from relative variance to real variance, which is 0.1 in order to fulfill the condition that a confidence factor of 10 corresponds to a relative variance of 2.5. Note, that the square root of the real variance is equal to the standard deviation and the confidence interval is two times the standard deviation.

The least-squares-adjustment method (as described in chapter 2.1.3) reduces the variance and thus relative variance values for the least squares-adjustment outputs are lower than the relative variance scores defined before the adjustment. Table 6-1 summarizes the relative variance outputs for the adjusted property data and shows the corresponding Cf calculated with equation (6-5). The Cf for Octa- and Nona-BDE were set to the highest Cf of the other congeners, since these values were extrapolated and therefore no relative variance value was available. The relative variance for Penta-BDE was set to the maximum of the values for BDE-99 and BDE-100.

Table 6-1: Confidence factors (Cf) derived from relative variances (Rv) for partition constants.

BDE	K_{aw}		K_{ow}		K_{oa}	
	Rv	Cf	Rv	Cf	Rv	Cf
Di-BDE	1.33	5.4	3.00	12.5	4.33	20.7
Tri-BDE	1.24	5.0	1.94	7.6	2.12	8.3
Tetra-BDE	1.38	5.5	1.97	7.7	2.16	8.5
Penta-BDE	1.79	7.0	2.04	8.0	2.30	9.1
Hexa-BDE	1.93	7.6	2.48	9.9	2.48	9.9
Hepta-BDE	4.00	18.4	3.00	12.5	3.00	9.9
Octa-BDE		*18.4*		*18.4*		*61.5*
Nona-BDE		*18.4*		*18.4*		*61.5*
Deca-BDE	4.00	18.4	4.00	18.4	8.00	61.5

There was usually only one literature value for each inner energy, which makes the value quite uncertain. However, the values do not differ much between different congeners. For ΔU_{aw} the highest deviation from the mean of all congeners is 26% (factor 1.26), for ΔU_{ow} the highest is 100% (factor 2) and for ΔU_{oa} the highest deviation is 21% (factor 1.21). The uncertainty for one congener is likely to be

somewhat lower than the deviation between different congeners. For all inner energy data a confidence factor of 1.3 has been assumed, which should be more on the conservative side.

In the study about uncertainty propagation in models (MacLeod et. al. 2002) a factor of 3 was assumed for degradation rates. This appears to be quite low, when considering the difference among measurements of photolysis rates for instance (see chapter 4.5.1). Additionally to the variation in laboratory measurements, there is some uncertainty regarding the appropriateness to use these degradation derived from laboratory experiments as degradation rates in the environment. Therefore the confidence factor for all degradation rates was set to 10.

Table 6-2: Definition of confidence factors for some compound specific parameters

Parameter	Description	Cf
U	inner energy	1.3
deg	degradation rates	10
$c_{input, a}$	concentration in air input	3
$c_{input, w}$	concentration in water input	5

Meteorological and hydrological data was given high accuracy since most of them are specific for the Lake Thun environment. The highest uncertainty (Cf=2) was assumed for the OH-concentrations since these represent average values for the latitude where Lake Thun is, but they not specific for the site. The wet and dry periods (twet and tdry) are attributed a Cf of 1.4 which should reflect the fact that the durations of rain events are very variable. Solar radiation and rainfall rates showed variability around 10-20% between stations that are close to each other (see chapter 3.2.2 and chapter 4.5.1) and therefore Cf of 1.2 was assumed. A Cf of 1.5 for wind was assumed which should reflect that the measuring station in Interlaken is not exactly in the valley of Lake Thun. Water runoff measurements should be somewhat more confident and therefore a Cf of 1.2 was chosen. The temperatures in air and in the water were assumed to have a maximum variability of about +/- 5° which results in a Cf of 1.02. For the bottom lake water the variability is lower and therefore the Cf was set to 1.01.

For the compartment sizes an error of about 5% was assumed. The volume of the lake, the length and width of the compartments and the surface areas thus have a Cf of 1.05. The atmospheric height and the sediment volume were given a Cf of 2 since they are not well defined by a physical border.

For the aerosol concentrations and the suspended particle concentrations a factor of 3 was assumed which is estimated from the measurement data presented in chapter 4.1.. The volume fraction of fish was given a Cf of 2 since the value is based on an approximate estimation. The volume fraction of solid sediment can only have values between 0 and 1. A factor of 2, which results in a fraction between 0.1 and 0.4, seemed to be appropriate. Organic mass and organic carbon fractions in aerosols, suspended particles and sediment were all attributed a Cf of 1.5. Note, that organic mass fractions in aerosols have to be within 0 and 1, and organic carbon fraction of suspended particles and sediment between 0 and ~0.5. The lipid

content in fish was attributed a Cf of 1.4 which is estimated based on the measurements (Bogdal, 2007 and Naef, M., personal communication). For density in sediment, density in particles, diffusion velocity in air and diffusion velocity in water, the values were taken from the uncertainty propagation study by MacLeod et al. (2002). Dry deposition rates were assumed to have higher accuracy than diffusion velocities and thus a Cf of 1.5 was used. The uncertainty of scavenging efficiencies is not known, but 1.2 seemed to be appropriate since the values have to lie within 0 and 1. The velocities describing water-sediment exchange were set to 2, which is in the range of the uncertainties for the exchange velocities for atmosphere-water processes. The activation energy of biodegradation was given a Cf of 1.3 which is the same as for the inner energies (see above). The scavenging ratio and the air-raindrop volume ratio is based on assumptions for raindrop diameter and cloud height which have some high uncertainty and therefore a factor of 2 was assumed. The Cf for the parameter 'b' describing the Koc based on Kow was taken from Seth et al. (1999). Finally, for the fractions of degradation leading to lower brominated congeners a Cf of 1.2 was used which was the maximum possible value since the fraction needs to lie between 0 and 1. The confidence factors for the parameters used in the model are shown in Table 6-2.

The confidence factors of PCB partition constants were all assumed to be 5. All other confidence factors were defined as for the PBDEs.

Table 6-3: Confidence factors for input parameters used in the model

Parameter[1)]	Description	Assumed Cf
Ta	Air temperature	1.02
Ts	Lake surface temperature	1.02
Tb	Lake bottom temperature	1.01
OH	OH concentration	2
Ir	Irradiance (=Solar radiation)	1.1
kr	rainfall rate	1.1
twet	duration of rain event	1.4
tdry	duration of dry periods	1.4
qw	Water runoff	1.2
wind	wind speed (ms-1)	1.5
V(2)	Volume bulk water	1.05
V(3)	Volume bulk sediment	2
P(2,1)	Volume fraction coarse aerosols	3
P(3,1)	Volume fraction fine aerosols	3
P(5,1)	Volume fraction suspended particles	3
P(6,1)	Volume fraction fish	2
P(7,1)	Volume fraction solid sediment	2
Ar(1,1)	lake surface area	1.05
Ar(2,1)	sediment area	1.05
focP	organic mass fraction in suspended particles	1.5
focS	organic mass fraction in sediment	1.5
Omc	organic mass fraction coarse aerosols	1.5
Omf	organic mass fraction fine aerosols	1.5
Lip	lipid content of fish	1.4
densP	density of particles	1.5
densS	density of sediment	1.5
ka	diffusion mass transfer coefficient in air (air-water interface)	3
kw	diffusion mass transfer coefficient in water (air water interface)	3
kddc	dry deposotion rate coarse aerosols	1.5
kddf	dry deposotion rate fine aerosols	1.5
Ec	Scavenging efficiency coarse aerosols	1.2
Ef	Scavenging efficiency fine aerosols	1.2
Vra	Volume ratio rain air	2
kws	mass transfer coefficient sediment-water	2
kd	mass transfer coefficient deposition (water-sediment)	2
kres	mass transfer coefficient resuspension (sediment-water)	2
ksb	sediment burial velocity	2
Ea	Activation energy biodegradation	1.3
Qs	scavenginig ratio	2
b	Kow - Koc conversion factor	2.7
ht	height of atmospheric compartment	2
wh	width of atmospheric compartment	1.05
lh	length of atmospheric compartment	1.05

1) Variable name as used in the model code

6.2.2. Monte Carlo simulation

Monte Carlo simulation is a good method when the distributions of input parameters is well-known and when the three assumptions of the analytical uncertainty method (namely linear input – output relationships, independent input parameters, log-normal distribution of parameters) are an issue. Monte Carlo analysis can be useful for confirmation of the results obtained with the analytical uncertainty propagation method. The high computational power nowadays make it possible to conduct many iterative simulations in short time and since inclusion of a random number generator into the model code was relatively simple, the option to perform Monte Carlo analysis was also included into the model. MacLeod et al. (2002) showed that there is a satisfactory agreement between the analytical uncertainty propagation method and a Monte Carlo simulation in a case study with two different multimedia models. However, the model presented here and the lake Thun case study deviate from the models tested in their study.

For the Monte Carlo analysis also a log-normal distribution was assumed for all parameters. This could easily be changed in the model code by individually allocating a distribution to each parameter if more information on parameters become available.

A Monte Carlo analysis with 5'000 runs was performed, whereas parameters were changed in each run randomly within their given distribution. The log-normal distribution is defined by the mean (μ) and the standard deviation (σ) of the corresponding normal distribution, which can be derived as follows:

$$\sigma = \frac{1}{2}\ln Cf \quad \text{(6-6)} \quad \text{and} \quad \mu = \ln(\mu^*) \quad \text{(6-7)}$$

where μ^* is the mean of the log-normally distributed parameter.

6.2.3. The issue of interdependent parameters

Sensitivity analysis for partition constants needs some special consideration since partition constants are interdependent. When varying one partition constant, the other partition constants need to be adjusted, otherwise the thermodynamic relation between the partition constants would be violated.

An easy way to address this problem is to provide only two partition constants (e.g. K_{aw} and K_{ow}) and calculate the third one (e.g. K_{oa}) based on the provided constants. By applying this approach, the thermodynamic constraint (i.e. equation 2-2) is always fulfilled. The drawback is, that sensitivity of the third (calculated) constant cannot be assessed.

In the calculation of model output uncertainty the problem that partition constants are dependent on each other again occurs. Again, the best solution is to provide only two partition constants together with their uncertainties. However, this approach causes some problems. By calculating the third partition constants on the basis of the two other partition constants, an uncertainty of the third constant based on the uncertainty of the other two can be calculated. However, due to available literature data of the third constant, there might be knowledge about the

uncertainty of the third constant and this uncertainty might be lower than the uncertainty calculated from the other constants.

A more sophisticated way in addressing the problem is by applying an adjustment procedure as described in chapter 2 after one partition constant has been changed in the sensitivity or uncertainty analysis respectively. This adjustment procedure would change the other two parameters according to their relative variance. Schenker et al. provide a excel spreadsheet to perform this adjustment procedure. An implementation of this procedure into the model was not considered so far. A major drawback is that the model would expected to become significantly slower which possibly outweighs the advantage of the more comprehensive method to adjust partition constants.

Finally, another option to address this problem should be mentioned here. Each partition constant can be derived from a ratio of two solubilities. Solubilities are independent substance properties and it would be advantageous to provide solubilities in a model and then calculate the partition constants based on them. However, solubilities are usually not directly measured. Therefore, they need to be calculated from measured partition constants. Again, a problem to define the uncertainty in solubilities arise, since the uncertainty seen in measured partitioning data need to be split in a certain way to the uncertainty of the two solubilities defining that partition constant.

It would therefore be good to develop a method how to split the uncertainty observed in measurements of partition constant to the uncertainty in the underlying solubilities.

In the model applied to Lake Thun, only K_{aw} and K_{ow} are provided. K_{oa} is calculated by applying the thermodynamic constraint:

$$K_{oa} = \frac{K^*_{ow}}{K_{aw}}$$

where K^*_{ow} is the partition constant between dry octanol and water. It can be calculated (as proposed Schenker et al., 2005) by:

$$\log K^*_{ow} = 1.36 \cdot \log K_{ow} - 1.6 \qquad (6\text{-}8)$$

Other interdependent parameters are the energies of phase transition (ΔU) and the velocities describing sedimentation, resuspension and sediment burial. In the model, ΔU_{ow} was calculated from U_{aw} and U_{oa}, which were more reliable since there were no measurements available for the U_{ow} of PBDEs and the sedimentation velocity was calculated from the resuspension velocity and sediment burial velocity, which have lower uncertainties as mentioned above (chapter 4.4.8).

7. Results and discussion

7.1. Concentrations in steady-state model (Level III model)

7.1.1. Standard model run

The standard model run includes the parameters that were derived in chapter 4. Tables with the parameters are included in the *Appendix IV – Variable parameters* Appendix IV – and *Appendix V – Constant parameters*.

Modeled concentrations in the lake water compartment and in sediment were compared with measured concentrations in these media. The following congeners were measured in the samples taken at Lake Thun (Bogdal, 2007.):

- Tri-BDE-28
- Tetra-BDE-47
- Penta-BDE-99
- Penta-BDE-100
- Hexa-BDE-153
- Hepta-BDE-183
- Deca-BDE-209

In order to compare measurements with modeled values, the measurements of the two Penta congeners (BDE-99, BDE-100) were summed up. Note that there are no measurements for Di-, Octa- and Nona- BDEs.

In the following paragraphs, modeled and measured values are compared. The uncertainty indicated for the modeled values represents the 95% confidence interval obtained with Monte Carlo simulation. All results of the level III steady state model are presented for the month July 2007. Seasonal variation will be addressed with the dynamic solution (level IV model).

Lake water compartment

Two water samples of the Lake Thun surface water have been taken at the deepest point of the lake and one water sample has been taken from the outflowing river (Aare) in Thun, which also represents lake water (Bogdal, 2007). Dissolved and particulate fraction have been measured (the threshold is at 0.7 µm). Compounds adsorbed to particles smaller than 0.7 µm are thus counted to the dissolved fraction. The filters were weighed before and after the sampling in order to determine the concentration of particles in the water sample (Bogdal, 2007). This is needed in order to take into account the particle concentration of the sample, which might deviate from the average particle concentration in the lake that has been used in the model. The measured particle bound concentration were converted as follows:

$$c_{i,p}\left(\frac{\text{mol}}{\text{m}^3}\right) \xrightarrow{+C_{p,sample}\left(\frac{kg}{l}\right)} c_{i,p}\left(\frac{\text{mol}}{\text{kg}}\right) \xrightarrow{\cdot C_{p,\text{mod}el}\left(\frac{kg}{l}\right)} c'_{i,p}\left(\frac{\text{mol}}{\text{m}^3}\right)$$

Thus, the particle bound concentration is obtained that would have been measured in a sample that had exactly the particle concentration used in the model.

Unfortunately there is quite high uncertainty in the particle concentration of the sample, since humidity during the filter weighting procedure was not well controlled and therefore the weight of the particle filters were not measured very accurately.

The analytics of water samples involve some difficulties, since PBDE solubility is extremely low in water. Unfortunately, the performance of chemical analytics is not yet so well elaborated, which is reflected by the fact that many measurements were close to the blank samples. Generally, no quantitative analysis is possible when the measurement does not exceed the blank by more than a factor of 5, which can be regarded as the limit of quantification.

Modeled and measured values for the water compartment are shown in Figure 7-1 and Figure 7-2. In the dissolved phase, the modeled values for Tri-, Tetra- and Penta- and Hepta-BDE match with the measured values. Modeled Hexa-concentrations seem to be a bit too low, but the measurements did not exceed 5-times the blank, therefore it is likely that the real value is below the measurements. A big difference is only seen in the Deca-BDE concentration.

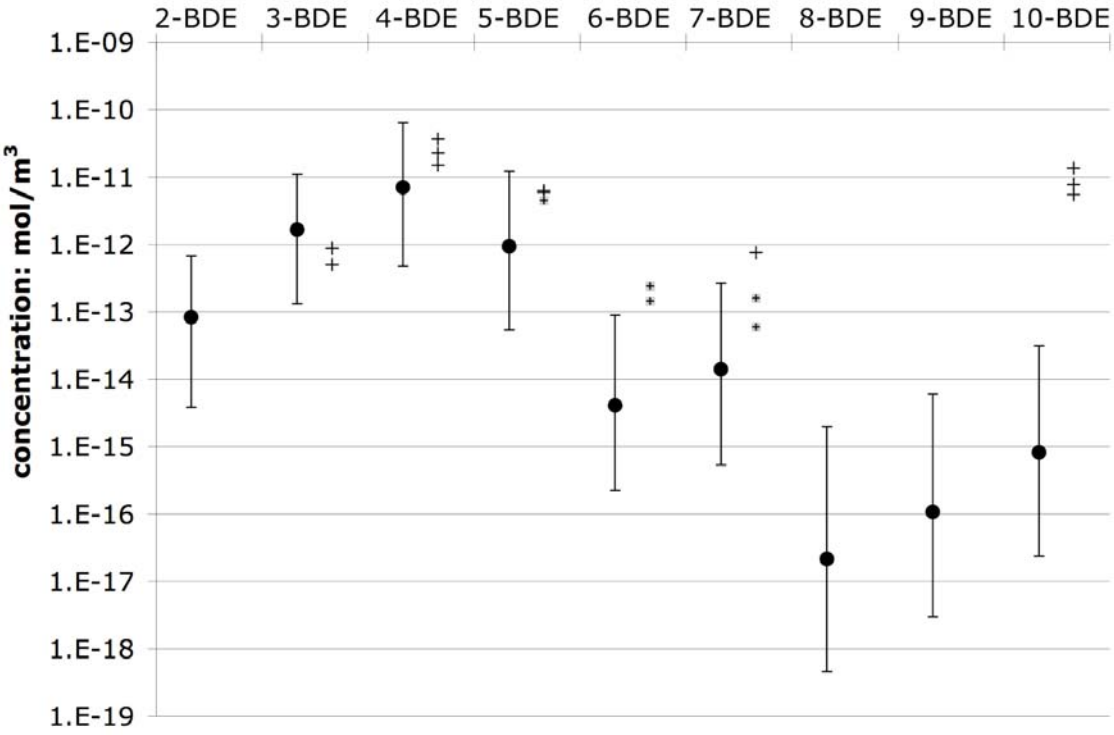

Figure 7-1: Dissolved concentrations in the lake water compartment. Black dots are point estimates of the model. The crosses represent measurements. Grey shaded crosses are measurements that do not exceed the blank measurement by more than a factor 5.

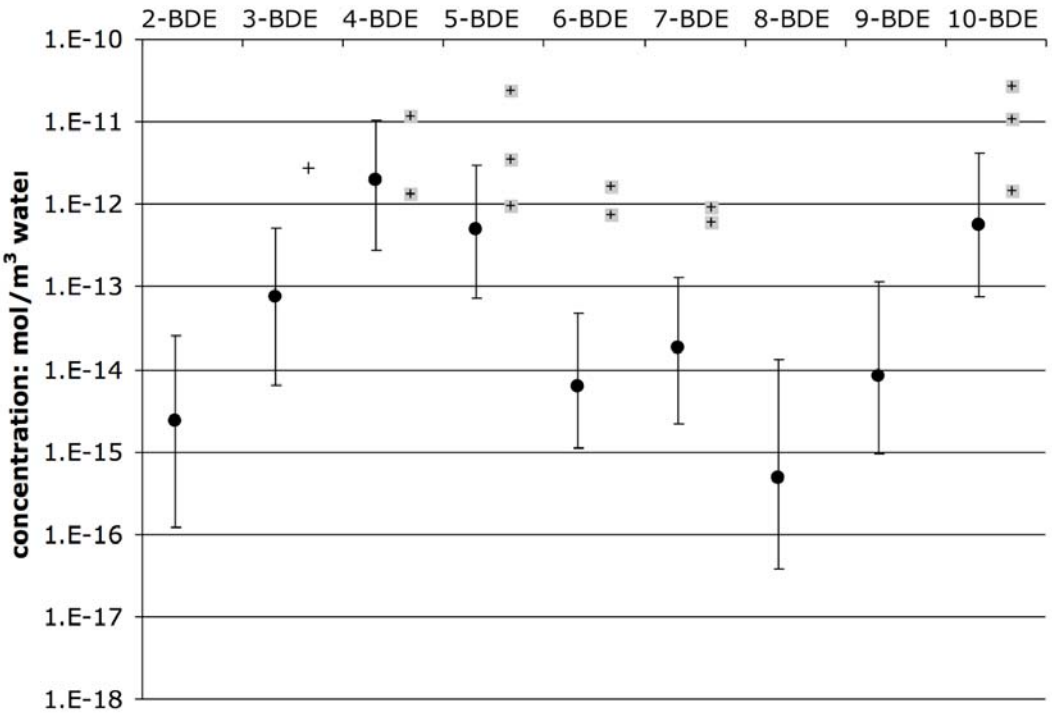

Figure 7-2: Particle bound concentrations in the lake water compartment. Black dots are point estimates of the model. The crosses represent measurements. Grey shaded crosses are measurements that do not exceed the blank measurement by more than a factor 5.

Except for Tri-BDE, the particle bound concentration does not exceed the limit of quantification in all samples and for all congeners. However, Tri-BDE was not detected in two of three samples, which increases the uncertainty in measurement for that value. The real concentration is therefore expected to lie below the measurements for all congeners, which is in correspondence with the modeled values, that tend to be lower than the measured values too.

Generally, there is good agreement between the modeled and the measured values in the water compartment. The exception is Deca-BDE. However, it seems that the error is in the measurement rather than in the model. The modeled values are representing the partition equilibrium (as presented in chapter 4.2). If the measured values followed the partition in equilibrium, the dissolved phase concentration should be almost 4 orders of magnitude lower or the particle bound concentration about 4 orders of magnitude higher. It is likely that the error is in the dissolved concentration, since it is unlikely that the particle bound concentration for Deca-BDE exceeds the one of other congeners by 4 orders of magnitude while on the other hand it is very likely that the measured dissolved concentrations are too high when considering the low water solubility of Deca-BDE.

The most reasonable explanation of the measurement error in the dissolved phase is that according to the measurement procedure, all particles that are smaller than 0.7 µm belong to the 'operationally dissolved' phase. Deca-BDE might be adsorbed to this fraction of small particles and therefore be counted to the dissolved fraction in the measurements. Additionally to small particles, there might be Deca-

BDE adsorbed to dissolved organic matter which further increases the measured dissolved concentration.

Samples of whitefish (*Coregonus sp.*) were taken in September 2005 and in autumn and winter 2006. In the first sample the fish were divided up into females and males and further into fish with and without deformations (Bogdal, 2007). The second samples were divided up into a total of 20 pools according to the ecotype (Brienzlig and Albock), sex, sampling site, and grade of gonad malformations (Naef, M., diploma thesis, personal communication). The objective of separately analyzing pools of fish with different characteristics was to investigate possible relations between malformations and increased concentrations of endocrine disrupting chemicals. More details about the fish samples is presented in the diploma thesis of Michal Naef (2007).

Here, the modeled fish concentration was compared with the concentrations of all samples. The samples of the second period have clearly lower concentrations than those of the first period. This seems to be more a result of improvements in the analytical method than an actual change of concentrations in the fish. The modeled values generally correspond well to the measured values when considering the uncertainty in the model. As in the water samples, Hexa-BDE concentrations are again modeled too low. There is thus some indication that the concentration in tributaries is modeled too low, which causes the concentrations in all media to be too low. Modeled and measured Deca-BDE concentrations are in agreement, which raises the confidence into the modeled water concentration and thus further puts the measured water (dissolved) concentration into question.

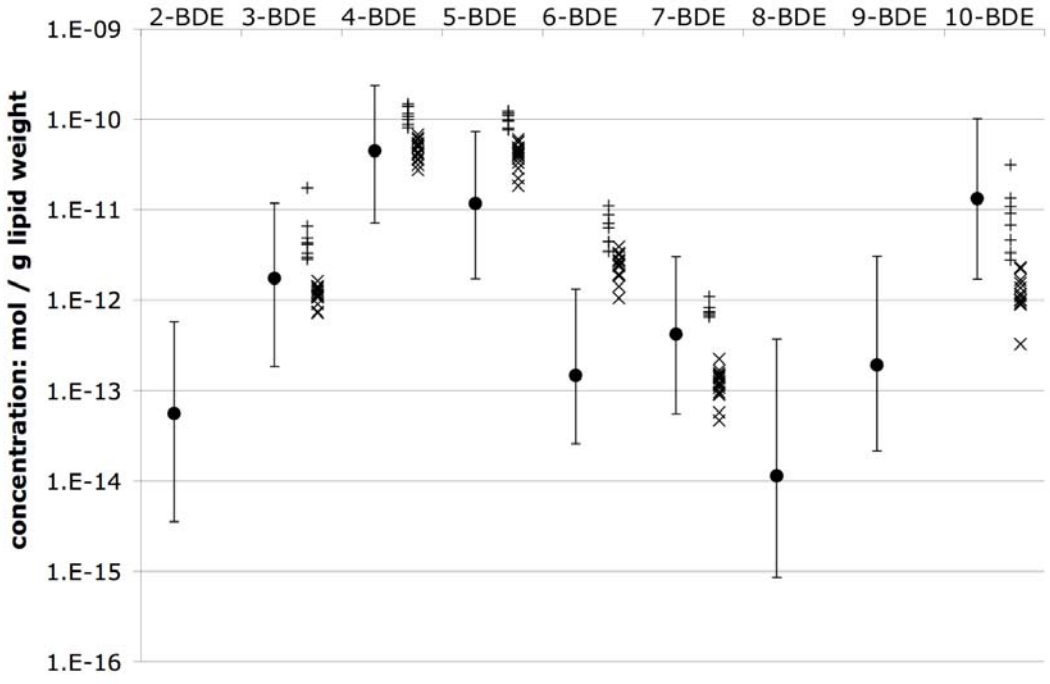

Figure 7-3. Concentrations in fish. Modeled: black dots, (+) measured first period (September 2005) and (x) second period (Autumn and Winter 2006).

It seems to be surprising that the model, which assumes equilibrium between the water and the fish lipid, suits well to calculate fish concentrations. This would mean

that there is no biomagnification of PBDEs in fish, since this would cause concentrations exceeding those expected in equilibrium with water.

Biomagnification occurs when the solubility of PBDE in the fish' diet is higher than in the fish' excretes, which is caused by lower organic content of excretes compared to diet. In this case, the uptake mass flow of PBDE into the fish is higher than the removal by excretion processes. Since the model presented here does not consider uptake and removal processes, it would be expected that the model underestimated the concentrations. One possible explanation for the fact that the concentrations still match is that the fish eliminates the PBDEs by degradation. This would be an additional removal processes in the fish that could compensate the difference between uptake and excretion. Several studies have shown that fish are able to degrade PBDEs (Tomy et al., 2004; Stapleton et al., 2004; Streets et al., 2006). However, exact degradation rates are difficult to determine since only depuration from fish can be measured which is the sum of degradation and excretion.

Sediment compartment

The sediment concentrations in the model represent the upper most part of the sediment. Consequently, they were compared with the measured concentrations in the top layer of the three sediment cores taken in Lake Thun in spring 2005. The top layer was dated on average with the year 2004 according to ^{137}Cs and ^{210}Pb measurements (Bogdal, 2007). Figure 7-4 shows both modeled and measured concentrations. The lower brominated congeners tend to be somewhat to high, but still match to the measured concentrations when model uncertainty is taken into account.

While the modeled concentration represents steady state concentration of the top sediment and thus the concentration for the modeled month, the measurement represent the year 2004, which is one year old sediment (core taken in spring 2005). The concentrations in the measurement could thus be lower due to (1) lower concentrations in 2004 in the lake water and therefore lower mass flow into the sediment and (2) biodegradation in the sediment. Biodegradation is faster for lower brominated congeners depicting the fact that the model tends to overestimate only the concentrations for lower brominated congeners. The biodegradation half-life of Penta-BDE for instance was assumed to be about one year. Thus, the effect of degradation could bring the modeled concentration 0.3 log-unit down (1 half-life) and thus closer to the measured values.

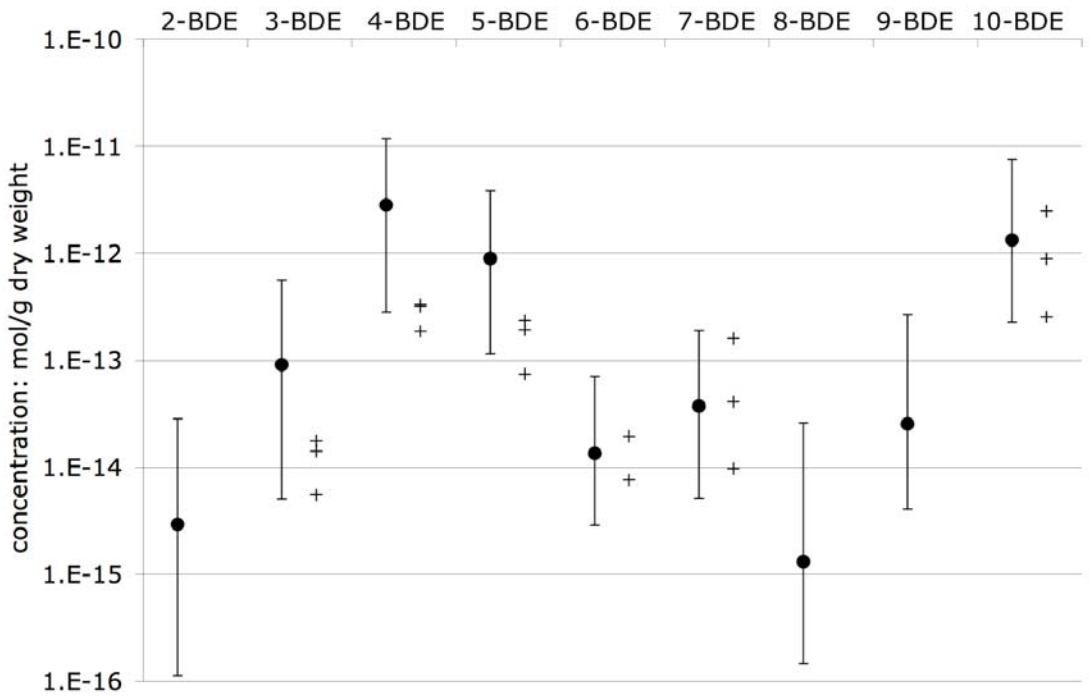

Figure 7-4: Concentrations in sediment. Black dots: Modeled point estimates. Crosses (+): Measured values.

Inventories in different compartments

Most of the chemicals with the modeled system are present in the solid sediment for all congeners. The fraction of the total mass in the model present in the solid sediment is 83% for Di-BDE, 88% for Tri-BDE and above 98% for the other PBDE homologues. 17% of Di-BDE, 11% of Tri-BDE, 1.7% for Tetra-BDE and less than 1% for other PDBEs are in the water compartment.

In the lake water compartment the highest fraction is in the dissolved phase for homologues up to Penta-BDE, and for higher brominated congeners most is in the suspended particle phase. The fraction in fish is increasing with degree of bromination, but does only reach 3% for Deca-BDE of the whole mass in the lake.

7.1.2. Other scenarios

Run without water input

The model was used to determine, whether the input by rivers is important. Hence, a scenario where input by rivers is turned off was assessed. Figure 7-5 compares the performance of the model scenario with water input with the scenario without water input. The deviation of the modeled from the geometric mean of the measured values is visualized. A specific data point is better modeled with the scenario where the deviation is smaller and consequently the points that are in the upper-left triangle are better modeled with the scenario 'without water input', while the points in the lower-right triangle are better modeled with the scenario 'with water input'. As seen in the figure, more points are in the lower right triangle,

depicting that the model scenario with water input fits better to the measurements. However, the difference between the scenarios is very small and uncertainties in the modeled values, which are about one order of magnitude (1 on logarithmic scale), are outweighing the differences.

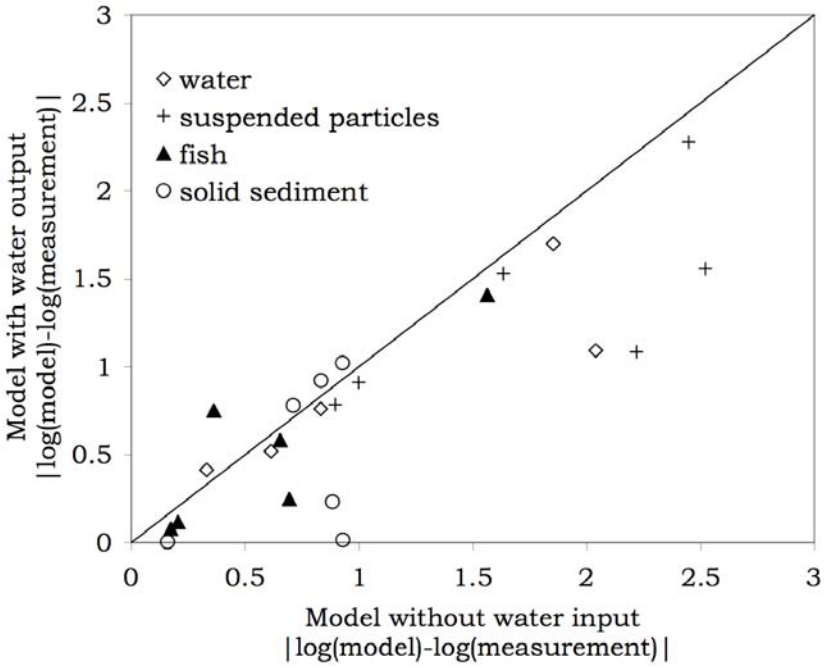

Figure 7-5: Deviation of the modeled from the mean of measured concentrations. The deviation for the model without water input is shown on the y-axis, the deviation of the model with water input is shown on the x-axis. For the data points in the upper left triangle, the model without water input performs better. For the data in the lower right triangle, the model with water input performs better.

Run without debromination

A run without debromination was carried out in order to investigate whether the assumptions in the standard model run regarding debromination are appropriate. The concentrations for Di-, Octa- and Nona-BDE obviously stay at zero, since they were not included in the air and water inputs. Besides these concentrations, there is only a visible change in the concentration of Tri-DBE. The Tri-BDE concentrations are lower in the scenario without debromination and consequently, the concentration in solid sediment and water are closer to the measurement in the scenario without debromination, while the concentrations in fish and in suspended particles are closer to the measurement in the scenario with debromination (compare with Figures 7-1 to 7-4).

Due to the low differences between the two scenarios (with and without debromination), no conclusion can be made whether the debromination is modeled well. In order to further analyze this, the model needed to be compared to measurements of Di-, Octa-, and Nona-BDE, if they become available.

7.1.3. Results for PCBs

PCBs were modeled in order to see whether the model have the same accuracy and to find differences between PBDE and PCBs.

The concentrations in the dissolved water phase are shown in Figure 7-6, those in the particle bound phase in Figure 7-7. Measured concentrations are within the uncertainty of the modeled concentrations. For the dissolved phase, modeled concentrations tend to be lower than the measured concentration. A trend that has already been observed with PBDEs. Again, one reason might be that measurements are higher since small particles (below 0.7 µm) and chemicals bound to dissolved organic matter are included.

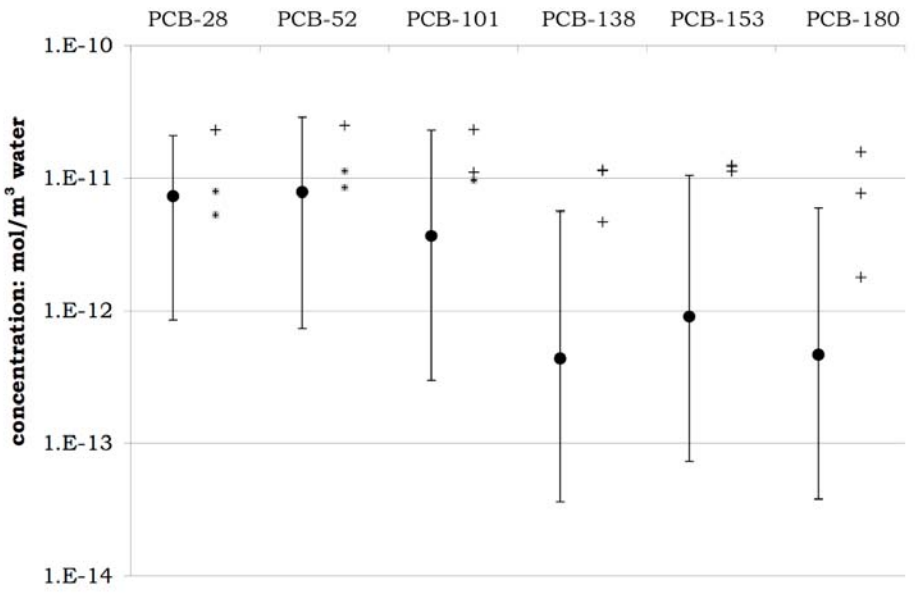

Figure 7-6: Modeled concentrations (black points) and measured concentrations (black crosses) in dissolved water phase. Measured data that does not exceed 5 times the blank value (below limit of quantification) are grey shaded.

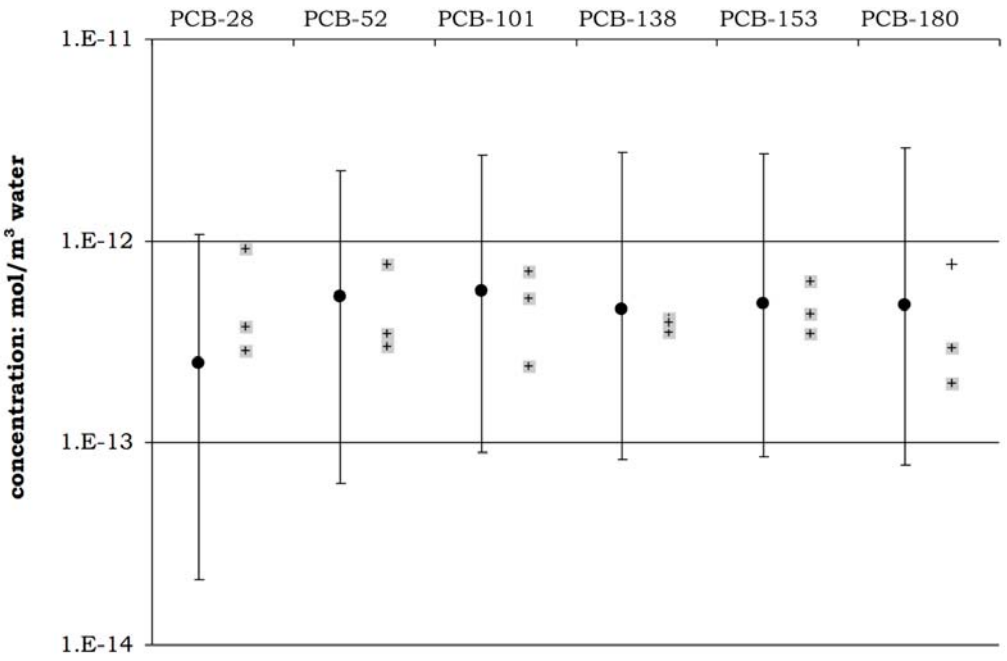

Figure 7-7: Modeled concentrations (black points) and measured concentrations (black crosses) in dissolved water phase. Measured data that does not exceed 5 times the blank value (below limit of quantification) are grey shaded.

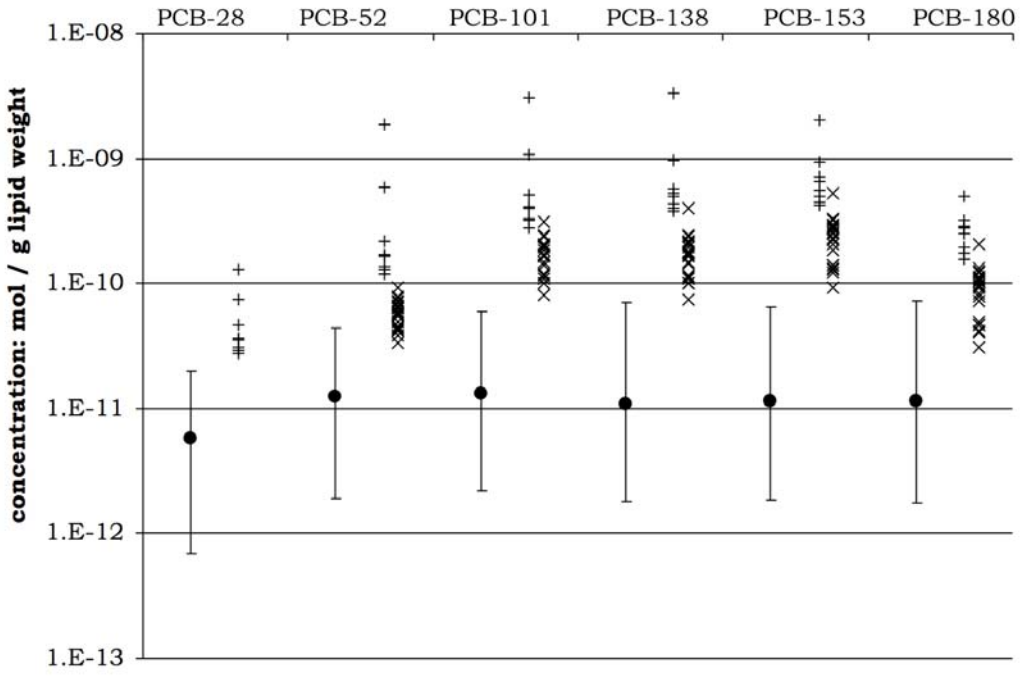

Figure 7-8: Concentrations in fish. Modeled: black dots; measured first period, September 2005: (+), and second period, Autumn and Winter 2006: (x).

Figure 7-8 shows the modeled and measured PCB concentrations in fish. The modeled values are clearly below the measured values. This is in contrast to the

PBDEs, where the model performed well. It seems that the equilibrium model assumed for the fish does not suit very well for the PCBs. Concentrations measured in the field exceed the concentrations that would be expected in equilibrium with water. Consequently, some biomagnification of PCBs in whitefish is observed.

Figure 1-1 shows that the modeled sediment concentrations are in agreement with the measured concentrations. There is no trend for overestimation of the model as observed for the PBDEs supporting the supposition that degradation in the sediment occurs for PBDEs. PCBs in contrast are degraded slower than PBDEs.

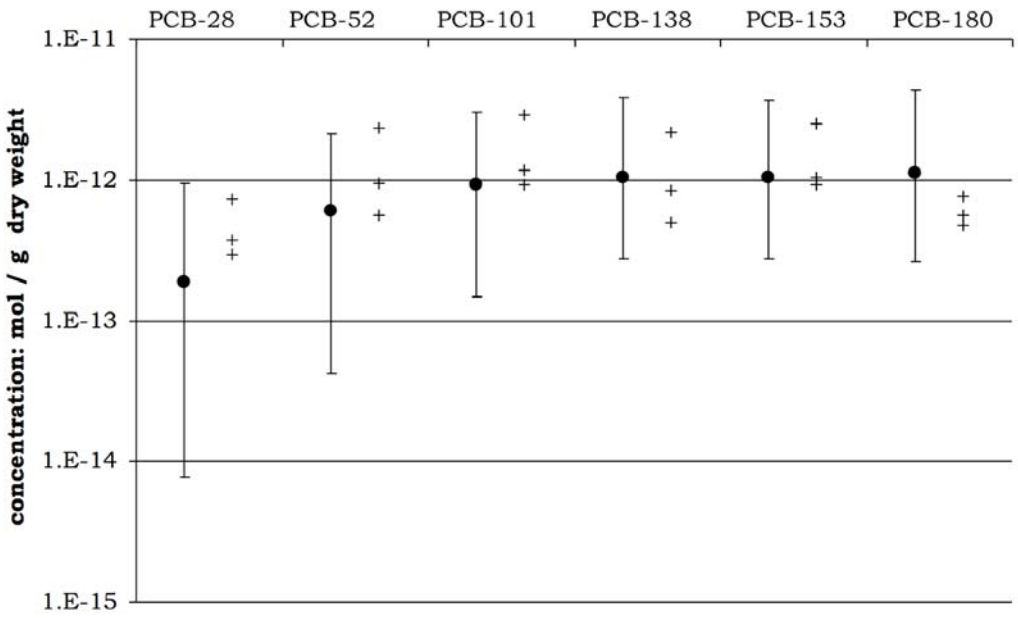

Figure 7-9: Concentrations of PCBs in sediment. Black dots: Modeled values. Crosses (+): Measured values.

7.2. Mass balance for lake compartment

The mass balance for the lake compartment was assessed in detail in order to determine the main input and output processes. The contribution of each input process is shown in Figure 7-10.

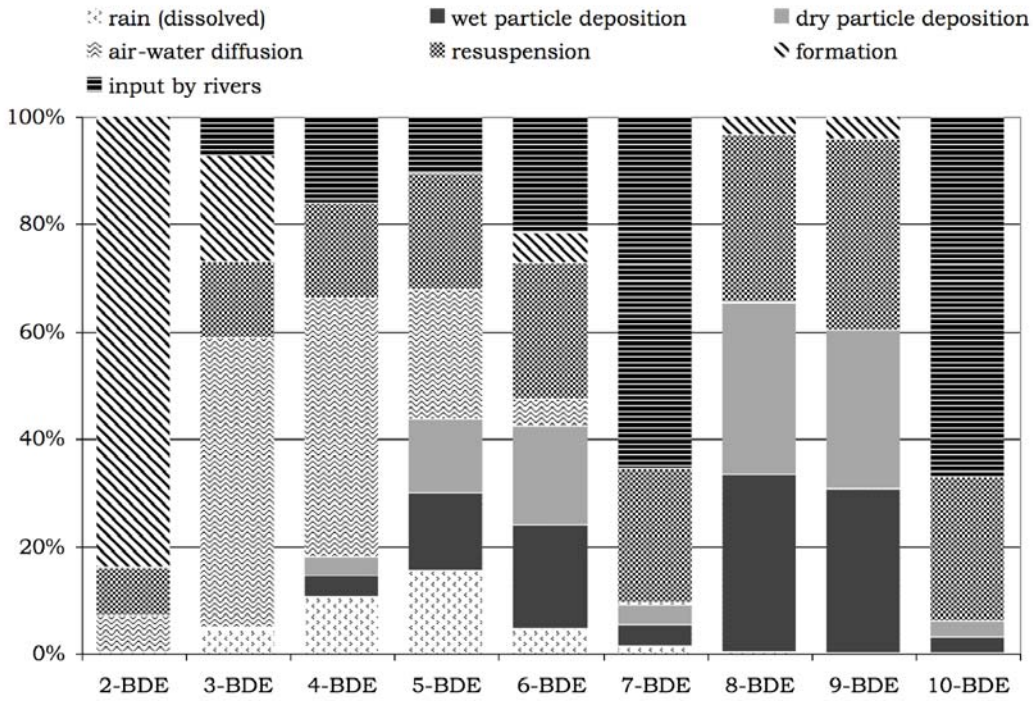

Figure 7-10: Input processes into the lake water compartment

Except for Hepta-BDE and Deca-BDE, the input mainly comes from the atmosphere. The pathway is mainly by particle deposition for higher brominated congeners and by diffusion for the lower brominated congeners. Resuspension from sediment is important for all congeners, but somewhat more prominent for higher brominated congeners due to their higher particle bound fraction. Dry and wet particle deposition have about equal importance. This is highly dependent on rainfall, which was extremely high in July 2007. In other months, dry deposition exceeds wet deposition. Formation is only important for Di-BDE. Since no Di-BDE were measured neither in the atmosphere nor in the river water, all Di-BDE in the model are formed by debromination. There is however some formation taking place already in the atmosphere and thus leading to an input of Di-BDE into the water by diffusion.

Figure 7-11 shows the total input into the lake, the inventory in the atmosphere and in the inventory in the lake water for the July 2007. Consider that input in the lake water does not equal the output from atmosphere. The difference between the inventory in the atmosphere and the total input into the lake shows how the congener pattern changes between the atmosphere and the lake. Apart from Di-BDE, Octa-BDE and Nona-BDE, which are only formed by debromination in the model, there is a visible shift in the congener pattern. The higher brominated PBDE become enriched in the water compared to the lower brominated. This is indicated by the smaller difference between the input into the lake water and the inventory in the atmosphere for higher brominated congeners. Note that the scale is logarithmic and the difference is therefore a measure of the ratio.

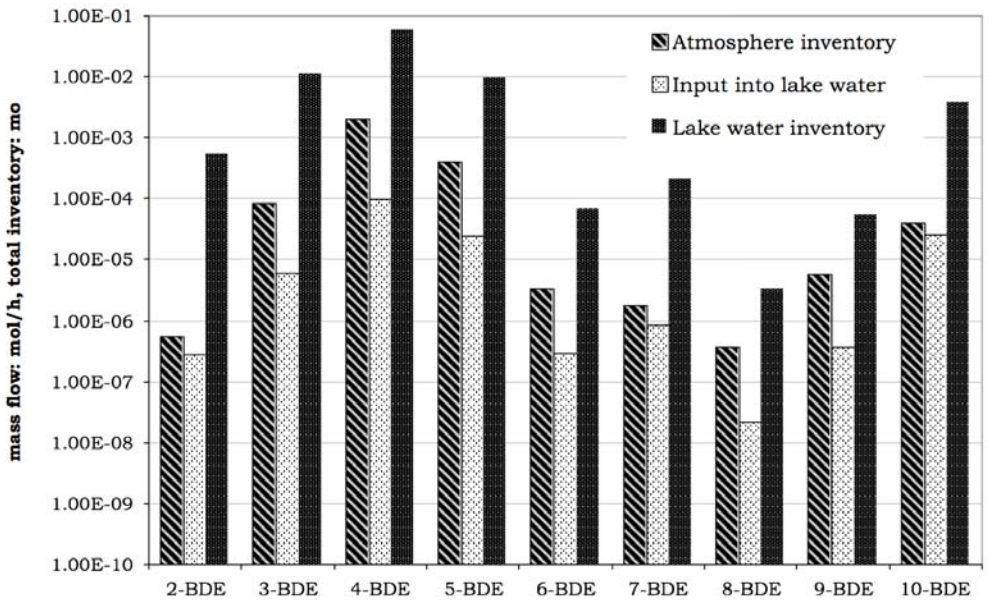

Figure 7-11: Input mass flow into the lake and inventory in the lake (total substance amount in the lake)

Total residence time in the lake water can be calculated from the data presented in Figure 7-11. The residence time has been calculated for October 2006, January 2007, April 2007 and July 2007 in order to see seasonal differences. Results are shown in Table 7-1.

Table 7-1: Residence time in the lake water compartment (in days) for different months.

	October 2006	January 2007	April 2007	July 2007
Meteorological conditions				
Temperature (°C)	11.5	2.3	13.1	17.2
Precipitation (mm)	47	62	37	343
Residence time of compounds in water (days)				
Di-BDE	100	99	95	82
Tri-BDE	95	98	92	79
Tetra-BDE	26	23	24	25
Penta-BDE	17	15	16	17
Hexa-BDE	10	10	10	10
Hepta-BDE	11	10	10	11
Octa-BDE	7	7	7	7
Nona-BDE	7	7	7	7
Deca-BDE	7	7	7	7

Output processes from the lake water compartment are shown in Figure 7-12. The most important process is sedimentation, except for Di-BDE, where degradation and output by rivers is higher. This can be explained by the fact that PBDEs are

mainly bound to particles and removal with particles is much faster than removal of the dissolved substances. The degradation reaction for Di-BDE is mainly biodegradation. Photodegradation is very slow for Di-BDE. In absolute terms, the degradation for Tri- and Tetra-BDE would be higher than for Di-BDE, but relatively compared to sedimentation degradation is highest in Di-BDE.

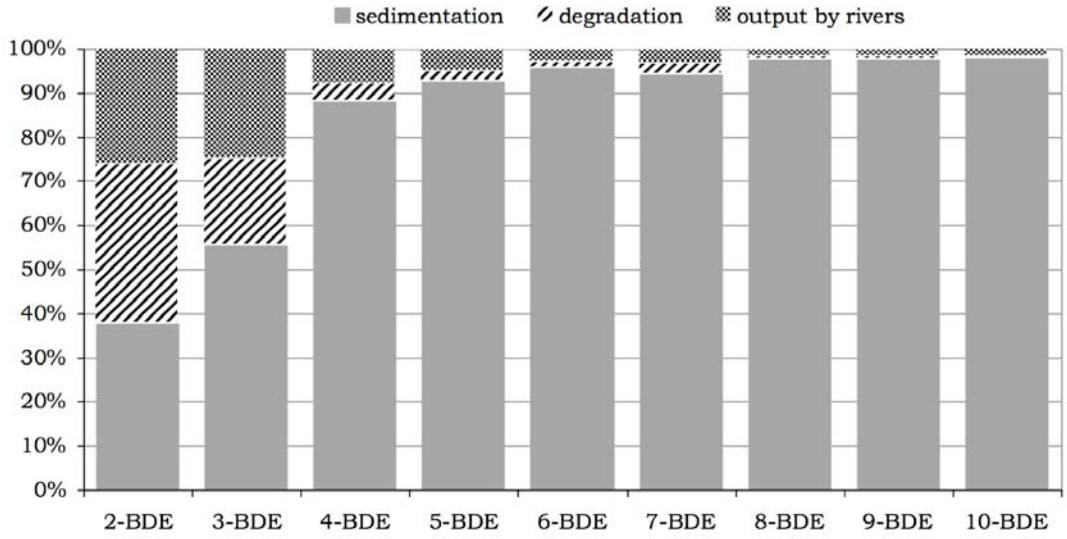

Figure 7-12: Output processes from lake water.

7.3. Sensitivity analysis and model uncertainty

The uncertainty of the model output is dependent on the uncertainty in the parameters and their influence on the output. The influence of one parameter to the output is described with the sensitivity index (see chapter 6).

On the following pages, sensitivity plots are shown. Each plot includes the parameters that induce the highest change in the output (highest relative sensitivity. The x-axis is the relative parameter change and the y-axis is the relative output change (relative sensitivity). The sensitivity index for each point is the slope of the line connecting the origin with the point. All parameters, which exceed a certain threshold with their relative sensitivity are shown. The threshold is defined for each plot individually.

Sensitivity plots are shown for the water concentration and for the solid sediment concentration. Concentrations in the other media would have similar plots and differences are discussed below. The Tri-, Tetra- and Deca-BDE concentrations were chosen as examples. Tetra- and Deca-BDE are chosen because they have the highest concentrations in the environment and in order to have representatives of low brominated homologues and high brominated congeners. Tri-BDE was chosen in order to investigate the influence of debromination. Tri-BDE is a better choice for this than Di-BDE, Octa-DBE or Nona-BDE, because for these the relative contributions of the processes in the model might not very well be reflected since they have not been measured in the input and are only formed by debromination in the model.

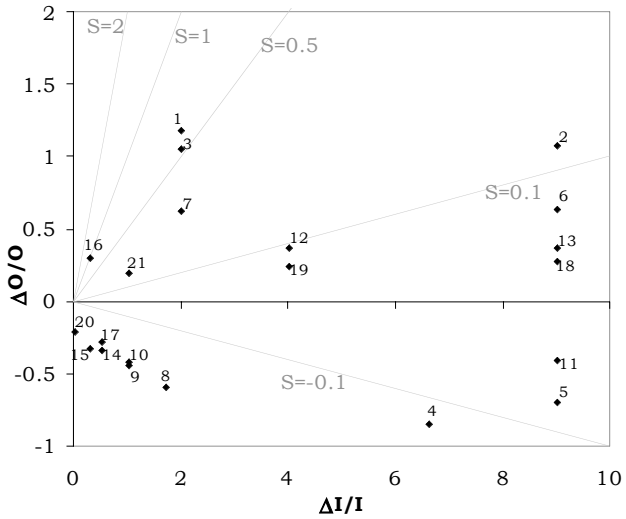

Figure 7-13: Sensitivity plot for Tri-BDE concentration in water (dissolved). Threshold for relative sensitivity: 0.2

1	Air side diffusion velocity
2	Photolysis rate of Tetra-BDE in air
3	Bulk conc. in atmospheric input of Tetra-BDE
4	Kow of Tri-BDE
5	Biodegradation rate of Tri-BDE in water
6	Photolysis rate of Tetra-BDE in water
7	Bulk conc. in atmospheric input of Tri-BDE
8	Kow - Koc conversion factor
9	Volume fraction of solid sediment
10	Sediment burial velocity
11	Biodeg. rate of Tri-BDE in solid sediment

12	Bulk conc. in water tributaries of Tetra-BDE
13	Biodegradation rate of Tetra-BDE in solid sediment
14	OC fraction in suspended particles
15	Uoa of Tri-BDE
16	Uaw of Tri-BDE
17	Density of sediment
18	Biodegradation rate of Tetra-BDE in water
19	Bulk conc. in water tributaries of Tri-BDE
20	Air temperature
21	Diffusion velocity sediment-water

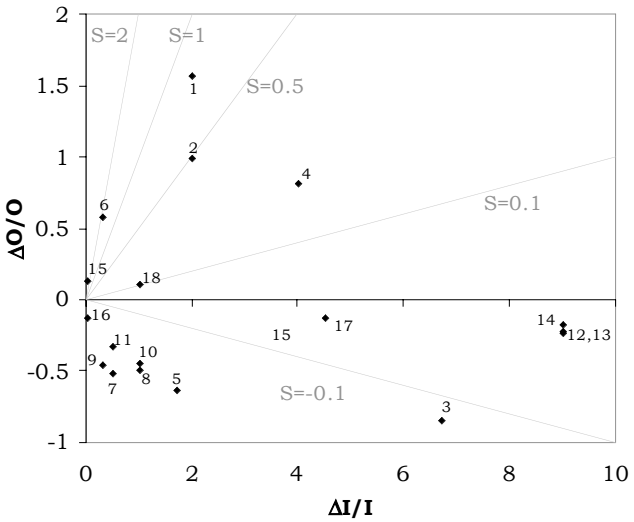

Figure 7-14: Sensitivity plot for Tetra-BDE concentration in water (dissolved). Threshold for relative sensitivity: 0.1

1	Bulk conc. in atmospheric input of Tetra-BDE
2	Air side diffusion velocity
3	Kow of Tetra-BDE
4	Bulk conc. in water tributaries of Tetra-BDE
5	Kow - Koc conversion factor
6	Uaw of Tetra-BDE
7	Organic carbon fraction in suspended particles
8	Volume fraction of solid sediment
9	Uoa of Tetra-BDE

11	Density of sediment
12	Biodegradation rate of Tetra-BDE in water
13	Biodeg. rate of Tetra-BDE in solid sediment
14	Photolysis rate of Tetra-BDE in air
15	Lake surface temperature
16	Air temperature
17	Kaw of Tetra-BDE
18	Diffusion velocity sediment-water

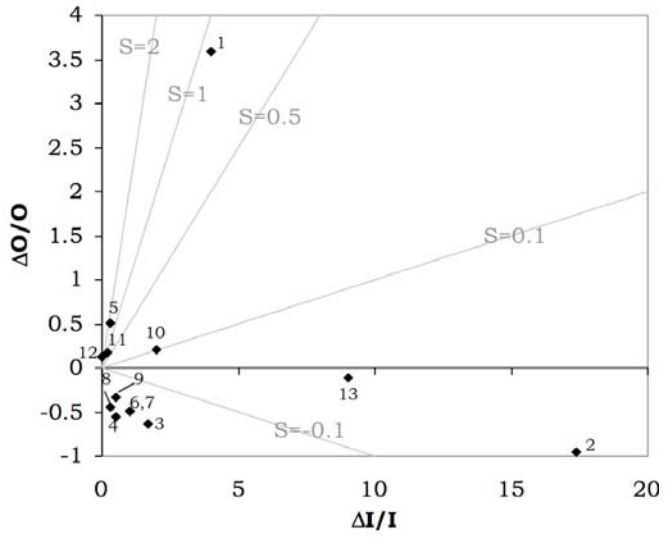

Figure 7-15: Sensitivity plot for Deca-BDE concentration in water (dissolved). Threshold for relative sensitivity: 0.1

1	Bulk conc. in water tributaries of Deca-BDE
2	Kow of Deca-BDE
3	Kow - Koc conversion factor
4	OC fraction in suspended particles
5	Uaw of Deca-BDE
6	Volume fraction of solid sediment
7	Sediment burial velocity
8	Uoa of Deca-BDE
9	Density of sediment
10	Bulk conc. in atmospheric input of Deca-BDE
11	Water runoff
12	Lake surface temperature
13	Biodeg. rate of Deca-BDE in solid sediment

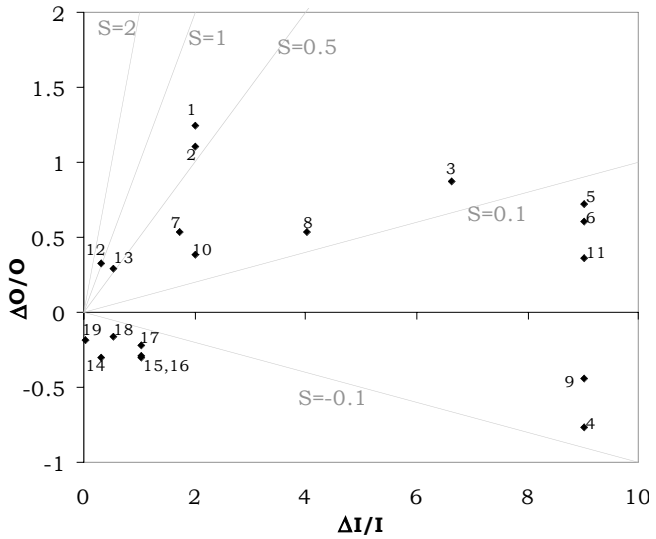

Figure 7-16: Sensitivity plot for Tri-BDE concentration in solid sediment. Threshold for relative sensitivity: 0.15

1	Bulk conc. in atmospheric input of Tetra-BDE
2	Air side diffusion velocity
3	Kow of Tri-BDE
4	Biodegr. rate of Tri-BDE in solid sediment
5	Biodegr. rate of Tetra-BDE in solid sediment
6	Photolysis rate of Tetra-BDE in air
7	Bulk conc. in water tributaries of Tetra-BDE
8	Kow - Koc conversion factor
9	Biodegradation rate of Tri-BDE in water
10	Bulk conc. in atmospheric input of Tri-BDE
11	Photolysis rate of Tetra-BDE in water
12	Uoa of Tri-BDE
13	OC fraction in suspended particles
14	Uaw of Tri-BDE
15	Sediment burial velocity
16	Volume fraction of solid sediment
17	Diffusion velocity sediment-water
18	Air temperature
19	Density of sediment

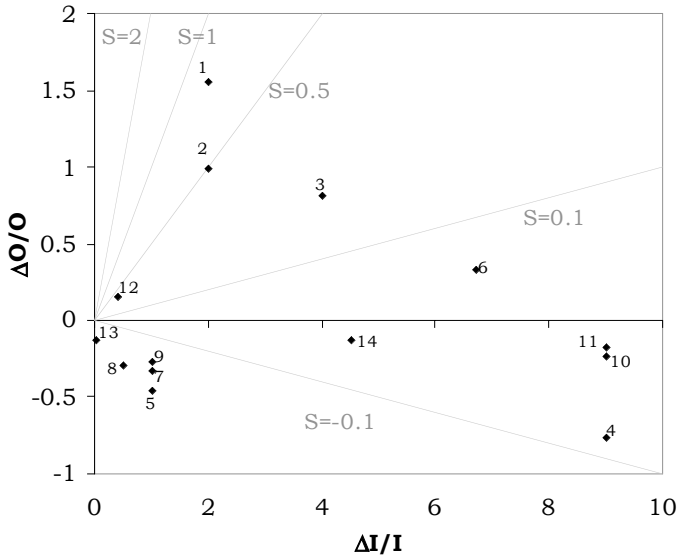

Figure 7-17: Sensitivity plot for Tetra-BDE concentrations in solid sediment. Threshold for relative sensitivity: 0.1

1	Bulk conc. in atmospheric input of Tetra-BDE	8	Density of sediment
2	Air side diffusion velocity	9	Volume bulk sediment
3	Bulk conc. in water tributaries of Tetra-BDE	10	Biodegradation rate of Tetra-BDE in water
4	Biodeg. rate of Tetra-BDE in solid sediment	11	Photolysis rate of Tetra-BDE in air
5	Volume fraction of solid sediment	12	Activation energy for biodegradation
6	Kow of Tetra-BDE	13	Air temperature
7	Sediment burial velocity	14	Kaw of Tetra-BDE

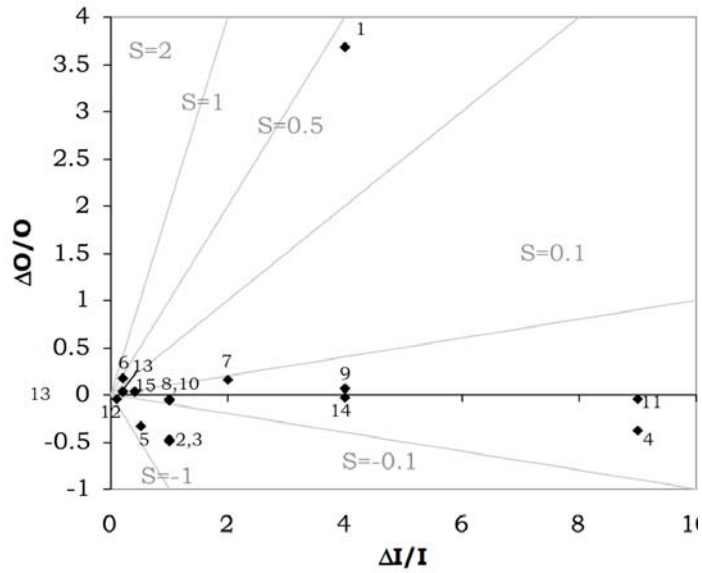

Figure 7-18: Sensitivity plot for Deca-BDE concentrations in solid sediment. Threshold for relative sensitivity: 0.02

1	Bulk conc. in water tributaries of Deca-BDE	9	Volume fraction of coarse aerosols
2	Volume fraction of solid sediment	10	Volume fraction of suspended particles
3	Sediment burial velocity	11	Photolysis rate of Deca-BDE on fine aerosols
4	Biodeg rate of Deca-BDE in solid sediment	12	Sediment area
5	Density of sediment	13	Scavenging ratio
6	Water runoff	14	Volume fraction of fine aerosols
7	Bulk conc. in atmospheric input of Deca-BDE	15	Activation energy for biodegradation
8	Volume bulk sediment		

High relative sensitivity for the Tri- and Tetra-BDE is seen for atmospheric input and the air side diffusion velocity. This highlights that the major pathway for these homologues into the lake is from the atmosphere via diffusion. Deca-BDE concentrations show the highest relative sensitivity (3.6) for concentrations in the input of tributaries. This reflects the fact that inflow by tributaries is the most important input process and that a change in the input concentration has almost proportional influence on the concentration in water (sensitivity index close to 1). The parameters that describe the partitioning between the dissolved phase and the particle bound phase, which are namely K_{ow}, K_{ow}-K_{oc} conversion factor (variable b in equation 4-4) and volume fraction of suspended particles are seen to have some high relative sensitivities for all shown homologues. This reflects the fact that the water – particles partitioning coefficients for PBDE are at the edge which determines whether the chemicals are mainly in the dissolved phase or mainly in the particle bound phase. Figure 7-19 (left) shows that the log K_{pw} switches from negative to positive values between Hepta- and Octa-BDE. This means that, homologues with 7 or less bromines are mainly in the dissolved phase, while homologues with 8 or more bromines are mainly particles bound. Changes in parameters describing this partitioning equilibrium will switch this edge toward higher or towards lower brominated homologues and therefore have a high influence on the water and also on the particle bound concentration for some PBDEs.

Interesting is the fact, that the Tri-BDE concentrations in water as well as in the sediment is highly influenced by parameters describing the fate of Tetra-BDE. This can be explained by the fact that Tetra-BDE is degrading into Tri-BDE and that Tetra-BDE has much higher concentrations than Tri-BDE.

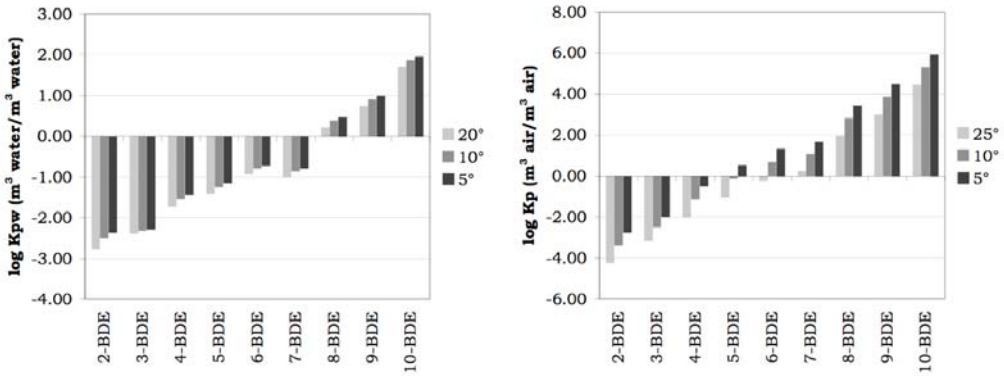

Figure 7-19: Water-particle partition coefficient in m3 water/m3 water (left) and Aerosol-air partition coefficient in m³/m³ (right). A coefficient of 0 (=1 in non-logarithmic form) means that the fractions in both phases are equal.

There are some parameters with high sensitivity indices and also high uncertainties. They have a high potential to improve the model, since it is likely that their uncertainty can be reduced by finding more appropriate data or improvements in measurement methods in the future. If the uncertainty of these parameters could be reduced, there would be a high improvement of the model output. These parameters include the concentrations in atmospheric input for Tri- and Tetra-BDE, the concentration of Deca-BDE in tributaries, the air-side diffusion velocity, the K_{ow}

of Deca-BDE, the volume fraction of solid sediment and the volume fraction of suspended particles.

The sensitivity index for all parameters to all model outputs was calculated with the model. Subsequently, it was analyzed which parameter output combination leads to a sensitivity index which is higher than 1 or lower than -1 respectively. This indicates a disproportionally high influence of the parameter on the output.

Air temperature has the highest sensitivity index, which is largest for the influence on the air concentrations: There, the sensitivity index ranges between 2 for Tri-BDE and 56 for Deca-BDE. Note that the influence of changing atmospheric input concentration depending on temperature (as described by equation 4-51) is not included in the sensitivity analysis for the air temperature. Thus, when the air temperature is changed, the input concentration still remains constant. The influence of the air temperature to concentration in all other media are negative, meaning that increasing temperature leads to lower concentrations, except for Octa-BDE. Since Octa-BDE is not present in the input it is formed only by debromination, which is higher, when more of the parent PDBEs (Nona-BDE and Deca-BDE) are in the gas phase. Temperature influences the partitioning between air and aerosols. This has a high effect to PBDEs, since a change in temperature can lead to a switch for the chemicals from being mainly in the gas phase to be mainly in the particle phase. This is illustrated in Figure 7-19 (right) with the aerosol-air partition coefficient.

The photolytic degradation is faster in the gas phase than on the aerosol and thus more Octa-BDE is formed at higher temperatures. This effect seems to be stronger than the effect that the partition equilibrium in the atmosphere is shifted in favor of the gas phase. Therefore, concentrations on aerosol for Octa-BDE increase with increasing temperature and this leads to higher deposition into the lake and finally to higher concentrations in all media.

The sensitivity index of water temperature on water concentrations is around 6 for all congeners, except for Tri-BDE where the sensitivity index is only 0.8. The sensitivity index of bottom water temperatures is higher than 1 for pore water (between 2.6 and 18) and lower than 1 for solid sediment (between -1.6 and -9.2). Bottom water temperature also affects the concentrations in the lake water, on suspended particles and in fish over-proportional.

For Di-BDE and Octa-BDE, solar radiation has a sensitivity index of about 1.4-1.7 depending on which media is regarded. This seems to be due to increased photodegradation of Tri-BDE or Nona-BDE (and also Deca-BDE), which have much higher concentrations than Di-BDE and Octa-BDE and thus over-proportionally influence these concentrations.

The sensitivity index of K_{ow} of Di-BDE and Tri-BDE on concentrations in the gas phase and on concentrations on aerosol is 2.6 and 2.1 respectively. The sensitivity index of other partition constants is always lower than 1 for all congeners and outputs. Since K_{oa} is calculated in the model based on K_{ow} and K_{aw} (see chapter 6.2.3) a change in K_{ow} also influences K_{oa}. K_{oa} determines the concentrations of chemicals in the gas phase and on aerosols, for which the high sensitivity index has been observed.

Sensitivity indices above 1 (1-2.2) for U_{aw} and below 1 (-1 - -1.6) for U_{oa} on the water concentration are observed. Inner energies are used to calculate the

temperature dependence of partition constants. Since the inner energies are in the exponential term, they have a high influence. (see equation 4-53).

7.3.1. Analytical uncertainty calculation and Monte Carlo simulation

The uncertainty output obtained with the analytical uncertainty propagation method was compared with a Monte Carlo simulation output. As seen in Figure 7-20, Monte Carlo simulation and the analytical uncertainty propagation method do not lead to the same result in all cases. Shown are the concentrations in various media (8) for all homologues (9) and all modeled months (20) leading to 1440 points for comparison. Most prominent are differences in the air and aerosol phase. The confidence factor of the Monte Carlo analysis was determined with two methods. First by dividing the standard output (model point estimate) by the lower percentile (0.025) of all Monte Carlo outputs and second by dividing the upper percentile (0.975) by the standard output. If the Monte Carlo outputs are log-normal distributed, this should lead to the same result. The results are shown in the left figure (first case) and the right figure (second case). Apparently, the two methods did not lead to the same result, which shows that the Monte Carlo output is not log-normal distributed. It is therefore not possible to determine a correct confidence factor for the output from Monte Carlo simulation, since this can only be defined when the output is log-normally distributed. The figures show that the confidence factor calculated with the higher percentile tends to be lower than the confidence factor calculated with the lower percentile. Conclusively, the distribution of output values has a shape that is shifted towards lower values compared to a log-normal distribution.

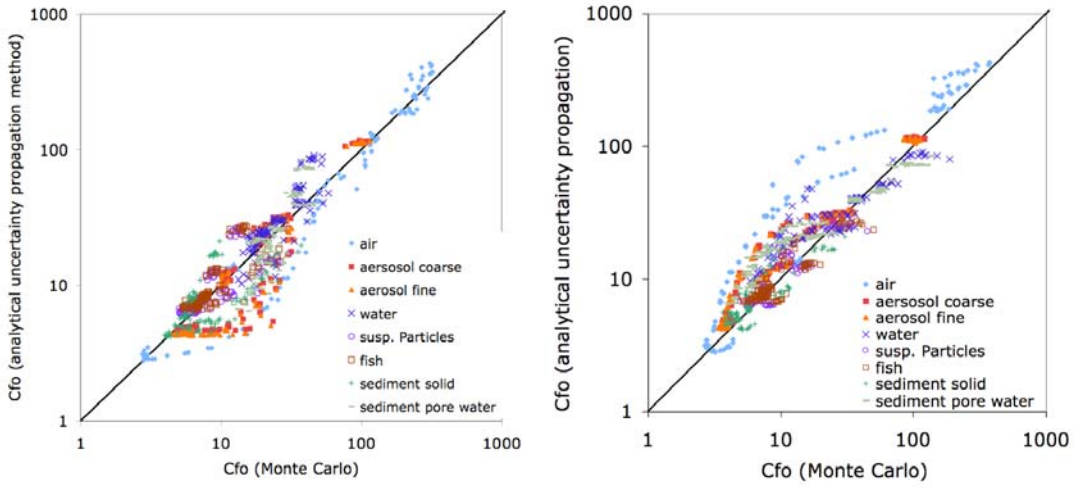

Figure 7-20: Comparison of output confidence factors (Cfo) obtained with analytical uncertainty and Monte Carlo analysis. Cfo from Monte Carlo output calculated by dividing the median with the lower percentile (0.025) (left figure), and by dividing the higher percentile (0.975) with the median (right figure).

The most probable reason behind this is that air temperature and the energy of phase transition from octanol to air have an exponential influence on the result (see

equation for calculating temperature dependence of partition constants). These non-linear relationships between input parameters and outputs lead to a change in the distribution.

The analytical uncertainty propagation is only correct in case of linear relationships and thus it assumes that the output will have the same distribution as the inputs, which is log-normal. Since obviously the model output is not log-normal distributed, it is concluded that the analytical uncertainty propagation method is not appropriate to estimate the model uncertainty.

Therefore, Monte Carlo outputs were used in the model as estimations of the model uncertainty, whereas the lower percentile (0.025) and the upper percentile (0.975) defined the 95% confidence interval of the model output.

7.4. Dynamic solution

7.4.1. Concentration profile

The results of the dynamic solution show the seasonal variability caused by changing environmental parameters. For the Lake Thun case study, air temperature, lake surface temperature, OH concentrations, Solar radiation, rainfall rates, runoff from lake and wind speed are changed each month. The monthly values are listed in *Appendix IV – Variable parameters*.

The dynamic solution was calculated for the time period January 2006 until August 2008. The steady state solution for January 2006 served as initial conditions.

Figure 7-21 and Figure 7-22 show the evolution of concentrations over the time period for Tetra-BDE and Deca-BDE. There are leaps in the concentrations at the end and beginning of a month. These are caused by the sudden change in the fugacity capacities due to temperature leaps. The model holds the mass in a compartment constant at the change of a month, but it cannot hold the concentrations in individual media constant at the same time. Hence, for each month there is a sudden shift from one media to the other within a compartment depending on how the partition coefficient changes between two months.

It is observed for both homologues that the seasonal variability is 0.5 to 1 order of magnitude for the different phases. The gas phase concentrations are higher in summer than winter for both homologues, the aerosol concentrations are lower in summer for Tetra-BDE but higher for Deca-BDE. This is a result of the definition for the atmospheric input concentration (see chapter 4.7), which is higher in summer and the partition equilibrium between aerosols and the gas phase, which is shifted to the gas phase at warmer temperatures. It is shown that the first effect outweighs the second for Deca-BDE.

The solid sediment concentration is increasing over the whole time period of the model. This indicates that in the sediment concentrations take a long time until they reach steady-state concentrations. At the end of the period, in August 2007, the steady state concentrations would be $2.5 \cdot 10^{-12}$ mol/g dry weight and $1.2 \cdot 10^{-12}$ mol/g dry weight for Tetra-BDE and Deca-BDE. The concentration in the dynamic model is still below. Apart from the long time it takes to reach steady-state, this lag

is caused by the fact that the steady state concentration in January 2006 was very low (used as initial concentrations in the dynamic model), because January 2006 had the coldest air temperature in the whole period and therefore the lowest input concentrations.

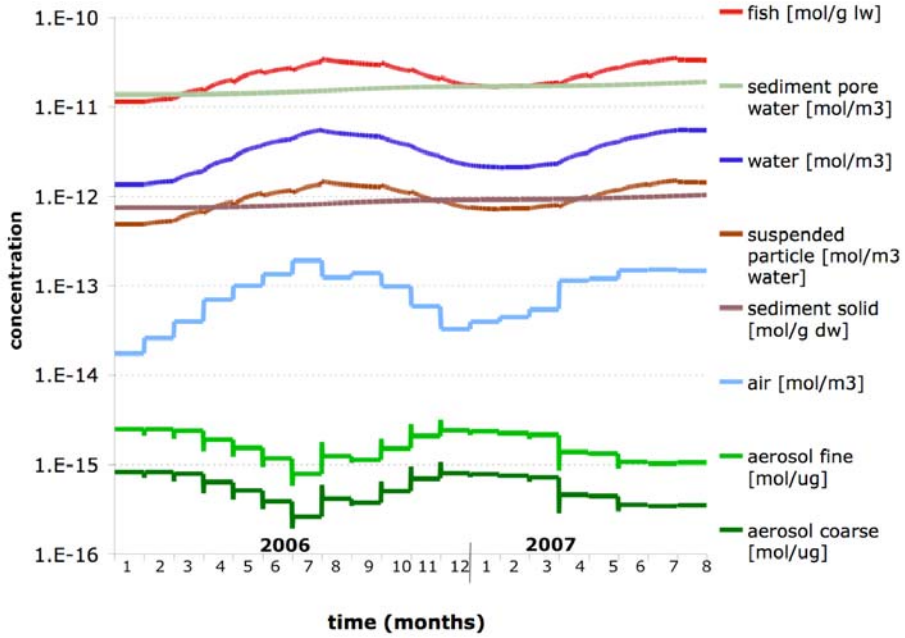

Figure 7-21: Concentration profile of Tetra-BDE in the time period January 2006 until August 2008. Concentrations in various media. Units are indicated in the legend.

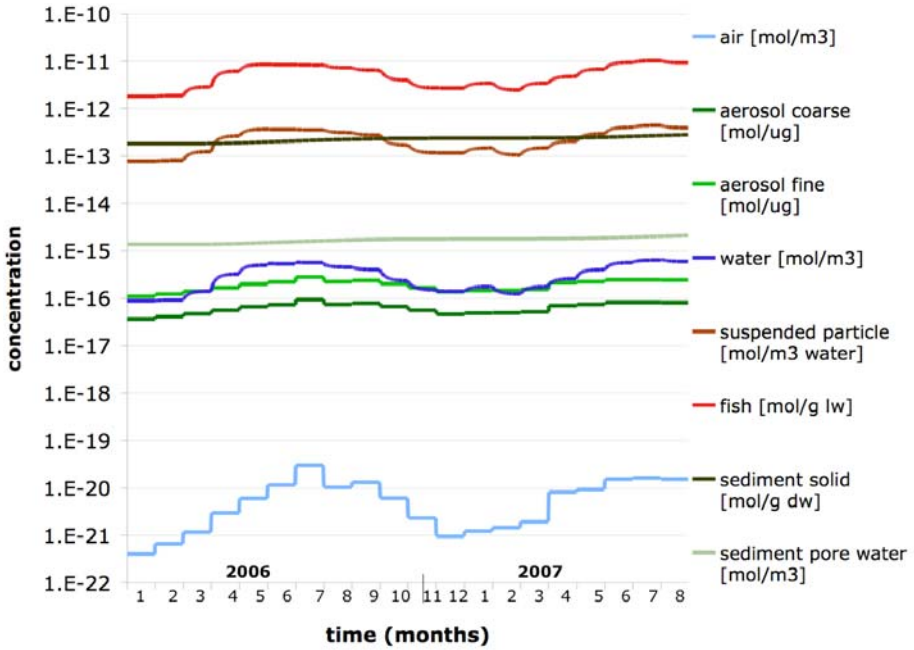

Figure 7-22: Concentration profile of Deca-BDE in the time period January 2006 until August 2008. Concentrations in various media. Units are indicated in the legend.

7.4.2. Comparison of mathematical solution alternatives

Three different solution alternatives were developed to solve the mass balance differential equation system. The comparison of the three methods showed, that there is agreement between the two numeric solution alternatives. Further, the analytic solution and the two numeric solutions match for the homologues up to Hexa-BDE and for all homologues regarding the gas and aerosol phase. However, there are some differences between the analytic solution and the two numeric solutions for the homologues from Hepta-BDE to Deca-BDE for the concentrations in the water, particle, fish, solid sediment and pore water. The highest differences have been observed in the solid sediment, which is shown in Figure 7-23. Shown is the ratio between the analytical and the numerical (self-made) solution. The differences are characterized by leaps at the beginning of new months followed by slow declinations. Interestingly there are no leaps during the summer months which decrease the difference between the two solutions. The differences in Octa-BDE and Nona-BDE are higher than in Deca-BDE. The mismatch can possibly be caused in the Deca-BDE and then transferred and somehow amplified to Nona- and Octa-BDE for which formation from Deca-BDE is the only input pathway.

Figure 7-24 shows the concentration profile for the analytical and the two numerical solutions in the solid sediment for Octa-BDE. This clearly shows that the leaps are encountered in the analytical solution. A closer look at the leaps however revealed that they are not actual leaps but fast increases and thus not caused by the sudden change in fugacity capacities at the end/beginning of a month, but seemingly by a fast process at the beginning which seems to be outbalanced after short time.

The result of this comparison was puzzling. The solution alternatives were then analyzed under different scenarios in order to find the reasons that cause these disagreements. A reduction in the small timestep (Δt) for the numeric solution (self-made), which increases its accuracy did not lead to a change in the gap between the analytic and numeric solution. Therefore, it seemed that the problem is not the inaccuracies caused by the numerical approximation. Further analysis showed that a model run without debromination led to equal solutions for the analytical and the numerical method. It was assumed that MATLAB encounters some problems with the model matrix describing the mass transfer terms. For the case without debromination, all B-matrices within the A-matrix (as described in chapter 5, equations (5-4) and (5-5)) are filled with zeros, while in the case with debromination, some of the B-matrices contain values differing from zero. Probably, the problem is caused in the algorithm that MATLAB uses for the inversion of the Matrix, which is needed in the analytical solution.

Due to these facts the numerical solution was used for the investigation of the dynamic behavior of the model and it is suggested to use the numerical solution unless the problems with the analytical solution can be solved.

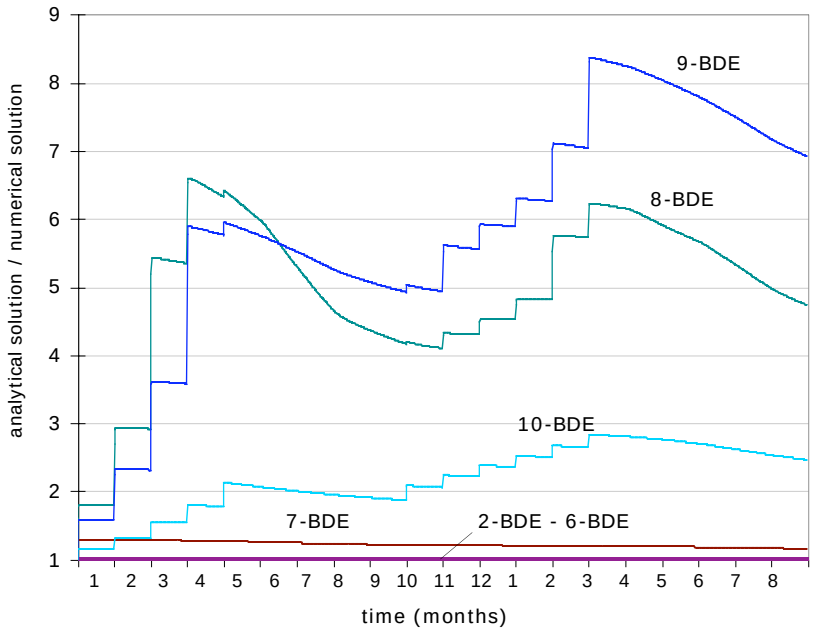

Figure 7-23: Difference between analytical solution and numerical solution. Shown is the ratio between the solutions.

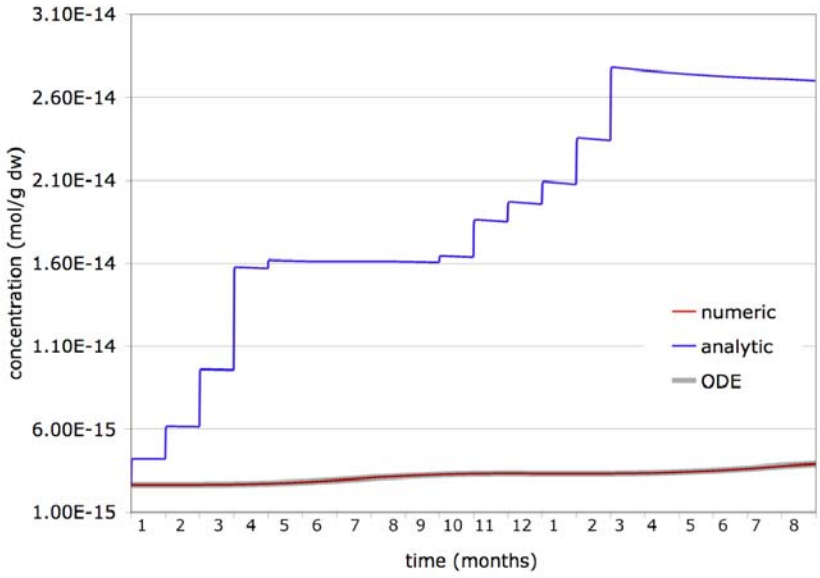

Figure 7-24: Concentration profile for Octa-BDE in solid sediment obtained with the analytical solution and the numerical solution.

7.4.3. Overall lifetime of compounds in the system

A dynamic model run without inputs and with the initial conditions set to the steady state solution of January 2006 was performed. This model run was used to determine the duration until the chemicals are depleted from the system when input is ceased. In order to investigate this, the model was run for 10 years following

August 2007, whereas the variable parameters defined for September 2006 until August 2007 were used for each of the 10 years.

The result shows an exponential decrease of the chemical mass in the system, caused by removal processes (outflow with river, burial to deeper sediment, diffusion to atmosphere and degradation). A half-life of the chemicals present in the lake water and sediment compartment was calculated. The results are shown in Figure 7-25. There is a trend to higher half-lives with increasing bromination. An exception are those homologues that are mainly formed by debromination (Di-, Tri-, Octa-, Nona-BDE), which have somewhat higher half-lives and lie apart from that trend. The basic reason behind this is that higher brominated homologues have a higher fraction in the sediment and that degradation in sediment and sediment burial are slower than degradation in the lake water and output with rivers. Furthermore, a higher fraction of the higher brominated homologues are present in fish, in which no degradation takes place and which are remaining in the lake. The half-life of the chemicals in the lake is much higher than the 'half-life' of lake water which is 1.3 years[11].

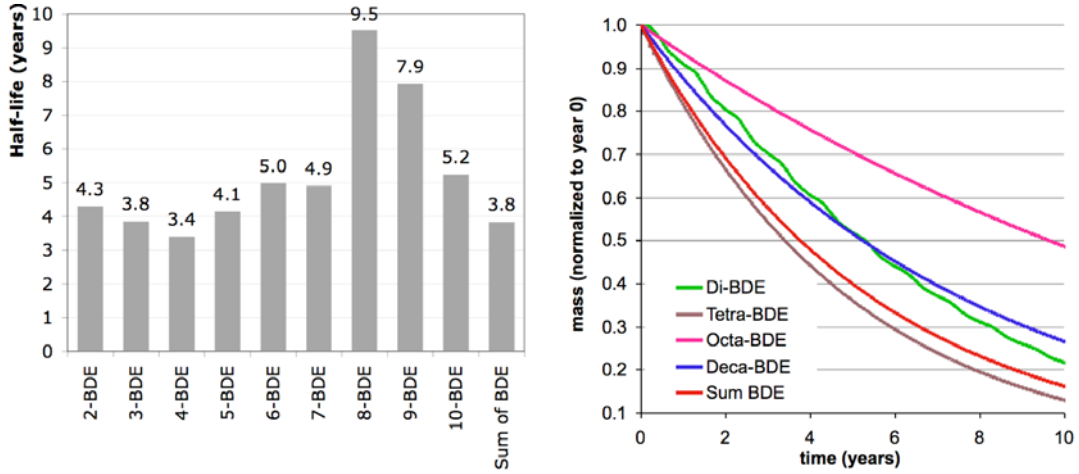

Figure 7-25: Depletion from the lake after input has ceased. The overall half-lives of the mass in the lake water and sediment together is shown in the left figure. The exponential decrease of four different homologues is shown in the right figure.

As seen in Figure 7-25 (right), a seasonal variation in the mass is only visible for Di-BDE. The reason for this is that for the lower brominated congeners, depletion by biodegradation and by diffusion from water to the atmosphere become important. Both processes are temperature dependent and therefore seasonal variation can be observed. For the higher brominated congeners depletion is mainly by sediment burial, which is not directly temperature dependent.

This fact indicates that the seasonal variations observed in Figure 7-21 and Figure 7-22 above are mainly caused by variations in the input concentrations.

[11] The average residence time of lake water is 684 days (Laboratory of Soil and Water Protection Bern, 2007). The 'half life' of the water in the lake is calculated by ln(2) · residence time.

The half-life obtained with this approach can be converted to a total depletion rate with:

$$k_{tot} = \frac{\ln(2)}{t_{1/2}} \quad (7\text{-}1)$$

This total rate can be determined for each PBDE individually or for the sum of PBDEs. Note that this k_{tot} is dependent on all the parameters used in the lake model and it is therefore also Lake Thun specific. Furthermore, it is an average rate over all months and therefore no seasonal variability can be described with this rate. The rates calculated for PBDEs are shown in Table 7-2

The time dependent mass in the modeled system (lake water + sediment) can then be described by:

$$\dot{M}(t) = k_{tot} M \quad (7\text{-}2) \quad \text{with the solution:} \quad M(t) = M_0 \cdot e^{-k_{tot} \cdot t} \quad (7\text{-}3),$$

M_0 is the initial mass in the system, which can be obtained from a stead-state solution. Expressions of this form can be determined for each PDBE individually or for the sum of PBDEs.

Equation (7-2) can be used for further analysis of various emission (substance input) scenarios. A term describing the input can thus be added to the equation (7-2), which leads to:

$$\dot{M}(t) = k_{tot} M + q(t) \quad (7\text{-}4)$$

q(t) describes the time dependent emissions into the modeled system. Various scenarios could be calculated with equation (7-4) by setting different functions for q(t) as for instance linearly or exponentially decreasing emissions.

Table 7-2: Total depletion rate for PBDEs.

BDE	**k_{tot} (y^{-1})**
Di-BDE	0.161
Tri-BDE	0.180
Tetra-BDE	0.204
Penta-BDE	0.167
Hexa-BDE	0.139
Hepta-BDE	0.141
Octa-BDE	0.073
Nona-BDE	0.087
Deca-BDE	0.132

8. Conclusions

8.1. Model development

A multimedia environmental fate model for a lake has been successfully developed and the different model runs performed in this thesis proved to deliver reasonable results. However, some problems have been observed with the analytical solution of the level IV model and it is therefore suggested to use the numerical solution unless the problems can be solved. Furthermore, uncertainty analysis with the analytical uncertainly calculation method showed some systematic deviations from a Monte Carlo simulation. The Monte Carlo simulation should provide a better estimate of the model uncertainty and therefore used in further assessments with the model.

The straightforward approach of modeling the lake as one box has the advantage that it is completely unspecific to the lake. In principal, the model can thus be applied to any lake. The model can also be applied to other chemicals, but it cannot be assured that the processes modeled and the parameterization is still appropriate when chemicals with completely different characteristics are modeled.

Two issues during the development of the model have led to the conclusion that using solubilities instead of partition constants as input values in models would be helpful in future modeling studies. One advantage of solubilities is that they can be used to calculate the temperature dependence of partition constants representing two media with different temperatures. The second advantage is that solubilities are not interdependent. The interdependency of partition constants causes problems in uncertainty and sensitivity analysis since a change in one partition constant needs an adaptation in the other partition constants in order to fulfill the thermodynamic constraint.

8.2. The case study of PBDEs in Lake Thun

Agreement between modeled and measured values for the Lake Thun case study demonstrates that the model performs well in calculating concentrations in various media. Some disagreements have been observed, which seem to be partly caused by errors or problems in measurements and partly by inaccuracies and simplifications in the model. However, it can be concluded, that the model includes the most important processes that determine the environmental fate of chemicals in a lake and that the effort in the parameterization has proved to be the road to success.

Most of the chemical mass in the modeled environment is present in the sediment, even though only the top layer (4 cm) has been modeled. This reflects the fact that the main removal process from lake water is sedimentation of suspended particles.

The main input into the lake comes from the atmosphere. However, the model seems to come closer to the measured values when an additional input by tributaries is included. So far, the model could not help in determing whether and to what extent debromination is happening in the environment.

An overall half-life for depletion from Lake Thun (water + sediment compartment) in case of ceasing input into the lake is between 3.4 and 9.5 years, whereas higher brominated homologues tend to be longer in the lake. This is rather high compared to a 1.3 years 'half-life' of water in the lake. It has been shown how the dynamic model can be used to determine a total rate of depletion from Lake Thun. This total rates can be used for analysis of different emission scenarios without actually using the model, since these total rates virtually incorporate the whole model in a single value.

Sensitivity and uncertainty analysis showed that PBDEs have some special characteristics that influence their fate. Namely, some PBDEs are at the edge of being either mainly particle bound or mainly in the gas phase (or dissolved). A change in temperature can therefore lead to a big change in the environmental fate of these chemicals. Consequently, site and time specific temperature data are important in modeling PBDEs.

8.3. Recommendations for further research

There are many possibilities for further investigations of the fate of PBDEs in Lake Thun and there are many points where the model and the Lake Thun case study could be improved.

One thing to emphasize is that the model should be applied again, when new and better data of water samples in the tributaries and in the air become available. The model output is very sensitive to the input concentration and therefore it is crucial to know them as accurately as possible. Further analyses with the model could include consideration of longer time periods and analyze different future emission scenarios or investigation of short-term meteorological variations by using a higher time resolution. Furthermore, the mathematical discrepancies between the analytical solution and the numerical solutions of the level IV model and the discrepancies between the analytical uncertainty calculation and the Monte Carlo simulation could be studied in more detail.

When more information becomes available regarding the pathway of debromination (i.e. which congeners are formed from which congeners), individual congeners rather than homologues could be modeled. This would be an advantage when modeled and measured concentrations are compared since measured data are always for individual congeners and not for homologue groups.

There are many possibilities to further extend the model. Additional processes and/or additional compartments could be added or existing compartments split into sub-compartments. Possible extensions depending which questions are focused on, would be:

- Division of water compartment into several sub-compartments. This could be horizontal or vertical divisions. Knowledge about the transfer processes between the compartments must be known to succeed in this. This could solve the issues that the environmental conditions (e.g. temperature) are highly variable with water depth.

- Development of an emissions scenario. This would make modelling possible without using the air measurements from Lake Thun for calibration.
- Inclusion of variable aerosol concentrations. This would mainly influence the seasonal variability and probably change the amount of chemicals deposited into the lake.

These are some suggestions and the list is definitely not complete. However, two things should be kept in mind prior to each model extension: (1) A model extension only makes sense if the added processes or compartments can be parameterized appropriately (e.g data on transfer processes or compartment dimensions must be available). (2) An extension can make the model more specific to a lake and there might thus be limitations to use the model for other lakes in the future.

References

Alaee, M., Arias, P., Sjodin, A., & Bergman, A. (2003). An overview of commercially used brominated flame retardants, their applications, their use patterns in different countries/regions and possible modes of release. *Environment International 29(6)*, 683-689.

Anderson, P.N., & Hites, R.A. (1996). OH radical reactions: The major removal pathway for polychlorinated biphenyls from the atmosphere. *Environmental Science & Technology 30(5)*, 1756-1763.

Arnot, J., Gouin, T., & Mackay, D. (2005). Practical methods for estimating environmental biodegradation rates. *Draft Guidance Report for Environment Canada in partial fulfillment of the Cooperative Agreement between Environment Canada and the Canadian Environmental Modelling Network*.

Atkinson, R. (1986). Kinetics and mechanisms of the gas-phase reactions of the hydroxyl radical with organic compounds under atmospheric conditions. *Chemical Reviews 86*, 69-201.

BAFU (Swiss Federal Office for the Environment). (2003). Modelling of PM10 and PM2.5 ambient concentrations in Switzerland 2000 and 2010. *available at: http://www.bafu.admin.ch/luft/00612/00624/index.html?lang=de*.

Bamford, H.A., Poster, D.L., & Baker, J.E. (2000). Henry's law constants of polychlorinated biphenyl congeners and their variation with temperature. *Journal of Chemical and Engineering Data 45(6)*, 1069-1074.

Bezares-Cruz, J., Jafvert, C.T., & Hua, I. (2004). Solar photodecomposition of decabromodiphenyl ether: Products and quantum yield. *Environmental Science & Technology 38(15)*, 4149-4156.

Bogdal, C. (2007a). Partitioning of polybrominated diphenyl ethers between air, water, sediment, and fish in Lake Thun (Switzerland). *Organohalogen Compounds 69*, 441-444.

Bogdal, C. (2007b). Historical profile of chlorinated paraffins and polychlorinated biphenyls in a sediment core from Lake Thun (Switzerland). *Organohalogen Compounds 69*, 335-338.

Braekevelt, E., Tittlemier, S.A., & Tomy, G.T. (2003). Direct measurement of octanol-water partition coefficients of some environmentally relevant brominated diphenyl ether congeners. *Chemosphere 51(7)*, 563-567.

Cetin, B., & Odabasi, M. (2005). Measurement of Henry's law constants of seven polybrominated diphenyl ether (PBDE) congeners as a function of temperature. *Atmospheric Environment 39(29)*, 5273-5280.

da Rosa, M.B., Kruger, H.U., Thomas, S., & Zetzsch, C. (2003). Photolytic debromination and degradation of decabromodiphenyl ether, an exploratory kinetic study in toluene. *Fresenius Environmental Bulletin 12(8)*, 940-945.

Darnerud, P.O. (2003). Toxic effects of brominated flame retardants in man and in wildlife. *Environment International 29(6)*, 841-853.

Darnerud, P.O., Eriksen, G.S., Johannesson, T., Larsen, P.B., & Viluksela, M. (2001). Polybrominated diphenyl ethers: Occurrence, dietary exposure, and toxicology. *Environmental Health Perspectives 109(Supplement 1)*, 49-68.

Ellinger, S., Hackenberg, R., & Ballschmitter, K. (2003). Determinnation of log Kow values for polybromo diphenyl ether (PBDEs) by Capillary Gas Chromatography and by Total Surface Area (TSA) Correlation. *Organohalogen Compounds 63*, 341-344.

Eriksson, J., Green, N., Marsh, G., & Bergman, A. (2004). Photochemical decomposition of 15 polybrominated diphenyl ether congeners in methanol/water. *Environmental Science & Technology 38(11)*, 3119-3125.

European Chemicals Bureau. (2000). European Union Risk Assessment Report: diphenyl ether, pentabromo deriv. *1st Priority List, available on ECB website: http://ecb.jrc.it/*.

European Chemicals Bureau. (2002). European Union Risk Assessment Report: bis(pentabromophenyl) ether. *1st Priority List, available on ECB website: http://ecb.jrc.it/*.

European Chemicals Bureau. (2003). European Union Risk Assessment Report: diphenyl ether, octabromo deriv. *1st Priority List, available on ECB website: http://ecb.jrc.it/*.

European Commission. (2003). Directive 2002/95/EC of the European Parliament and of the Council of 27 January 23 on the restriction of the use of certain hazardous substances in electrical and electronic equipment.

Finger, D., Lorenz, J., & Wüest, A. (2006). Auswirkungen der Stauseen auf den Schwebstoffhaushalt und auf die Primärproduktion des Brienzersees. Veränderungen im Ökosystem Brienzersee. Schlussbericht des Teilprojektes C. *Eawag report. Available at: http://www.eawag.ch/organisation/abteilungen/surf/publikationen/2006_brienzersee*.

Gandhi, N., Bhavsar, S.P., Gewurtz, S.B., Diamond, M.L., Evenset, A., Christensen, G.N., & Gregor, D. (2006). Development of a multichemical food web model: Application to PBDEs in Lake Ellasjoen, Bear Island, Norway. *Environmental Science & Technology 40(15)*, 4714-4721.

Gerecke, A.C. (2006). Photodegradation of decabromodiphenyl ether: kinetics, reaction quantum yield and penetration of light into kaolinite. *Organohalogen Compounds 68*, 1979-1982.

Gerecke, A.C., Hartmann, P.C., Heeb, N.V., Kohler, H.P.E., Giger, W., Schmid, P., Zennegg, M., & Kohler, M. (2005). Anaerobic degradation of decabromodiphenyl ether. *Environmental Science & Technology 39(4)*, 1078-1083.

Götz, C.W., Scheringer, M., MacLeod, M., Roth, C.M., & Hungerbuhler, K. (2007a). Alternative Approaches for Modeling Gas-Particle Partitioning of Semivolatile Organic Chemicals: Model Development and Comparison. *Environ. Sci. Technol. 41(4)*, 1272-1278.

Götz, C.W., Scheringer, M., MacLeod, M., Wegmann, F., & Hungerbuhler, K. (2007b). Regional differences in gas-particle partitioning and deposition of semivolatile organic compounds on a global scale. *Atmospheric Environment (accepted)*.

Gouin, T., & Harner, T. (2003). Modelling the environmental fate of the polybrominated diphenyl ethers. *Environment International 29(6)*, 717-724.

Harner, T., & Bidleman, T.F. (1998). Octanol-air partition coefficient for describing particle/gas partitioning of aromatic compounds in urban air. *Environmental Science & Technology 32(10)*, 1494-1502.

Harner, T., & Shoeib, M. (2002). Measurements of octanol-air partition coefficients (K-OA) for polybrominated diphenyl ethers (PBDEs): Predicting partitioning in the environment. *Journal of Chemical and Engineering Data 47(2)*, 228-232.

Hites, R.A. (2004). Polybrominated diphenyl ethers in the environment and in people: A meta-analysis of concentrations. *Environmental Science & Technology 38(4)*, 945-956.

Hueglin, C., Gehrig, R., Baltensperger, U., Gysel, M., Monn, C., & Vonmont, H. (2005). Chemical characterisation of PM2.5, PM10 and coarse particles at urban, near-city and rural sites in Switzerland. *Atmospheric Environment 39(4)*, 637-651.

Ikonomou, M.G., Rayne, S., & Addison, R.F. (2002). Exponential increases of the brominated flame retardants, polybrominated diphenyl ethers, in the Canadian arctic from 1981 to 2000. *Environmental Science & Technology 36(9)*, 1886-1892.

Inspectorate of fisheries Canton Bern. (2007). Fischfangstatistik 2005/2006. *available at: http://www.vol.be.ch/site/home/lanat/fischerei/fischerei-fangstatistiken.htm*.

Jolliet, O., & Hauschild, M. (2005). Modeling the influence of intermittent rain events on long-term fate and transport of organic air pollutants. *Environmental Science & Technology 39(12)*, 4513-4522.

Keum, Y.S., & Li, Q.X. (2005). Reductive debromination of polybrominated diphenyl ethers by zerovalent iron. *Environmental Science & Technology 39(7)*, 2280-2286.

Kirchhofer, A. (1990). Limnologische und ichtiologische Untersuchungen im Brienzersee unter besonderer Berücksichtigung der sympatrischen Felchenpopulationen. Doktorarbeit, Philosophisch-naturwissenschaftliche Fakultät, Bern.

Kuramochi, H., Maeda, K., & Kawamoto, K. (2007). Physicochemical properties of selected polybrominated diphenyl ethers and extension of the UNIFAC model to brominated aromatic compounds. *Chemosphere 67(9)*, 1858-1865.

Kwok, E.S.C., & Atkinson, R. (1995). Estimation of Hydroxyl Radical Reaction-Rate Constants for Gas-Phase Organic-Compounds Using a Structure-Reactivity Relationship - an Update. *Atmospheric Environment 29(14)*, 1685-1695.

Laboratory of soil and water protection Canton Bern. (2007). Seen im Kanton Bern (overview brochure). *available at: http://www.bve.be.ch/site/index/gsa/bve_gsa_gwq_seen.htm*.

Lau, F., Destaillats, H., & Charles, M.J. (2003). Expermimentally determined Henry's law constants for six brominated diphenyl ether congeners. *Organohalogen Compounds 63*, 333-336.

Lau, F.K., Charles, M.J., & Cahill, T.M. (2006). Evaluation of gas-stripping methods for the determination of Henry's law constants for polybrominated diphenyl

ethers and polychlorinated biphenyls. *Journal of Chemical and Engineering Data 51(3)*, 871-878.

Law, R.J., Allchin, C.R., de Boer, J., Covaci, A., Herzke, D., Lepom, P., Morris, S., Tronczynski, J., & de Wit, C.A. (2006). Levels and trends of brominated flame retardants in the European environment. *Chemosphere 64(2)*, 187-208.

Li, N., Wania, F., Lei, Y.D., & Daly, G.L. (2003). A comprehensive and critical compilation, evaluation, and selection of physical-chemical property data for selected polychlorinated biphenyls. *J. Phys. Chem. Ref. Data 32(4)*, 1545-1590.

Mackay, D. (2001). Multimedia Environmental Models - The Fugacity Approach. Boca Raton; CRC Press LLC.

Mackay, D., Paterson, S., & Shiu, W.Y. (1992). Generic Models for Evaluating the Regional Fate of Chemicals. *Chemosphere 24(6)*, 695-717.

MacLeod, M., Fraser, A.J., & Mackay, D. (2002). Evaluating and expressing the propagation of uncertainty in chemical fate and bioaccumulation models. *Environmental Toxicology and Chemistry 21(4)*, 700-709.

McKone, T.E., & Lawrence, E.O. (1997). CalTOX Version 2.3 Description of Modifications and Revisions. Manual for the CalTOX multimedia model. *available at: http://www.dtsc.ca.gov/AssessingRisk/ctox_model.cfm*.

Palm, A., Cousins, I.T., Mackay, D., Tysklind, M., Metcalfe, C., & Alaee, M. (2002). Assessing the environmental fate of chemicals of emerging concern: a case study of the polybrominated diphenyl ethers. *Environmental Pollution 117(2)*, 195-213.

Palm, W.U., Kopetzky, R., Sossinka, W., Ruck, W., & Zetzsch, C. (2004). Photochemical reactions of brominated diphenylethers in organic solvents and adsorbed on silicon dioxide in aqueous suspension. *Organohalogen Compounds 66*, 4105-4110.

Peterman, P.H., Orazio, C.E., & Feltz, K.P. (2003). Sunlight photolysis of 39 mono-hepta PBDE congeners in lipid. *Organohalogen Compounds 63*, 357-360.

Putaud, J.P., Raes, F., Van Dingenen, R., Bruggemann, E., Facchini, M.C., Decesari, S., Fuzzi, S., Gehrig, R., Huglin, C., Laj, P., Lorbeer, G., Maenhaut, W., Mihalopoulos, N., Mulller, K., Querol, X., Rodriguez, S., Schneider, J., Spindler, G., ten Brink, H., Torseth, K., & Wiedensohler, A. (2004). European aerosol phenomenology-2: chemical characteristics of particulate matter at kerbside, urban, rural and background sites in Europe. *Atmospheric Environment 38(16)*, 2579-2595.

Raff, J.D., & Hites, R.A. (2006). Gas-phase reactions of brominated diphenyl ethers with OH radicals. *Journal of Physical Chemistry A 110(37)*, 10783-10792.

Raff, J.D., & Hites, R.A. (2007). Deposition versus Photochemical Removal of PBDEs from Lake Superior Air. *Environmental Science & Technology*.

Rayne, S., Wan, P., & Ikonomou, M. (2006). Photochemistry of a major commercial polybrominated diphenyl ether flame retardant congener: 2,2 ',4,4 ',5,5 '-Hexabromodiphenyl ether (BDE153). *Environment International 32(5)*, 575-585.

Sanchez-Prado, L., Llompart, M., Lores, M., Garcia-Jares, C., & Cela, R. (2005). Investigation of photodegradation products generated after UV-irradiation of five polybrominated diphenyl ethers using photo solid-phase microextraction. *Journal of Chromatography A 1071(1-2)*, 85-92.

Schenker, U., MacLeod, M., Scheringer, M., & Hungerbuhler, K. (2005). Improving data quality for environmental fate models: A least-squares adjustment procedure for harmonizing physicochemical properties of organic compounds. *Environmental Science & Technology 39(21)*, 8434-8441.

Scheringer, M., Wegmann, F., Fenner, K., & Hungerbuhler, K. (2000). Investigation of the cold condensation of persistent organic pollutants with a global multimedia fate model. *Environmental Science & Technology 34(9)*, 1842-1850.

Schwarzenbach, R.P., Gschwend, P.M., & Imboden, D.M. (2003). Environmental Organic Chemistry. John Wiley & Sons, Hoboken, New Jersey.

Seinfeld, J.H., & Pandis, S.N. (1998). Atmospheric Chemistry and Physics. Wiley-Interscience, New York.

Seth, R., Mackay, D., & Muncke, J. (1999). Estimating the organic carbon partition coefficient and its variability for hydrophobic chemicals. *Environmental Science & Technology 33(14)*, 2390-2394.

Söderstrom, G., Sellström, U., De Wit, C.A., & Tysklind, M. (2004). Photolytic debromination of decabromodiphenyl ether (BDE 209). *Environmental Science & Technology 38(1)*, 127-132.

Spivakovsky, C.M., Logan, J.A., Montzka, S.A., Balkanski, Y.J., Foreman-Fowler, M., Jones, D.B.A., Horowitz, L.W., Fusco, A.C., Brenninkmeijer, C.A.M., Prather, M.J., Wofsy, S.C., & McElroy, M.B. (2000). Three-dimensional climatological distribution of tropospheric OH: Update and evaluation. *Journal of Geophysical Research-Atmospheres 105(D7)*, 8931-8980.

Stapleton, H.M., Alaee, M., Letcher, R.J., & Baker, J.E. (2004). Debromination of the flame retardant decabromodiphenyl ether by juvenile carp (Cyprinus carpio) following dietary exposure. *Environmental Science & Technology 38(1)*, 112-119.

Streets, S.S., Henderson, S.A., Stoner, A.D., Carlson, D.L., Simcik, M.F., & Swackhamer, D.L. (2006). Partitioning and bioaccumulation of PBDEs and PCBs in Lake Michigan. *Environmental Science & Technology 40(23)*, 7263-7269.

Sturm, M., & Matter, A. (1972). Sedimente und Sedimentationsvorgänge im Thunersee. *Eclogae Geologicae Helveticae 65(3)*, 563-590.

Tittlemier, S.A., Halldorson, T., Stern, G.A., & Tomy, G.T. (2002). Vapor pressures, aqueous solubilities, and Henry's law constants of some brominated flame retardants. *Environmental Toxicology and Chemistry 21(9)*, 1804-1810.

Tomy, G.T., Palace, V.P., Halldorson, T., Braekevelt, E., Danell, R., Wautier, K., Evans, B., Brinkworth, L., & Fisk, A.T. (2004). Bioaccumulation, biotransformation, and biochemical effects of brominated diphenyl ethers in juvenile lake trout (Salvelinus namaycush). *Environmental Science & Technology 38(5)*, 1496-1504.

Wania, F., & Daly, G.L. (2002). Estimating the contribution of degradation in air and deposition to the deep sea to the global loss of PCBs. *Atmospheric Environment 36(36-37)*, 5581-5593.

Wania, F., & Dugani, C.B. (2003). Assessing the long-range transport potential of polybrominated diphenyl ethers: A comparison of four multimedia models. *Environmental Toxicology and Chemistry 22(6)*, 1252-1261.

Watanabe, I., Tatsukawa, R. (1989). Anthropogenic brominated aromatics in the Japanese environment. *Proceedings, Workshop on brominated aromatic flaame retardants, Skokloster, Sweden*, 63-71.

Wong, A., Lei, Y.D., Alaee, M., & Wania, F. (2001). Vapor pressures of the polybrominated diphenyl ethers. *Journal of Chemical and Engineering Data 46(2)*, 239-242.

Wurl, O., Lam, P.K.S., & Obbard, J.P. (2006). Occurrence and distribution of polybrominated diphenyl ethers (PBDEs) in the dissolved and suspended phases of the sea-surface microlayer and seawater in Hong Kong, China. *Chemosphere 65(9)*, 1660-1666.

Zennegg, M., Kohler, M., Gerecke, A.C., & Schmid, P. (2003). Polybrominated diphenyl ethers in whitefish from Swiss lakes and farmed rainbow trout. *Chemosphere 51(7)*, 545-553.

Zetzsch, C., Palm, W.U., & Krueger, H.U. (2004). Photochemistry of 2,2',4,4',5,5'-HexaBDE (BDE-153) in THF and adsorbed on SiO2: First observation of OH reactivity of BDEs an aerosol. *Organohalogen Compounds 66*, 2256 - 2261.

Property estimation tools

EPIWIN Version 3.20 (February 2007). Software package provided by the United States Environmental Protection Agency for estimation of various chemical properties (AOPWIN and BIOWIN are part of the EPIWIN software package). http://www.epa.gov/oppt/exposure/pubs/episuitedl.htm

AOPWIN Version 1.92. OH-radical reaction estimation tool. Part of the EPI Suite Software package. Based on methods developed by Atkinson (1986). Details on the EPA website (http://www.epa.gov/opptintr/exposure/pubs/episuite.htm) and in the help files for the program (download on the same page).

BIOWIN Version 4.10. Biodegradation rates estimation tool, part of the EPI Suite Software package. Details about the underlying predictive methods can be found on the EPA website (http://www.epa.gov/opptintr/exposure/pubs/episuite.htm) and in the help files for the program (download on the same page).

SPARC (Sparc performs automated reasoning in chemistry) Version January 2007; http://www.epa.gov/athens/research/projects/sparc/index.html

Data sources

MeteoSwiss (Swiss Federal Office of Meteorology and Climatology)

(1) Data obtained from Climap-net database queries

(2) Data obtained directly from the MeteoSwiss webpage:
http://www.meteoschweiz.admin.ch/web/en/climate/climate_norm_values/tabellen.html

(1) Weather station Interlaken	Data for 2006 and 2007 - Precipitation (sum) - Air temperature - Solar radiation - Wind speed and direction
(1) Weather stations Zurich and Kloten	Data for 21st September 2005 (hourly) - Solar radiation
(2) Weather stations Hondrich and Thun	Mean values 1961-1990 for precipitation

BAFU (Swiss Federal Office for the Environment), Hydrology division

Access: http://www.hydrodaten.admin.ch

Stations: Aare - Ringgenberg, Goldswil Aare – Thun Kander – Hondrich Simme – Latterbach[1)]	Monthly runoff data for 2006 and 2007

1) data set including water from power station Simmenfluh-Wimmis

Canton Bern, pollutant measurements

Access: http://www.vol.be.ch/site/home/beco/beco-imm.htm

Station Thun, Pestalozzi	PM10 data for 2006 and 2007

Canton Bern, Laboratory of Soil and Water protection

Obtained from Markus Zeh via personal communication.

Lake Thun, deepest point (coordinates: 632'300/170'050)	Surface temperature data for 2006 and 2007. Total non-dissolved matter for the period 2003-2007

Weather station Thun, privately operated weather station

Access: http://www.thunerwetter.ch/

No data were used for the model from this station.

List of personal communications

Christian Bogdal Christian.Bogdal@empa.ch Dr. Martin Kohler Martin.Kohler@empa.ch Dr. Andreas Gerecke Andreas.Gerecke@empa.ch Michael Naef Michael.Naef@empa.ch	Empa Analytische Chemie Ueberlandstrasse 129 CH-8600 Duebendorf +41 44 823 4260 (Christian Bogdal)
Dr. Markus Zeh	Amt für Gewässerschutz und Abfallwirtschaft (GSA) des Kantons Bern Gewässer- und Bodenschutzlabor (GBL) Schermenweg 11 CH-3014 Bern +41 31 634 23 84 markus.zeh@bve.be.ch
Christoph Küng	Bereichsleiter Fischereiwirtschaft Fischereiinspektorat Kanton Bern Amt für Landwirtschaft und Natur Schwand CH-3110 Münsingen +41 31 720 32 40 christoph.kueng@vol.be.ch

Appendix I – Substances

Polybrominated diphenyl ethers (PBDEs)

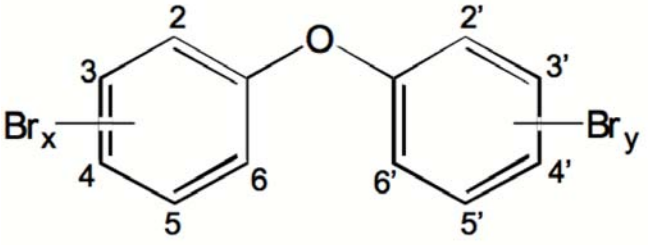

PBDE number (IUPAC)	PBDE name
PBDEs used in the model	
Di-BDE-15	4,4'-dibromodiphenyl ether
Tri-BDE-28	2,4,4'-tribromodiphenyl ether
Tetra-BDE-47	2,2',4,4'-tetrabromodiphenyl ether
Penta-BDE-99	2,2',4,4',5-pentabromodiphenyl ether
Penta-BDE-100	2,2',4,4',6-pentabromodiphenyl ether
Hexa-BDE-153	2,2',4,4',5,5'-hexabromodiphenyl ether
Hepta-BDE-183	2,2',3,4,4',5',6-heptabromodiphenyl ether
Deca-BDE-209	2,2',3,3',4,4',5,5',6,6'-decabromodiphenyl ether
Only mentioned in the text	
Tri-BDE-17	2,2',4-tribromodiphenyl ether
Hexa-BDE-154	2,2',4,4',5,6'-hexabromodiphenyl ether

Annotation:

‚PBDE-15', 'BDE-15' and 'Di-BDE-15' represent the same substance. The prefix ('Di-') is just used sometimes to illustrate the number of bromine substitutions. (applies to all PBDEs)

Polychlorinated biphenyls (PCBs)

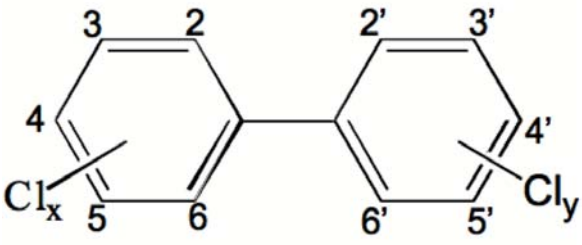

PCB number (IUPAC)	PCB name
PCBs used in the model	
Tri-CB-28	2,4,4'-Trichlorobiphenyl
Tetra-CB-52	2,2',5,5'-Tetrachlorobiphenyl
Penta-CB-101	2,2',4,5,5'-Pentachlorobiphenyl
Hexa-CB-138	2,2',3,4,4',5'-Hexachlorobiphenyl
Hexa-CB-153	2,2',4,4',5,5'-Hexachlorobiphenyl
Hepta-CB-180	2,2',3,4,4',5,5'-Heptachlorobiphenyl

Annotation:

'PCB-28', 'CB-28' and 'Tri-CB-28' represent the same substance. The prefix ('Tri-') is just used sometimes to illustrate the number of chlorine substitutions. (applies to all PCBs)

Appendix II – PBDE property data

LDV: Literature derived value. This is the geometric mean of all used values

Range: The difference between the minimum and maximum of the used values

Relative variance: Set to 2, 3 or 4 according to the definition in chapter 2

FAV: Final adjusted value, obtained with the least-squares adjustment method presented in chapter 2.

Italic: Excluded values

Vapor pressure (P)

MEASURED

BDE	*Norris et al. (1973)*[1)]	Tittlemier et al. (2002)	Watanabe and Tatsukawa (1989)[2)]	Wong et al. (2001)
BDE-15		1.73E-02	1.55E-02	9.84E-03
BDE-28	-	2.19E-03	2.08E-03	
BDE-47		1.86E-04	2.92E-04	3.19E-04
BDE-99		1.76E-05	4.63E-05	6.82E-05
BDE-100		2.86E-05	4.63E-05	
BDE-153		2.09E-06	6.31E-06	8.43E-06
BDE-183		4.68E-07		
BDE-209	*4.63E-06*			

1) Value obtained from EU Risk Assessment Report (European Chemicals Bureau, 2002)

2) Value obtained from Wania and Dugani (2003)

CALCULATED/ESTIMATED

BDE	*EPIWIN1*	*EPIWIN2*	*Sparc*	*Wong et al. (2001)*	*Palm et al. (2002)*
BDE-15	*1.49E-02*		*2.64E-03*		
BDE-28	*3.11E-04*	*8.91E-05*	*1.63E-04*	*1.60E-03*	
BDE-47	*9.31E-06*	*3.21E-05*	*8.28E-06*		*8.18E-05*
BDE-99	*4.12E-06*	*3.25E-06*	*2.63E-07*		*7.64E-06*
BDE-100		*3.25E-06*	*1.69E-07*		
BDE-153		*3.82E-07*	*1.99E-09*		
BDE-183		*4.38E-08*	*7.17E-11*		
BDE-209		*6.21E-10*	*2.56E-16*	*2.95E-09*	*5.42E-11*

Exclusions: BDE-209 from Norris et al. (1973) because he measured the commercial product. Values from Wong et al. (2001) and Palm et al. (2002) because they are based on linear extrapolations from other literature values

FINAL VALUES

BDE	LDV (Pa)	Number of values	Range (log units)	Relative variance	FAV (Pa)
BDE-15	1.38E-02	3	0.25	2	1.37E-02
BDE-28	2.13E-03	2	0.02	2	2.11E-03
BDE-47	2.59E-04	3	0.23	2	2.40E-04
BDE-99	3.82E-05	3	0.59	3	3.92E-05
BDE-100	3.64E-05	2	0.21	2	6.01E-05
BDE-153	4.81E-06	3	0.61	3	4.33E-06
BDE-183	4.68E-07	1	0.00	4	1.87E-06
BDE-209	--	0	--		9.03E-08

Water solubility (subcooled liquid) (S_w)

The water solubility data found in the literature represent the solution from the solid state. For the least-squares adjustment procedure water solubilities for the subcooled liquid state were needed. These were calculated by dividing the water solubilities shown here by the fugacity ratio. Fugacity ratios for all congeners have been found in the supporting information of Wania and Dugani (2003).

BDE	Fugacity ratio
BDE-15	0.477
BDE-28	0.409
BDE-47	0.261
BDE-99	0.215
BDE-100	0.179
BDE-153	0.045
BDE-183	0.035
BDE-209	0.00179

MEASURED

BDE	Kuramochi et al. (2007)	*Norris et al. (1973)*[1)]	Stenzel and Markley (1997)[2)]	Tittlemier et al. (2002)	Wania and Dugani (2003)[3)]
BDE-15	1.38E-03			8.21E-04	
BDE-28				4.16E-04	
BDE-47	1.16E-04			1.17E-04	
BDE-99	3.60E-05		1.98E-05	7.71E-05	
BDE-100				3.96E-04	
BDE-153	1.74E-06			3.00E-05	
BDE-183				5.81E-05	
BDE-209		1.34E-02			2.33E-06

1) Value obtained from EU Risk Assessment Report (European Chemicals Bureau, 2002)
2) Value obtained from Wania and Dugani (2003)
3) Wania and Dugani (2003) obtained the value from the Environmental Chemistry and Ecotoxicology Research Group at the Environmental Science Department, Lancaster University. The website indicated in the reference list is not valid anymore.

CALCULATED

BDE	*EPIWIN1*	*EPIWIN2*	*EPIWIN3*	*Sparc*	*Palm et al. (2002)*
BDE-15		*4.63E-02*	*5.64E-04*	*3.15E-03*	
BDE-28	*1.61E-03*			*1.27E-03*	
BDE-47		*4.28E-04*	*1.15E-05*	*2.62E-04*	*7.35E-05*
BDE-99		*8.81E-05*	*6.47E-07*	*2.11E-04*	*8.40E-06*
BDE-100		*1.06E-04*	*7.78E-07*	*2.39E-04*	
BDE-153		*7.15E-05*	*1.43E-07*	*1.52E-04*	
BDE-183		*2.94E-06*	*4.38E-10*	*4.88E-05*	
BDE-209	*1.53E+01*	*1.49E-06*	*3.76E-10*	*4.10E-06*	*7.57E-09*

Exclusions: BDE-209 from Norris et al. (1973) because he measured the commercial product, all values from estimation software programs, values from Palm et al. (2002) because they are based on extrapolations from other literature data.

FINAL VALUES

BDE	Average (mol m^{-3})	Number of values	Range (log units)	Relative variance	Final value (mol m^{-3})
BDE-15	1.06E-03	2	0.22	2	1.07E-03
BDE-28	4.16E-04	1	0.00	4	4.27E-04
BDE-47	1.17E-04	2	0.00	2	1.26E-04
BDE-99	3.80E-05	3	0.59	3	3.70E-05
BDE-100	3.96E-04	1	0.00	4	1.45E-04
BDE-153	7.22E-06	2	1.24	4	8.29E-06
BDE-183	5.81E-05	1	0.00	4	1.45E-05
BDE-209	2.33E-06	1	0.00	4	2.33E-06

Air - water partition constant (K_{aw})

MEASURED

BDE	Cetin and Odabasi (2005)	Lau et al. (2006) IGSM	Lau et al. (2006) MGSM	*Lau et al. (2003)*
BDE-15		-2.25	-2.33	*-1.83*
BDE-28	-2.71	-2.28	-2.43	*-2.22*
BDE-47	-3.50	-2.64	-2.59	*-1.77*
BDE-99	-3.62	-2.92	-3.20	
BDE-100	-4.03	-2.91	-2.93	
BDE-153	-4.00			
BDE-183				
BDE-209	-4.81			

CALCULATED

BDE	*Cetin and Odabasi (2005)*	*EPIWIN*	*Tittlemier et al. (2002)*	*Wania and Dugani (2003)*
BDE-15		*-2.91*	*-2.07*	*-2.78*
BDE-28		*-3.30*	*-2.69*	*-3.11*
BDE-47		*-3.69*	*-3.22*	*-3.35*
BDE-99		*-4.08*	*-4.03*	*-3.67*
BDE-100		*-4.08*	*-4.56*	*-3.81*
BDE-153		*-4.47*	*-4.57*	*-3.86*
BDE-183	*-4.27*	*-5.51*	*-5.52*	
BDE-209		*-6.03*		

Exclusions: Values estimated by EPIWIN software, Values from Lau et al. (2003) due to unreliable measurement method (GSM – Gas stripping method). Values from Tittlemier et al. (2002) because they are calculated from vapor pressure and solubility in water data, values from Wania and Dugani (2003) which are based on other literature values and another adjustment method.

FINAL VALUES

BDE	Average (log)	Number of values	Range (log units)	Relative variance	Final value (log)
BDE-15	-2.29	2	0.08	2	-2.29
BDE-28	-2.53	3	0.43	2	-2.70
BDE-47	-3.06	3	0.92	3	-3.12
BDE-99	-3.34	3	0.71	3	-3.37
BDE-100	-3.47	3	1.12	4	-3.78
BDE-153	-4.00	1	0.00	4	-3.68
BDE-183		0	0.00	--	-4.28
BDE-209	-4.81	1	0.00	4	-4.81

Octanol – water partition constant (K_{ow})

MEASURED

BDE	Braekevelt et al. (2003)	*European Chemicals Bureau (2002)*	Kuramochi et al. (2007)	Tomy et al. (2001)[1)]	Watanabe and Tatsukawa (1989)
BDE-15			5.86		5.03
BDE-28	5.94				5.53
BDE-47	6.81		6.78	6.19	6.02
BDE-99	7.32		7.39	6.53	6.72
BDE-100	7.24			6.30	6.72
BDE-153	7.90		8.05	6.87	7.39
BDE-183	8.27			7.14	
BDE-209		*6.27*			9.97

1) Value obtained from Wania and Dugani (2003)

CALCULATED

BDE	*EPIWIN*	*Sparc*	Wurl et al. (2006)	*Palm et al. (2002)*	*Ellinger et al. (2003)*	*Tittlemier et al. (2002)*
BDE-15	*5.83*	*5.91*				*5.55*
BDE-28	*5.88*	*6.83*				*5.98*
BDE-47	*6.77*	*7.74*		*6.67*	*7.40*	*6.55*
BDE-99	*7.66*	*8.75*		*7.42*	*7.90*	*7.13*
BDE-100	*7.66*	*8.73*			*7.80*	*6.86*
BDE-153	*8.55*	*9.77*			*8.30*	*7.90*
BDE-183	*10.33*	*10.73*				
BDE-209	*12.11*	*13.73*	8.70	*11.15*	*9.30*	

Excluded: Values from estimation softwars (EPIWIN, Sparc), Values from Palm et al. (2002) because they are based on linear regressions from other literature data, values from Ellinger et al. (2003) based on gas chromatography retention times an selective correlations with PCB congeners, values from Tittlemier et al. (2002) based on values for polychlorinated diphenyl ethers and fragment constants for bromine and chlorine.

FINAL VALUES

BDE	Average (log)	Number of values	Range (log units)	Relative variance	Final value (log)
BDE-15	5.45	2	0.83	3	5.44
BDE-28	5.73	2	0.42	3	5.92
BDE-47	6.45	4	0.80	3	6.53
BDE-99	6.99	4	0.86	3	7.00
BDE-100	6.75	3	0.94	3	6.68
BDE-153	7.55	4	1.18	4	7.36
BDE-183	7.71	2	1.13	4	7.26
BDE-209	9.97	1	0.00	4	9.97

Annotation: K_{ow} was converted to K_{ow}* with the equation (given in Schenker et al., 2005):

$$\log K_{ow}^{*} = 1.36 \cdot \log K_{ow} - 1.6$$

Octanol – air partition constant (K_{oa})

	MEASURED	*CALCULATED*
BDE	**Harner and Shoeib (2002)**	***Harner and Shoeib (2002)***
BDE-15		*8.79*
BDE-28	9.50	
BDE-47	10.53	
BDE-99	11.31	
BDE-100	11.13	
BDE-153	11.82	
BDE-183	11.96	
BDE-209		*14.40*

Excluded: Values for BDE-15 and BDE-209 from Harner and Shoeib (2002), because the BDE-15 value was obtained by calculation from relative retention time and BDE-209 was obtained by extrapolation from the other congeners

BDE	Average (log)	Number of values	Range (log units)	Relative variance	Final value (log)
BDE-15		1	0	4	8.09
BDE-28	9.50	1	0	4	9.16
BDE-47	10.53	1	0	4	10.39
BDE-99	11.31	1	0	4	11.29
BDE-100	11.13	1	0	4	11.26
BDE-153	11.82	1	0	4	12.08
BDE-183	11.96	1	0	4	12.56
BDE-209		1	0	4	16.77

ΔU_{vap}

	Measured		Calculated
BDE	**Tittlemier et al. (2002)**	**Wong et al. (2001)**	**Tittlemier et al. (2002) and Wong et al. (2001)**
BDE-15	65'121	75'521	
BDE-28	77'221		
BDE-47	92'121	89'521	
BDE-99	105'521	97'821	
BDE-100	99'521		
BDE-153	107'521	105'121	
BDE-183	115'521		
BDE-209			145'022[1)]

1) obtained with linear regression of the values from Tittlemier et al. (2002) an Wong et al. (2001) versus bromine number.

BDE	Average ($J\ mol^{-1}$)	Number of values	Range	Relative variance	Final value ($kJ\ mol^{-1}$)
BDE-15	70'321	2	10'400	3	70'321
BDE-28	77'221	1	0	4	77'221
BDE-47	90'821	2	2'600	3	86'730
BDE-99	101'671	2	7'700	3	94'768
BDE-100	99'521	1	0	4	99'521
BDE-153	106'321	2	2'400	3	97'242
BDE-183	115'521	1	0	4	115'521
BDE-209	145'022	1	0	4	145'022

Inner energy of solution in water (ΔU_w) (for liquid-> dissolved)

As with the values for solubility in water the values for inner energy of solution in water need to be converted. The values obtained from the literature represent the inner energy for the transition from the solid to the dissolved state. The value needed in the least-squares adjustment is the inner energy for the transition from the liquid to the dissolved state. This value was calculated by subtracting the inner energy of fusion (solid to liquid state) from the inner energy from solid to dissolved state. The inner energy of fusion was obtained from measurements by Kuramochi et al. (2007).

BDE	Kuramochi et al. (2007) ΔUw (solid –> dissolved)	Kuramochi et al. (2007) ΔUfus	ΔUw (liquid -> dissolved)
BDE-15	40'500	19'600	20'900
BDE-47	32'200	17'300	14'900
BDE-99	30'600	27'500	3'100
BDE-153	38'600	30'200	8'400

FINAL VALUES

BDE	Average (J mol^{-1})	Number of values	Range	Relative variance	Final value (J mol^{-1})
BDE-15	20900	1	0	4	20'900
BDE-28		0	--	4	15'501
BDE-47	14900	1	0	4	20'354
BDE-99	3100	1	0	4	12'304
BDE-100		0	--	4	42'873
BDE-153	8400	1	0	4	20'506
BDE-183		0	--	4	
BDE-209		0	--	4	79'345

Inner energy of air to water phase transfer (ΔU_{aw})

Measured

BDE	Cetin and Odabasi (2005)
BDE-15	
BDE-28	61720
BDE-47	60922
BDE-99	73260
BDE-100	56648
BDE-153	64630
BDE-183	
BDE-209	65677

FINAL VALUES

BDE	Average (J mol^{-1})	Number of values	Range	Relative variance	Final value (J mol^{-1})
BDE-15		0	--	4	49'421
BDE-28	61'720	1	0	4	61'720
BDE-47	60'922	1	0	4	66'376
BDE-99	73'260	1	0	4	82'464
BDE-100	56'648	1	0	4	56'648
BDE-153	64'630	1	0	4	76'736
BDE-183		0	--	4	
BDE-209	65'677	1	0	4	65'677

Inner energy of octanol to air phase transfer (ΔU_{oa})

Measured

BDE	Harner and Shoeib (2002)[1)]
BDE-15	
BDE-28	-72800
BDE-47	-97000
BDE-99	-91100
BDE-100	-105000
BDE-153	-98200
BDE-183	-89500
BDE-209	

1) Original literature values are erroneously given as positive values and they are reported to be enthalpies, but actually represent inner energies since the underlying partition constant in the measurements was defined on a concentration basis.

FINAL VALUES

BDE	Average ($J\ mol^{-1}$)	Number of values	Range	Relative variance	Final value ($J\ mol^{-1}$)
BDE-15		0	--	4	
BDE-28	-72'800	1	0	4	-72'800
BDE-47	-97'000	1	0	4	-97'000
BDE-99	-91'100	1	0	4	-91'100
BDE-100	-105'000	1	0	4	-105'000
BDE-153	-98'200	1	0	4	-98'200
BDE-183	-89'500	1	0	4	-89'500
BDE-209		0	--	4	-

Appendix III – PBDE degradation data

Photolysis half-lives (per h of sunlight).

		Eriksson et al. ,2004	Da Rosa et al., 2003	Zetzsch, et al., 2004	Petermann et al., 2003	Eriksson et al., 2004	Eriksson et al. ,2004	Bezares-Cruz et al., 2004	Palm et al., 2004	Gerecke, 2006	Söderström et al., 2004
# of Br	solution medium	methanol/water	toluene	aerosol (UV)	lipid	methanol	tetrahydrofuran	hexane	SiO_2 in water	kaolinite	sand
1											
2											
3											
4		290									
5		64									
6		47		24							
7		29	4.38		2						
8		6.4	3.38								
9		1	1.75								
10		0.5	0.64			0.3	0.25	0.13	6.1	1.25	13

Appendix IV – Variable parameters

month	Ta K	Ts K	OH molec./ cm^3	Ir W m^{-2}	kr m/h (average)	qw m3/s (average)	wind m/s (average)
Jan 06	270.0	277.5	6.0E+04	52.6	6.28E-05	29.9	1.4
Feb 06	272.5	277.4	2.1E+05	64.6	6.55E-05	31	1.5
Mar 06	275.5	277.7	3.6E+05	115.0	1.65E-04	55.5	2.0
Apr 06	280.7	281.1	5.2E+05	158.0	1.58E-04	143	1.7
May 06	284.6	285.7	6.9E+05	191.5	2.67E-04	205	1.9
Jun 06	288.6	289.9	8.5E+05	283.9	1.03E-04	203	1.8
Jul 06	294.1	293.6	1.0E+06	238.6	1.27E-04	194	1.6
Aug 06	287.6	289.5	8.0E+05	151.7	2.76E-04	164	1.5
Sep 06	289.1	289.5	5.7E+05	142.3	1.11E-04	144	1.3
Oct 06	284.6	286.5	3.5E+05	90.8	6.28E-05	79	1.1
Nov 06	278.9	283.6	2.5E+05	45.9	6.90E-05	47	1.3
Dez 06	274.2	280.8	1.6E+05	26.7	1.14E-04	47.3	1.4
Jan 07	275.5	279.8	6.0E+04	31	8.37E-05	67.3	1.4
Feb 07	276.6	278.9	2.1E+05	65	1.30E-04	39.6	1.4
Mar 07	278.2	279.1	3.6E+05	128	1.41E-04	66.5	1.8
Apr 07	286.3	282.2	5.2E+05	227	5.15E-05	101	1.9
May 07	286.9	286.5	6.9E+05	187	2.80E-04	151	2.0
Jun 07	290.0	287.5	8.5E+05	216	2.73E-04	220	1.8
Jul 07	290.4	289.0	1.0E+06	209	4.61E-04	240	1.8
Aug 07	290.0	291.2	8.0E+05	174	2.38E-04	214	1.5

Appendix V – Constant parameters

Annotation: The variables have the nomenclature as used in the model code

Parameter	Description	Value	Unit	
Tb	Lake bottom temperature	278	K	1)
twet	Duration of rain event	9.5	h	1)
tdry	Duration of dry periods	35.6	h	1)
V(1)	Volume of atmospheric compartment	12'394'200'000	m^3	2)
V(2)	Volume of lake water compartment	6'420'000'000	m^3	
V(3)	Volume of sediment compartment	1'906'800	m^3	
P(2)	Fraction of coarse aerosols	3.6	$\mu m/m^3$	
P(3)	Fraction of fine aerosols	11.6	$\mu m/m^3$	
P(5)	Fraction of suspended particles	6.50E-04	kg/m^3	
P(6)	Fraction of fish	2.30E-08	m^3/m^3	
P(7)	Fraction of solid sediment	0.2	m^3/m^3	
P(8)	Fraction of pore water	0.8	m^3/m^3	
Ar(1)	Lake surface area	47'670'000	m^2	2)
Ar(2)	Sediment area	47'670'000	m^2	
focP	Organic carbon fraction in suspended particles	0.02	kg/kg	
focS	Organic carbon fraction in sediment	0.02	kg/kg	
OMc	Organic mass fraction in coarse aerosols	0.10	kg/kg	
OMf	Organic mass fraction in fine aerosols	0.30	kg/kg	
Lip	Lipid content of fish	0.057	kg/kg	
densP	Density of particles	1'500	kg/m^3	
densS	Density of sediment	2'400	kg/m^3	
ka	Diffusion velocity in air (air-water interface)	5.7	m/h	
kw	Diffusion velocity in water (air water interface)	0.007	m/h	
kddc	Dry deposition velocity coarse aerosols	18.0	m/h	
kddf	Dry deposition velocty fine aerosols	3.6	m/h	
Ec	Scavenging efficiency coarse aerosols	0.5	-	
Ef	Scavenging efficiency fine aerosols	0.01	-	
Vra	Volume ratio rain air	6.0E-08	m^3/m^3	
kws	Diffusion velocity water-sediment	0.004	m/h	
kd	Sedimentation velocity	0.9	m/h	3)
kres	Resuspension velocity	2.30E-07	m/h	3)
ksb	Sediment burial velocity	5.60E-07	m/h	3)
Ea	Activation energy biodegradation	50'000	$J\ mol^{-1}$	
Qs	Scavenging ratio	200'000	m^3/m^3	
b	Kow - Koc conversion factor	0.33	$l\ m^3/kg\ m^3$	
ht	Height of atmospheric compartment	260	m	2)
wh	Width of atmospheric compartment	3'000	m	2)
lh	Length of atmospheric compartment	15'890	m	2)

1) For these parameters the model includes the possibility to use variable data (time dependent), but for the Lake Thun case study constant (annual averages) were used.
2) Atmospheric volume, surface area and length, width and height of the compartment must be correlated.
3) Sedimentation velocity, resuspension velocity and sediment burial velocity must be correlated as given in equation (4-41)

Appendix VI – List of variables

The variables used for describing vectors and matrices in chapter 5 are not included in this list. The explanations in chapter 5 should be considered directly.

Variables used in the model code are not included here neither. A list of the variables used for the input parameters in the model code is provided in *Appendix VII– Short model description*.

A_{aw}	Interface area between atmosphere and lake compartment = lake surface area	m^2
Ac	Sediment accumulation	kg m^{-2} h^{-1}
A_{ws}	Interface area between lake and sediment compartment	m^2
c_w^{eq}	Theoretic concentration in water in equilibrium with atmosphere	mol m^{-3}
$c_{air,bulk,i}$	Bulk concentration in air	mol/m^3
Cf	Confidence factor	-
C_{PM}	Aerosol concentration in air	µg / m^3
$C_{PM,coarse}$	Coarse aerosol concentration in air	µg m^{-3}
$C_{PM,fine}$	Fine aerosol concentration in air	µg m^{-3}
$C_{PM.0}$	Concentration of particulate matter (aerosols) at the surface	µg m^{-3}
$C_{PM.z}$	Concentration of particulate matter (aerosols) at height z	µg m^{-3}
C_{SP}	Concentration of suspended particles	kg m^{-3}
c_w	Concentration in water	mol m^{-3}
D	D-value	mol Pa^{-1} h^{-1}
D_{wet}^{max}	Maximal D-value for wet deposition	mol Pa^{-1} h^{-1}
D^*_i	Diffusivity of compound i.	m^2 h^{-1}
D^*_{ia}	Diffusivity in air of compound i	cm^2 s^{-1}
D^*_{iw}	Diffusivity in water of compound i	cm^2 s^{-1}
$D_{a,out}$	D-value for output with wind	mol Pa^{-1} h^{-1}
D_{awd}	D-value for diffusive exchange	mol Pa^{-1} h^{-1}
D_{dd}	D-value for dry deposition	mol Pa^{-1} h^{-1}
D_{deg}	D-value for degradation in media i by reaction j	mol Pa^{-1} h^{-1}
D_{res}	D-value for resuspension of sediments	mol Pa^{-1} h^{-1}
D_{rw}	D-value for rain washout	mol Pa^{-1} h^{-1}
D_{sb}	D-value for sediment burial	mol Pa^{-1} h^{-1}
D_{sed}	D-value for sedimentation of suspended particles	mol Pa^{-1} h^{-1}
$D_{w,out}$	D-value for output with water	mol Pa^{-1} h^{-1}
D_{wp}	D-value for wet particle deposition	mol Pa^{-1} h^{-1}
D_{wsd}	D-value for diffusion between sediment pore water and lake water	mol Pa^{-1} h^{-1}
E	Scavenging efficiency	-

f	Fugacity	Pa
$F_{a->w}$	Flux from atmosphere to water	mol m^{-2} h^{-1}
f_{OC}	Organic carbon mass fraction	kg/kg
f_{OM}	Mass fraction of organic matter	kg/kg
g	Gravity constant	9.81 m s^{-2}
h	Height of atmospheric compartment	m
h_s	Scaling height.	m
I	Input parameter	-
I_0	Light intensity at the surface	W m^{-2}
I_z	Light intensity at depth z	W m^{-2}
k_a	Water side diffusive exchange velocity	m h^{-1}
K_{aw}	Air-water partition constant	m^3/m^3
k_{aw}	Total exchange velocity	m h^{-1}
k_{diff}	Diffusion velocity	m h^{-1}
k_{deg}	Degradation rate in media i for reaction j	h^{-1}
k_{dry}	Dry deposition velocity	m h^{-1}
K_{FW}	Partition coefficient between fish and water	m^3 water/m^3 fish
K_o	Light attenuation coefficient	m^{-1}
K_{oa}	Octanol – air partition constant	m^3/m^3
K_{OC}	Partition coefficient between organic carbon and water	l/kg
K_{OW}	Octanol-water partition constant	m^3 /m^3
K_{ow}*	Dry octanol-water partition constant	m^3/m^3
K_p	Aerosol - air partition coefficient	$m^3/\mu g$
K_{pw}	Partition coefficient between particles (or sediment) and water	m^3/ kg
k_r	Rainfall rate	m h^{-1}
k_{res}	Resuspension velocity	m h^{-1}
k_{sb}	Sediment burial velocity	m h^{-1}
k_{sed}	Sedimentation velocity	m h^{-1}
k_w	Air side diffusive exchange velocity	m h^{-1}
k_{ws}	Pore water – lake water diffusion velocity	m h^{-1}
k_{wet}^{max}	Maximal removal rate from atmosphere by wet deposition	h^{-1}
L	Lipid content of the fish	m^3/m^3
M_{air}	Average molar mass of air	28.97 g mol^{-1}
M_i	Molar mass of chemical i	g mol^{-1}
M_O,	Molar mass of octanol	g mol^{-1}
M_{OM}	Molar mass of organic matter	g mol^{-1}
N	Mass flow	mol h^{-1}
O	Model output value	-
P	Vapor pressure (for an individual substance)	Pa
p	Atmospheric pressure (for total air)	atm

Q	Scavenging ratio	m^3/m^3
q_a	Wind output	$m^3\ s^{-1}$
$q_{a,i}$	Input mass flow for chemical i into the atmospheric compartment	$mol\ h^{-1}$
q_w	Water volume flow	$m^3\ h^{-1}$
r	Particle radius	m
R	Universal gas constant	$8.314\ J\ K^{-1}\ mol^{-1}$
Rv	Relative variance	-
S	Sensitivity index	-
S_A	Solubility in air	mol/m^3
S_o	Solubility in octanol	mol/m^3
Sr	Relative sensitivity	-
S_w	Solubility in water	mol/m^3
T	Absolute temperature	K
τ_{air}^{min}	Minimal residence time in the atmosphere	h
t_{dry}	Average duration of dry period	h
t_{wet}	Average duration of wet period	h
ΔU_a	Inner energy of solution in air (=vaporization)	$J\ mol^{-1}$
ΔU_w	Inner energy of solution in water	$J\ mol^{-1}$
ΔU_o	Inner energy of solution in octanol	$J\ mol^{-1}$
ΔU_{aw}	Inner energy of air – water phase transfer	$J\ mol^{-1}$
ΔU_{ow}	Inner energy of octanol – water phase transfer	$J\ mol^{-1}$
ΔU_{oa}	Inner energy of octanol – air phase transfe	$J\ mol^{-1}$
V_a	Volume of atmospheric compartment	m^3
$\overline{V}_{air}$	Average molar volume of the gases in air	$\sim 20.1\ cm^3\ mol^{-1}$
V_i	Molar volume of the chemical	$cm^3\ mol^{-1}$
w	Width of atmospheric compartment	m
w_i	Misclosure errors (i = 1 to 5)	various
V_i	Molar volume of chemical i	$cm^3\ mol^{-1}$
wind	Wind speed	$m\ h^{-1}$
z	Height in atmosphere or depth in lake	m
Z	Fugacity capacity	dependent on the unit of 'c'
Z_a	Fugacity capacity of air (gas phase)	$mol\ m^{-3}\ Pa^{-1}$
$Z_{bulk,a}$	Bulk fugacity capacity in atmosphere	$mol\ m^{-3}\ Pa^{-1}$
Z_p	Fugacity capacity of aerosols	$mol\ \mu g^{-1}\ Pa^{-1}$
$Z_{p,coarse}$	Fugacity capacity of coarse aerosols	$mol\ \mu g^{-1}\ Pa^{-1}$
$Z_{p,fine}$	Fugacity capacity of fine aerosols	$mol\ \mu g^{-1}\ Pa^{-1}$
$Z_{raindrop}$	Fugacity capacity of raindrop	$mol\ m^{-3}\ Pa^{-1}$
Z_s	Fugacity capacity of solid sediment	$mol\ m^{-3}\ Pa^{-1}$

Z_{sp}	Fugacity capacity of suspended particles	mol kg^{-1} Pa^{-1}
Z_w	Fugacity capacity of water (dissolved phase)	mol m^{-3} Pa^{-1}
a	Form factor, = 1 for spheres	-
μ	mean value	
γ_O,	Activity coefficient of chemical in octanol	-
γ_{OM}	Activity coefficient of chemical in organic matter	-
δ	Diffusion path length	m
η	Viscosity of water	kg m^{-1} s^{-1}
ρ_{sed}	Sediment density	kg m^{-3}
ρ_{sp}	Density of suspended particles	kg m^{-3}
ρ_w	Density of water	kg m^{-3}
σ	standard deviation	-
ϕ_i	Mass or volume fraction of the media i (compared to compartment volume or mass)	various
ϕ_s	Volume fraction of solids in sediment	m^{-3} solids / m^{-3} bulk sediment

Appendix VII– Short model description

This is a short introduction to the Lake model and should help a user to learn how the model works in order to (1) use the model and (2) know how the code works and thus learn where future refinements and improvements can be added.

This overview does not cover the modeling theory, i.e. the fugacity approach and the description of environmental processes.

More details are found in comments directly included in the model code.

Input files

All input files consist of two parts, a header describing the content of the file and the 'data' part, where the model will actually start reading the data. The header part can be edited without affecting the model.

Table VII-1: Input files needed to run the model

FILE	CONTENT
control.dat	Definition which calculations should be performed
properties.dat	Partition and energy of phase transition data for all compounds
deg_rates.dat	Degradation rates for OH-, photo- and biodegradation in all phases
parameters.dat	Constant environmental parameters
variable_parameters.dat	Seasonal variable environmental parameters
compartments.dat	Definition of the compartment's sizes
phases.dat	Definition of the phase's mass or volume fractions in their compartment
inp_conc_air.dat	Bulk concentration of the compounds in the input air (for each season)
inp_conc_water.dat	Bulk concentration of the compounds in the input water (for each season)
atm_conc.dat	Bulk concentration in air (for modus 2)
biodegradation_scheme.dat	Debromination scheme indicating which compound is formed from which compound (biodegradation)
photodegradation_scheme.dat	Debromination scheme indicating which compound is formed from which compound (photodegradation)
confidence_factors.dat	Confidence factors for all parameters. Sequence as indicated in confidence_factors.xls

Functions

The following figure gives a short overview of how the model works. The boxes represent individual functions of the model. Shown are only the most important functions. The central function is called 'START', which is also the command to

enter in order to start the model. The functions are then called clockwise (in the figure) starting with 'read parameters' and ending with 'write output'.

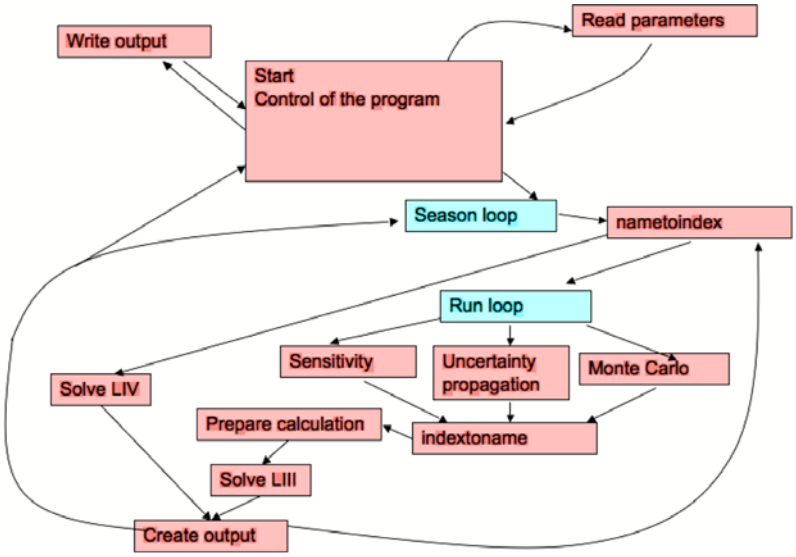

Figure VII-1: Scheme of the functions in the model

A list of all functions of the model with a short description is given in Table VII-2. For more details about the functions, the code should be read directly. Many comments have been included in the code in order to explain the individual steps in each function.

Table VII-2: Functions in the MATLAB code of the Lake model

FUNCTION (order as occurring in the code)	Short description
startV5	Model steering code. Determines which calculations should be performed. Starting loop for seasons. Setting parameters for sensitivity analysis.
level4	Steering file for the Level 4 solutions
read_parameters	Reading all parameters stored in the input files
prepare_calculation	Preparing the mass balance equations. Define the partition coefficients and fugacity capacity Calculate temperature dependence Define D-values Set up mass balance equation system (multichemical)
SolveIII_modus1	Solve mass balance equations for steady-state with given input (atmosphere and water)
SolveIII_modus2	Solve mass balance equation for steady-state with given atmospheric concentrations and water input
Level 4 prepare	Prepare L4 solution: Define differential equations for fugacity.
SolveIV_analytic	Analytical solution for the differential equation system (Solution from CliMoChem)
SolveIV_numericODE	Solution of the differential equation system with MATLAB ODE Solver

SolveIV_numeric2	Numerical solution of differential equation system. (self-made)
reshape fugacity	Reshape fugacity from (3*c) to (3,c)
calc_concentration	Calculate concentrations and mass from fugacity
create_output	Create outputs, namely concentration, mass and mass flow tables
monte_carlo_output	Create the output of Monte Carlo calculations. Output for mean, lower and upper quantile
monte_carlo_write	Write Monte Carlo output
sensoutput	Calculate relative sensitivity and sensitivity index
uncertainty_propagation	Calculate the uncertainty propagation with confidence factors and sensitivities (according to Macleod, 2002)
write_output	Write the outputs to files
write_sensitivity	Write the sensitivity outputs to files
degscheme	Build the degradation scheme matrices defining formation of compounds from other compounds
monte_carlo	Random number generator for Monte Carlo analysis
nametoindex	Store all the parameters in one variable (parameters)
indextoname	Restore all the parameters from the parameters variable

Table VII-3: Output files

output.txt	Level III outputs
sensindex1.txt sensindex2.txt	Sensitivity index (split into two files due to large content)
relsensitivity1.txt relsensitivity2.txt	Relative sensitivity (split into two files due to large content)
cfo.txt	Confidence factors for outputs
ctoutput.txt ctoutput2.txt ctoutput3.txt	Level 4 solution: Concentration as function of time for (1) analytical solution, (2) numeric ODE-Solver solution, (3) numeric (self-made) solution
mtoutput.txt mtoutput2.txt mtoutput3.txt	Level 4 solution: Mass as function of time for (1) analytical solution, (2) numeric ODE-Solver solution, (3) numeric (self-made) solution
mc_median.txt	Monte Carlo output. Median of the output values of all Monte Carlo runs
mc_lower.txt	Monte Carlo output. Lower quantile (0.025) of the output values of all Monte Carlo runs
mc_upper.txt	Monte Carlo output. Upper quantile (0.975) of the output values of all Monte Carlo runs
mc_parameter.txt	Monte Carlo output. Parameter mean and confidence factor calculated from random generated parameters (for checking the Monte Carlo calculation).

Table VII-4: Variables used in the model

Ta	Air temperature
Ts	Lake surface temperature
Tb	Lake bottom temperature
OH	OH concentration
Ir	Irradiance
kr	rainfall rate
twet	duration of rain event
tdry	duration of dry periods
qw	Water runoff
wind	wind speed (ms-1)
V(1)	Volume bulk air
V(2)	Volume bulk water
V(3)	Volume bulk sediment
P(2,1)	Volume fraction coarse aerosols
P(3,1)	Volume fraction fine aerosols
P(5,1)	Volume fraction suspended particles
P(6,1)	Volume fraction fish
P(7,1)	Volume fraction solid sediment
P(8,1)	Volume fraction pore water
Ar(1,1)	lake surface area
Ar(2,1)	sediment area
focP	organic mass fraction in suspended particles
focS	organic mass fraction in sediment
Omc	organic mass fraction coarse aerosols
Omf	organic mass fraction fine aerosols
Lip	lipid content of fish
densP	density of particles
densS	density of sediment
ka	diffusion mass transfer coefficient in air (air-water interface)
kw	diffusion mass transfer coefficient in water (air water interface)
kddc	dry deposotion rate coarse aerosols
kddf	dry deposotion rate fine aerosols
Ec	Scavenging efficiency coarse aerosols
Ef	Scavenging efficiency fine aerosols
Vra	Volume ratio rain air
kws	mass transfer coefficient sediment-water

kd	mass transfer coefficient deposition (water-sediment)
kres	mass transfer coefficient resuspension (sediment-water)
ksb	sediment burial velocity
Ea	Activation energy biodegradation
Qs	scavenginig ratio
b	Kow - Koc conversion factor
ht	height of air compartment
wh	width of air-water comps
lh	length of compartments
Kc(1)	Kaw
Kc(2)	Kow
Kc(3)	Koa
E(1)	ΔU_{aw}
E(2)	ΔU_{ow}
E(3)	ΔU_{oa}
dgr(i,j)	degradation rate (i=medium, j: 1=biodegradation, 2=Photolysis, 3 = OH reaction)
cinpair	concentration in air input
cinpwater	concentration in water input
ca	bulk concentration in atmosphere
Fbio	Debromination scheme for biodegradation
Fphoto	Debromination scheme for photodegradation